GEOTECHNICAL RESEARCH CENTRE

PARTIALLY SATURATED SOILS COMPOSITION, SOIL SUCTION AND SLOPE STABILITY

by

G.R.C. STAFF

SOIL MECHANICS SERIES No. 44

December 1981

McGill University
Montreal, Que Canada

ISSN 0541-6329

FOREWORD

THE following four papers deal with various aspects of partially saturated soils. The first paper is reprinted from Geotechnical Engineering, whilst the other three papers have been presented at the ASCE Specialty Conference on *Engineering and Construction in Tropical and Residual Soils*, held in Hawaii, January 11-14, 1982, and are published in the Proceedings of this Specialty Conference.

1. Yong, R.N. (1980) *Some Aspects of Soil Suction, Shear Strength and Soil Stability*, Geotechnical Engineering, Vol.11, pp.55-76.

2. Yong, R.N., Sweere, G.T.N., Sadana, M.L., Moh, Z.C. and Chiang, Y.C. (1982) *Compositional Effect on Suction of a Residual Soil*, Proceedings, ASCE Specialty Conference on "Engineering and Construction in Tropical and Residual Soils", Hawaii.

3. Boonsinsuk, P. and Yong, R.N. (1982) *Analyses of Hong Kong Residual Soil Slopes*, Proceedings, ASCE Specialty Conference on "Engineering and Construction in Tropical and Residual Soils", Hawaii.

4. Yong, R.N., Siu, S.K.H. and Sciadas, N. (1982) *Stability Analysis of Unsaturated Soil Slopes*, Proceedings, ASCE Specialty Conference on "Engineering and Construction in Tropical and Residual Soils", Hawaii.

Published in GEOTECHNICAL ENGINEERING (1980) Vol.11, pp.55-76

SOME ASPECTS OF SOIL SUCTION, SHEAR STRENGTH AND SOIL STABILITY†

RAYMOND N. YONG*

SYNOPSIS

The interrelationships between soil and water in terms of degrees of saturation of soil masses are reviewed. The elements of soil-water potential involved are clearly defined and the primary components—osmotic, gravitational and pressure—identified. Typical laboratory and field equipment for measuring soil-water potential are described before examples of test results on both laboratory prepared and natural clay soils are presented. Further examination of the data in relation to dry density of the soils and shear strength show that shear strengths lie on a surface which provide a unique relationship between soil-water potential, shear strength and dry density. Finally, attention is paid to the wetting of soil profiles as a result of infiltration from rainfall.

INTRODUCTION

The problems of analysis and determination of soil stability are generally addressed and solved in terms of:

(a) determination and establishment of the pertinent soil properties.

(b) formulation of a physical model which accurately describes the interaction of the various physical components providing stability of the soil mass—or potential instability, and

(c) development of the associated analytical technique to represent the physical model for computational purposes leading to usage in terms of prediction or design.

In situations where the soil mass is fully saturated, standard techniques have been developed which permit the procurement of representative laboratory test measurements subject to conditions which purport to represent field loading situations. By permitting latitude in examination in terms of total and effective stresses, various modelling techniques can be applied which implicitly rely on the saturated nature of the soil mass. Thus the identification of pore water pressure, in a fully saturated soil mass for example, becomes a most relevant and important parameter. The measurement of pore water

† Presented at the SEASSE Geotechnical Engineering Seminar, Hong Kong, July 31, 1979.

* Director, Geotechnical Research Center, and William Scott Professor of Civil Engineering and Applied Mechanics, McGill University, Montreal, Canada.

pressure and its role in the control of stability or instability of a soil mass has been thoroughly examined in many studies and can well be appreciated.

Laboratory test systems, appropriate analytical modelling techniques which address the reduction of laboratory test measurements, and also problems of mass instability, have all been developed in relation to a saturated soil mass system. The various difficulties that might arise relate to the appropriateness or viability of a model describing mass and stability, the various stages of loading which impact on the boundary condition, specification of initial conditions, and the exact role of pore water pressure.

However, in situations where the soil is not fully saturated, difficulties arise not only in the establishment of the pertinent shear strength parameters, but also in the understanding and associated development of the kind of physical model which best describes not only soil performance but also mass stability or instability. These situations are complicated not only because of soil unsaturation, but because of the various stages of dehydration or hydration as the soil moisture content changes in sympathy with the various seasonal and daily rainfall fluctuations and other local environmental factors. Thus one is faced not only with problems of fluctuation in water content but also in the role of pore water pressure and the gnawing doubt that perhaps hysteresis might also play a significant part in the control of soil performance. The problem, therefore, is one which requires attention to the proper development of theories which would allow for a means for prediction of soil strength, in relation to its present dynamic equilibrium status, and application of the relevant soil strength values or parameters to an acceptable working model which would describe mass stability or instability.

THE SOIL-WATER ENERGY CHARACTERISTIC

In an unbonded natural soil system the energy with which water is held to the soil particles and their particle units (flocs, aggregate groups, etc.) will describe the intrinsic energy of the soil mass itself. This phenomenon is especially useful in the description of soil strength and stability in situations where the degree of soil unsaturation is an issue.

Taking advantage of this fact, we note therefore that the intrinsic energy of a partly saturated unbonded soil or of remoulded soils, can be characterized by the energy relations of soil for water. By and large, these are multiple-valued functions that depend on the moisture history of the soil itself. This accountability for the effects or influences of wetting and drying can be factored into the evaluation of this intrinsic energy. When volume changes

occur because of changes in the moisture regime and stress environment, it will be observed that corresponding changes will occur in the intrinsic energy of the soil.

Soil water potential measurements are generally used to describe the energy status with soils. These can be usefully thought of as defining the integrity or stability of the soil system. One measures soil water potential in the laboratory to define the energy or equilibrium relationship between soil-water potential and water content for a representative soil sample. In the field one measures soil-water potential with the aid of psychrometry. Through other means soil suction measurements are made for purposes of establishment of water movement, water availability and other purposes. The relationship between soil water potential and soil water suction is essentially one which is described in terms of concepts via thermodynamics or concepts via engineering. In research, energy with which water is held in soils is best described with thermodynamic terminology giving rise therefore to the description in terms of soil-water potential. The potential is given in terms of the water phase and it is noted that the potential would decrease as the water content increases. This indicates that the water is held more strongly by dry soil than by wet soil and that movement of soil-water would be from a point of low potential to one of higher potential - analogous to the flow of heat in a conductor. If one therefore considers the potential in terms of water-phase, we note then that the values are generally negative. Figure 1 illustrates the concept of potential of soil-water. We note from Figure 1 that two component potentials are shown which combine to form the total potential. In actual fact, one could divide the total soil-water potential into six components defined by various researchers and summarized recently by YONG AND WARKENTIN (1975) as follows:

(1) $\Delta\psi_t$, the total potential, is the work required to transfer a unit quantity of water from the reference pool to the point in the soil. It is a negative number.

(2) $\Delta\psi_m$, the matric potential, is a soil matrix property. This is the equivalent of Buckingham's capillary potential. It is the work required to transfer a unit quantity of soil solution, from a reference pool at the same elevation and temperature as the soil, to the point in the soil. ψ_m cannot be calculated except for uniform spheres where it is related to curvature of air-water interfaces and $\psi_m = S[(1/r_1) + (1/r_2)]$, or in freely-swelling clay plates where $\psi_m = RT \cosh(y_c - 1)$. S = surface tension of the air-water interface; r_1, r_2 = radii of curvature of the air-water interface; R = universal gas constant;

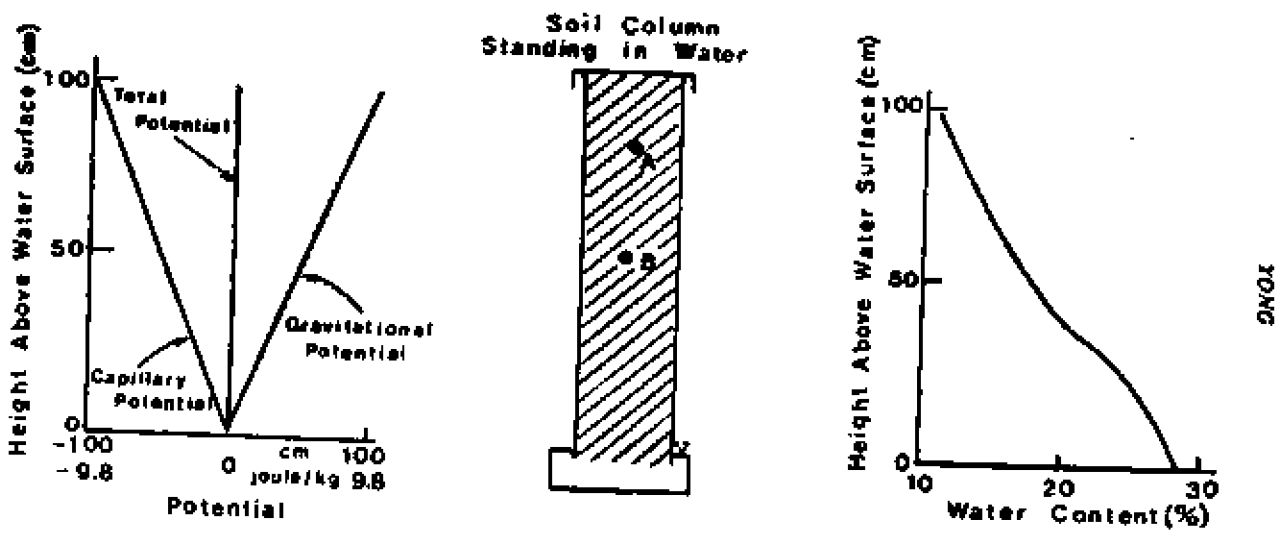

Fig. 1. Illustration of potential concept of soil water.

T = absolute temperature; ψ_c = electrical potential midway between two clay plates. ψ_m can be subdivided into a component related to swelling forces and a component from air-water interface forces, but these components cannot be separated experimentally.

(3) $\Delta\psi_g$, the gravitational potential, is the work required to transfer water from the reference elevation to the soil elevation.

$$\psi_g = -\gamma_w g h$$

where γ_w = density of water.

(4) $\Delta\psi_\pi$, the osmotic potential, is the work required to transfer water from a reference pool of pore water to a pool of soil solution at the same elevation, temperature, etc.

$$\Delta\psi_\pi = n\,RTc$$

where n = number of molecules per mole of salt; R = universal gas constant; T = absolute temperature; c = concentration of salt.

(5) $\Delta\psi_p$, the piezometric or submergence potential, is the work required to transfer water to a point below the water table.

$$\Delta\psi_p = \gamma_w g d$$

where d = depth below free water level.

(6) $\Delta\psi_a$, the pneumatic of a pressure potential, refers to transfer of water from atmospheric pressure to the air pressure, P, on the soil.

$$\Delta\psi_a = P$$

The three component potentials, matric, piezometric and pneumatic are often taken together as the pressure potential, $\Delta\psi_p$.

$$\Delta\psi_p = \Delta\psi_m + \Delta\psi_p + \Delta\psi_a$$

This therefore leaves us with the total potential as being comprised primarily of the osmotic, the gravitational and the pressure components. In laboratory experiments where the soil samples used for testing do not involve gravitational head differences, we note that the total potential measurements made will be comprised only of the osmotic and the pressure (matrix) components. Two representative laboratory techniques to provide soil-water potential measurements can be applied using the set-up described in Figure 2.

From Figure 2, we can now begin to relate the concept of soil suction to the soil-water potential. We observe that the samples are subjected to in-

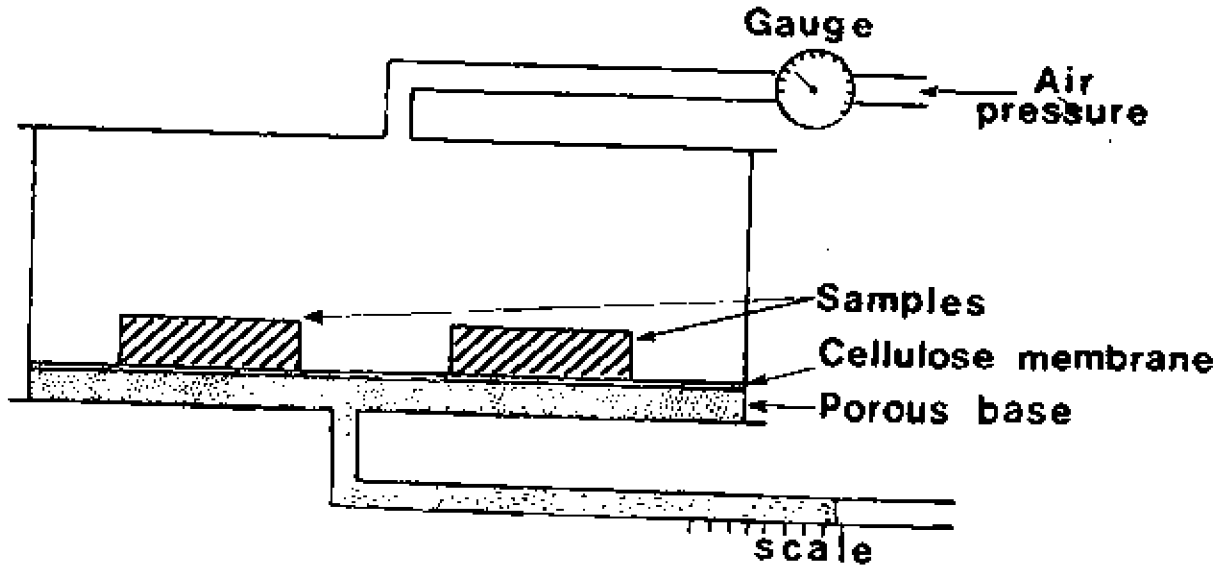

Fig. 2. Pressure plate apparatus for measurement of soil-water potential.

creasing air pressure within the chamber which serves to drive the pore water out from the test sample. The air pressure can be increased monotonically and set at various stages to allow for equilibrium to be established after each pore-water extrusion. Thus the air pressure-water content relationships (i.e. water content remaining in the soil samples) will essentially describe the amount of air pressure at equilibrium with the water content in the soil—i.e. the tension established between the soil water and the soil particles which allows the soil moisture to remain in equilibrium with the applied air pressure. This describes the equivalent energy relationship established between soil particles and the pore water which produces soil integrity.

Alternatively, instead of using air pressure to drive the water out to establish various stages of equilibrium between air pressure and water remaining in the soil samples, another procedure can be used which requires that a suction be applied at the bottom end of the porous plate as shown in Figure 2. Applying the suction to the water would draw the water out from the samples and, in effect, establish a soil suction principle in a more visually rewarding form. It is not unusual therefore to equate this actual experimental test system using suction measurements directly and describing these in terms of negative pore-water pressures. Thus one might argue that the negative pore-water pressure derived in this fashion is identical to that used for computations for derivation of effective stress. Whilst one might accept that soil suction measurements obtained directly through the suction technique, in the range of suction capability for the test apparatus less than − 1 atmosphere, could be directly equated to the negative pore-water pressure used for effective stress computations, the many problems and complications associated with the suction technique for pore water measurements below one atmosphere will not allow for a simple relationship to be easily established between soil suction measurements and negative pore-water pressure.

In the techniques used for field measurement, the two general devices shown in Figures 3 and 4 include either a soil-water tensiometer, or a thermocouple psychrometer. In Figure 3, water in the tensiometer is in contact with soil-water through the ceramic tip. Thus as the soil dries, a tension is exerted on the water in the tensiometer which is measured with a manometer or a Bourdon gauge. Note also that a tensiometer may be used to measure positive pressures or heads, making it, therefore, an ordinary piezometer. It is also useful to note that the tensiometer will only function until a negative pressure is reached at which air bubbles through the ceramic tip. The air-entry value of the ceramic tip can be manipulated within a very small range of interest in the testing procedure, but by and large the air entry values for most tensiome-

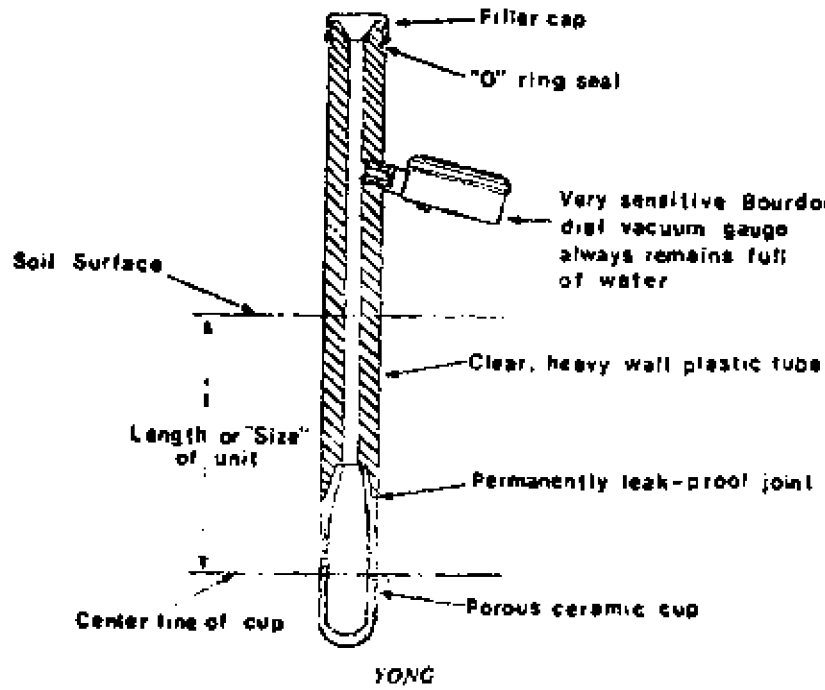

Fig. 3. Soil-water tensiometer for field use.

ters is about −0.85 bar. If, perchance, the soil dries considerably and the actual dehydration process will yield tension values much lower than −0.85 bar, the readings derived from the tensiometer will not necessarily indicate the true value of tension in the soil water. Thus, under those circumstances, it becomes extremely difficult to fully appreciate the real "tension" status of the pore-water and serious error can therefore result in both measurement and subsequent use of the measurement for analysis of soil integrity.

In situations where one might expect the values for soil-moisture tension to vary considerably — (and beyond the capability of the tensiometer) — the thermocouple psychrometer shown in Figure 4 should prove to be most useful. The instrument shown in Figure 4 determines the soil-water potential by measurement of the vapour pressure within the test bulb. This is a well-defined thermodynamic quantity which depends on both the matric and osmotic components of the total potential. The thermocouple end, which is fixed inside the small ceramic bulb, shown in Figure 4, is subject to a cooling current

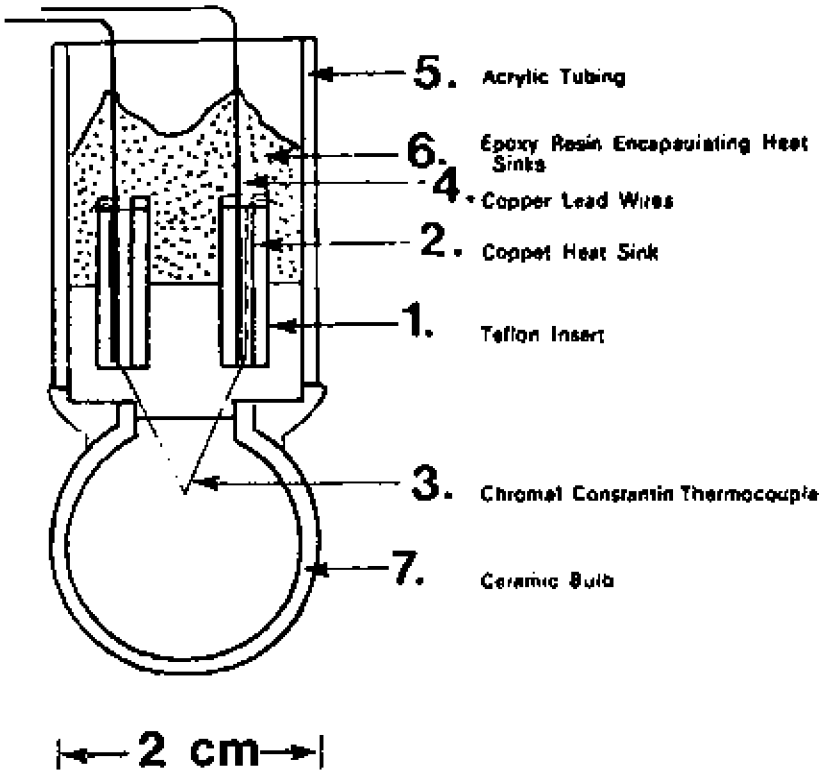

Fig. 4. Cross-section of a thermocouple psychrometer for in situ measurement of soil-water potential showing teflon insert (1), copper heat sink (2), chromel-constantin thermocouple (3), copper lead wires (4), acrylic tubing (5), epoxy resin encapsulating heat sinks (6), and ceramic bulb (7). Water is condensed on the thermocouple junction by Peltier cooling immediately preceding each measurement.

which condenses a minute amount of water on the junction. As this water evaporates, the junction is cooled. Computations can be made which will evaluate the rate of evaporation with respect to the vapour pressure in the bulb. These computations between osmotic pressure and vapour pressure will then provide one with the soil-water potential.

It is useful to note that the precision of the psychrometer as used in the laboratory, is usually about ± 0.1 bar. However, this precision is not readily accessible in the field. In the field, the precision is more easily ± 0.5 bar. It is therefore more useful at low potentials (high suction) or in situations where

the tensiometer will not work. At potentials around −15 bars, vapour equilibrium is established quickly and the readings take only a few minutes. However at higher potentials such as −1 bar (low suction) the readings may take hours to reach equilibrium.

SOIL-WATER POTENTIAL AND SHEAR STRENGTH

Recalling that the soil-water potential describes the energy status of soils, and that these can be measured experimentally in the laboratory or in the field, it is useful to show a typical set of results illustrating the adsorption or desorption characteristics of a laboratory prepared clay and a natural clay.[1] Note that in the desorption process, water is expelled from the test sample in the pressure chamber following application of the air pressure. In the adsorption process, the soil sample is allowed to take up water and the corresponding measurements of the suction required to maintain equilibrium are made. Because of the volume changes of the soil samples associated with the extrusion or entry of water similar to those observed in the consolidation and rebound tests, the adsorption and desorption curves do not necessarily coincide.

The typical soil-water potential results for kaolinite and a natural soil identified as Ste Rosalie clay obtained from the suction and pressure plate tests, shown in Figure 5a, include the dry densities of the samples at equilibrium for the particular water potential identified. This figure demonstrates the normal relationships expected, where the hysteresis encountered between desorption and adsorption is primarily due to irrecoverable changes in the fabric (i.e. volume change hysteresis). The term "fabric" refers to the geometrical arrangement of particles (including particle spacing) and does not take into account the forces between particles.

The relationship between the soil-water potential and shear strength for these samples can be seen in Figure 6. It is noted that, in the desorption process, the kaolinite sample begins to desaturate at a potential value somewhere between −10 and −100 millibars, (i.e. about pF 1 to pF 2). Between −1 and −100 millibars soil-water potential, the shear strength is seen to remain relatively constant. However, the shear strength increases very rapidly once desaturation begins to occur. A similar trend in the relationship between shear strength and soil-water potential is shown in the adsorption portion of the cycle. It would appear that the sample strives to reach complete saturation

[1] For comparison it might be interesting to see the results shown in Fig. 5b for soil water potential tests on three natural soils, demonstrating the differences between soil water potential and soil water, for desorption and adsorption test techniques. Note that these are not cyclic, but separate tests.

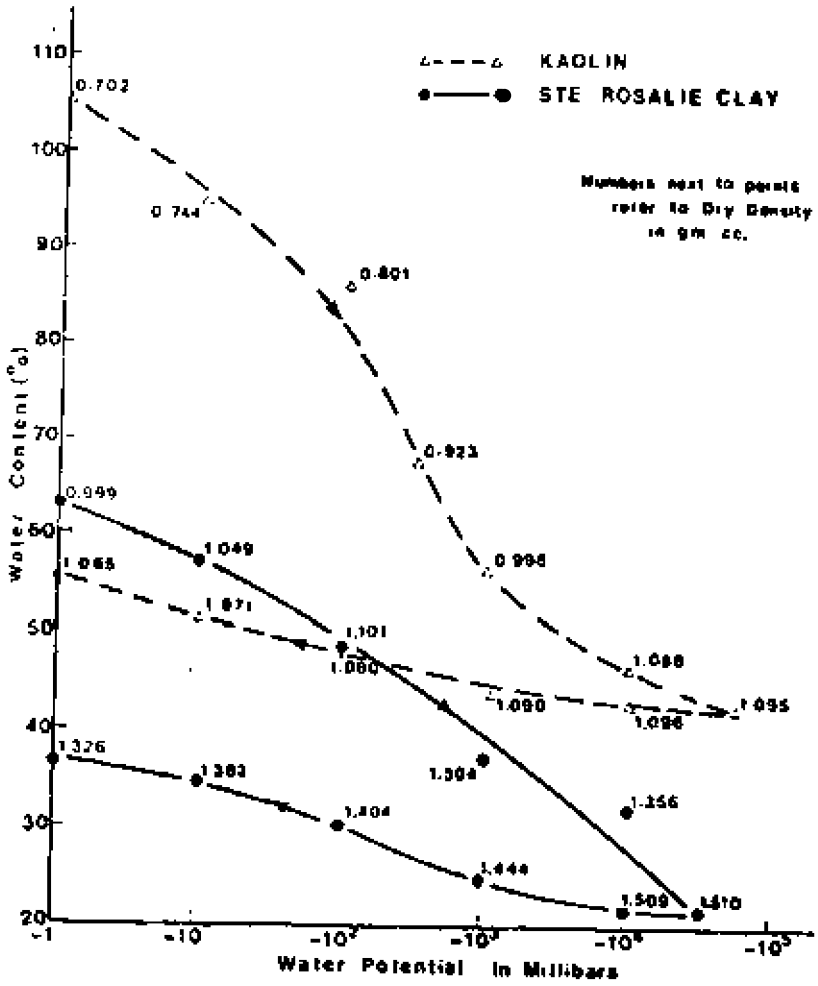

Fig. 5a. Soil-water potential curves for kaolinite and Ste Rosalie clay.

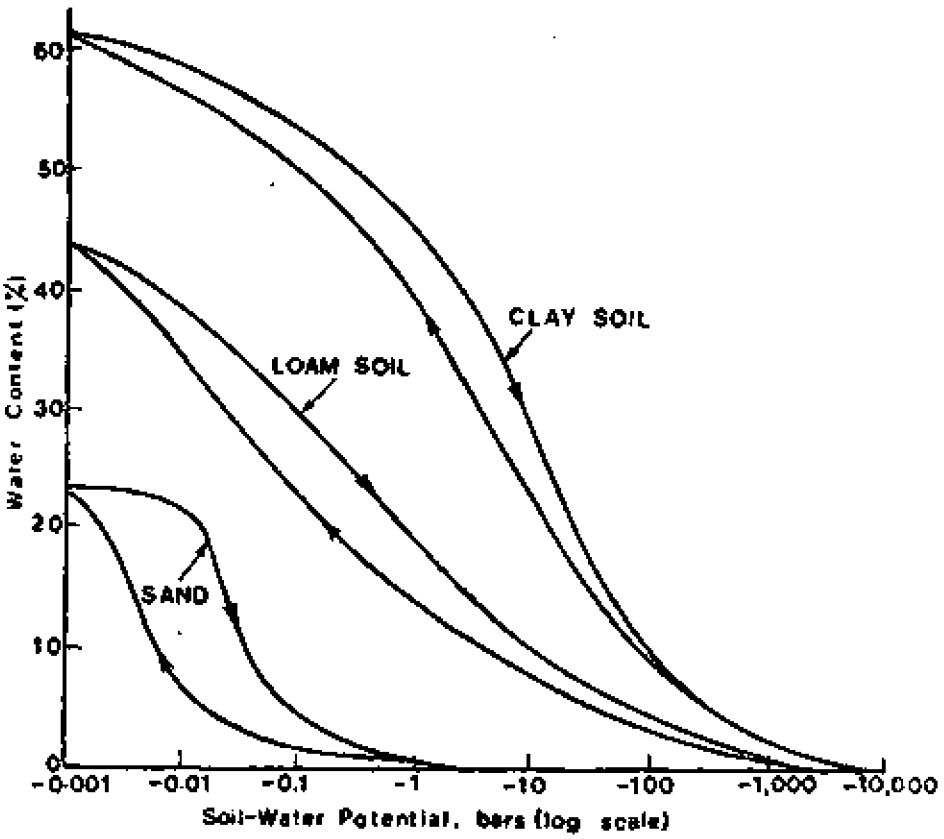

Fig. 5b. Representative water-retention curves. Relationship between potential and water content for different soils.

in the adsorption process and the strength thus begins to decrease less rapidly below potential values of −100 millibars.

Similar trends can be noted in the Ste Rosalie clay although it would appear that the unsaturated state for the Ste Rosalie clay begins at a much earlier stage, probably around a soil-water potential value of −10 to −50 millibars. From Figures 5a and 6 it is noted that irrecoverable fabric changes occur in the desorption process which, in turn, render different values for shear strength

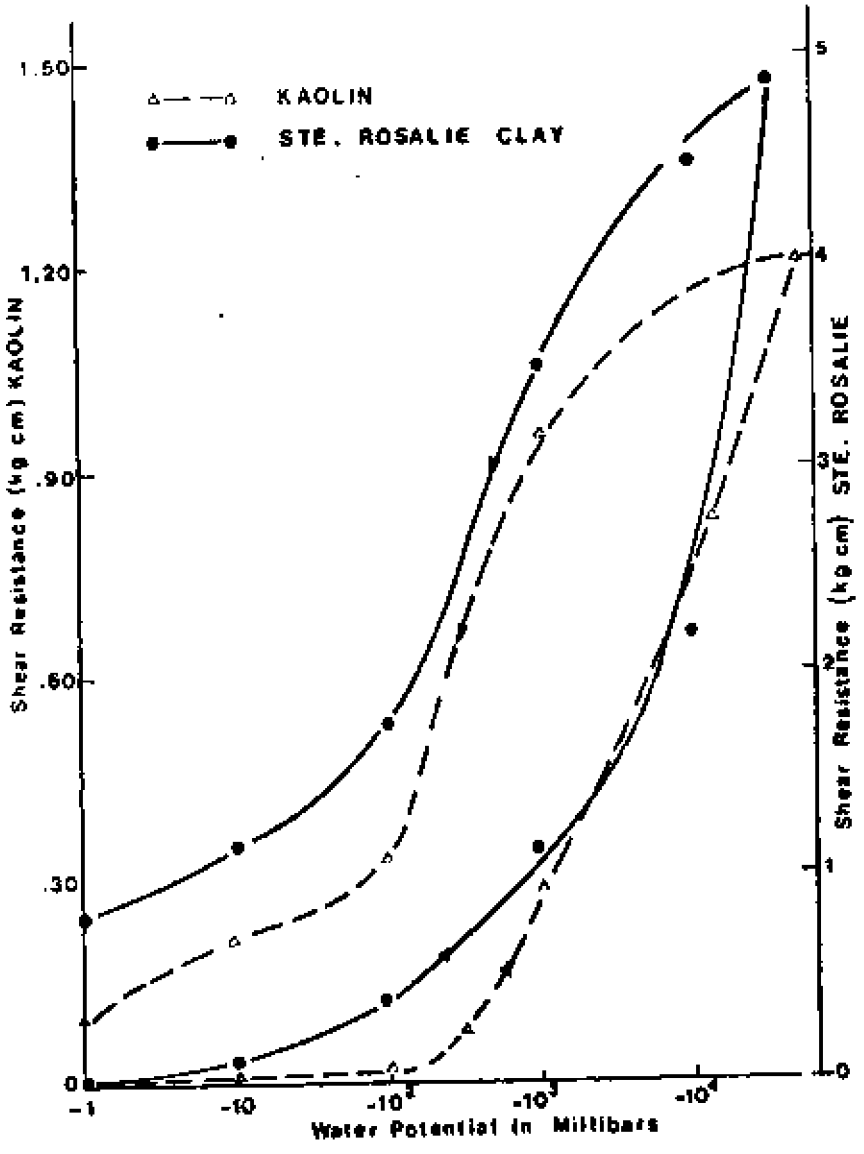

Fig. 4. Soil-water potential and shear strength relationships for kaolinite and Ste Rosalie clay.

at the same soil-water potential value on the adsorption cycle. Thus, one observes that, for the same soil-water potential, it is possible to obtain at least two different values of shear strength. However, if water contents, sample saturation and dry densities are taken into account, it will be seen that these are in no way similar, i.e. for the same soil-water potential it is possible to obtain different values of water content (Figure 5a), saturation, and dry density. The changes in fabric which are reflected in corresponding changes in dry density are not unlike those obtained in samples subject to the loading and unloading cycles in the standard consolidation test.

Whilst in general the soil-water potential may be determined for the desorption or drying process, the results shown in Figure 5a for both the desorption and adsorption process have been obtained to demonstrate the influence of moisture history. Since volume changes are measurable in terms of resultant effects on dry density (i.e. dry weight of solids divided by the bulk volume), it is seen that, if dry densities are obtained, a singular soil-water potential surface independent of moisture history can be obtained which identifies the energy status of the clay soil (see Figure 7 for a typical case). By using dry density as the identifying parameter, water contents, saturation and bulk volume must be taken into account. It is interesting to note that for a given soil type, there exists a singular soil-water potential surface which shows the interdependence between water content, dry density and soil-water potential.

Since one can obtain different values of shear strength for the same soil-water potential depending upon whether one is on the adsorption or desorption portion of the cycle, it is thus possible to obtain a unique value of shear strength in terms of the persistent (i.e. at that particular time) soil-water potential, provided that information on soil dry density is available. From measurements of soil sample volume, it is seen that a significant reason for the differences in shear strength between the adsorption and desorption cycle is due to the resultant existing volume of the sample at each particular potential value. Whilst water retention measurements provide quantitative values for the total water holding capacity of the soil, it must be realized that where solute effects are negligible (as in the case of the soils shown here), the matric suction which accounts for the total soil suction depends on both soil fabric and soil-water interaction. In actual fact, therefore, the matric suction is directly related to dry density.

In Figures 8 and 9, the shear strength, dry density and soil-water potential values for Kaolinite and Ste Rosalie clay respectively are shown on a three-dimensional plot. It is seen that the shear strengths lie on a surface which

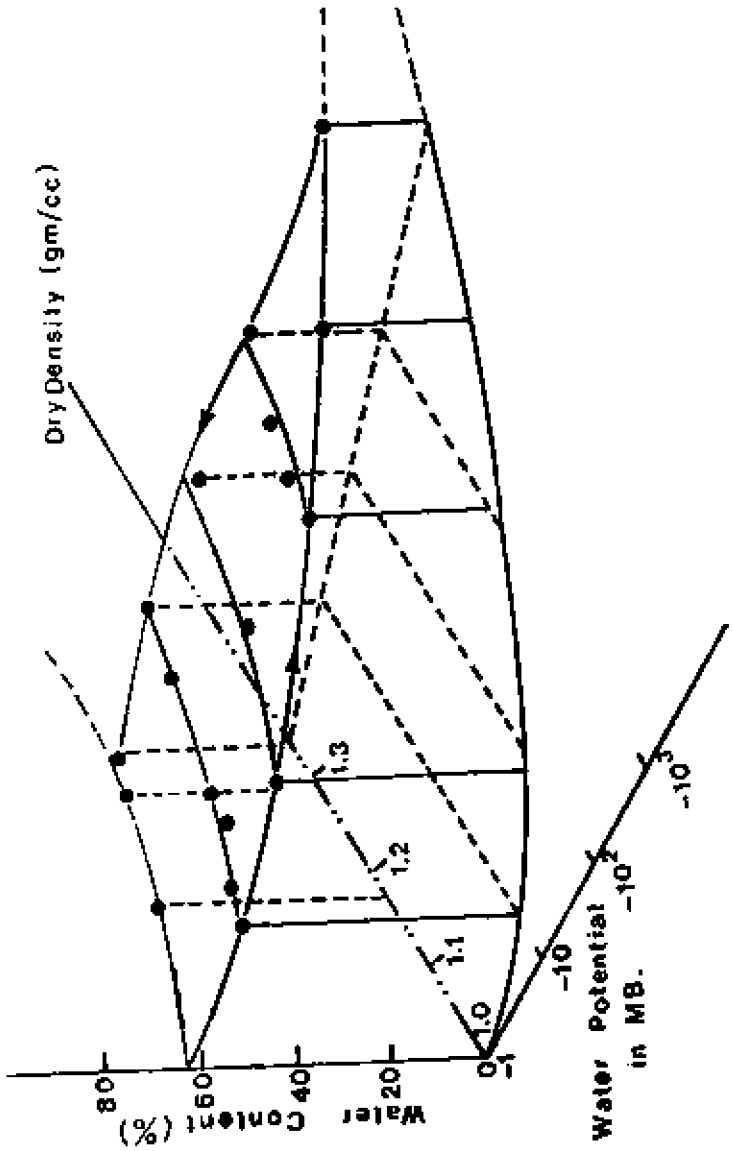

Fig. 7. Soil-water potential surface for Site Reveille clay.

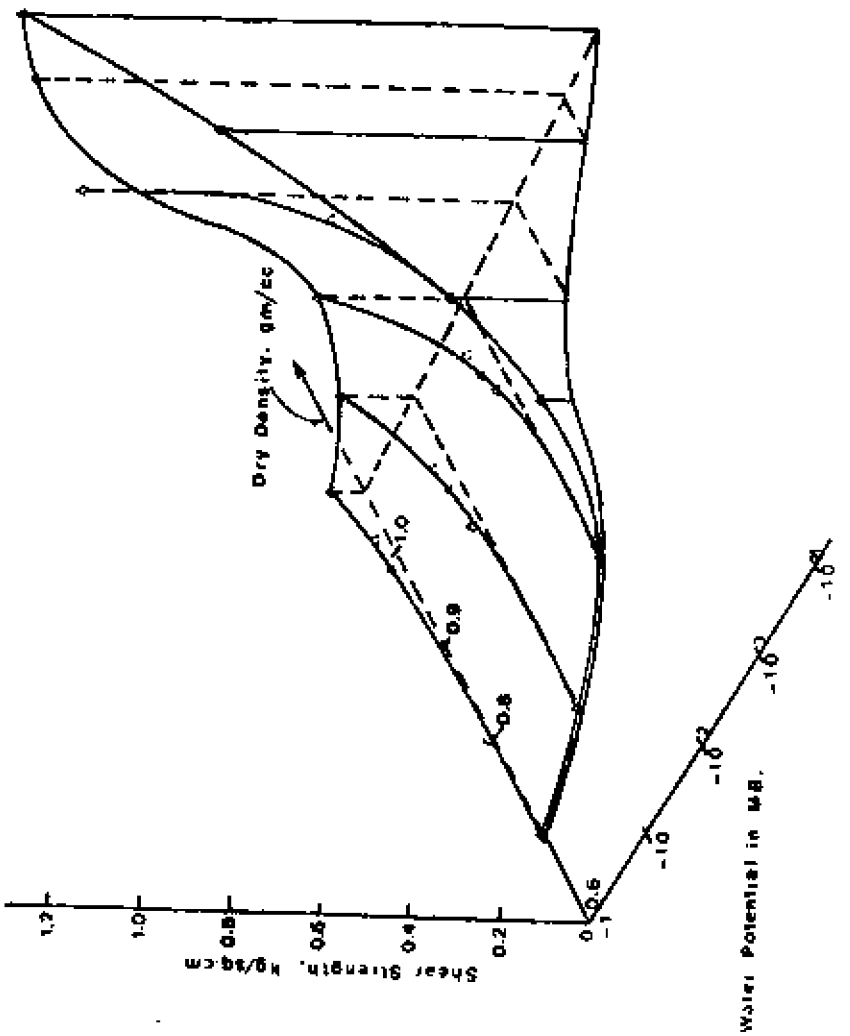

Fig. 8. Soil-water potential-shear strength surface for kaolin clay.

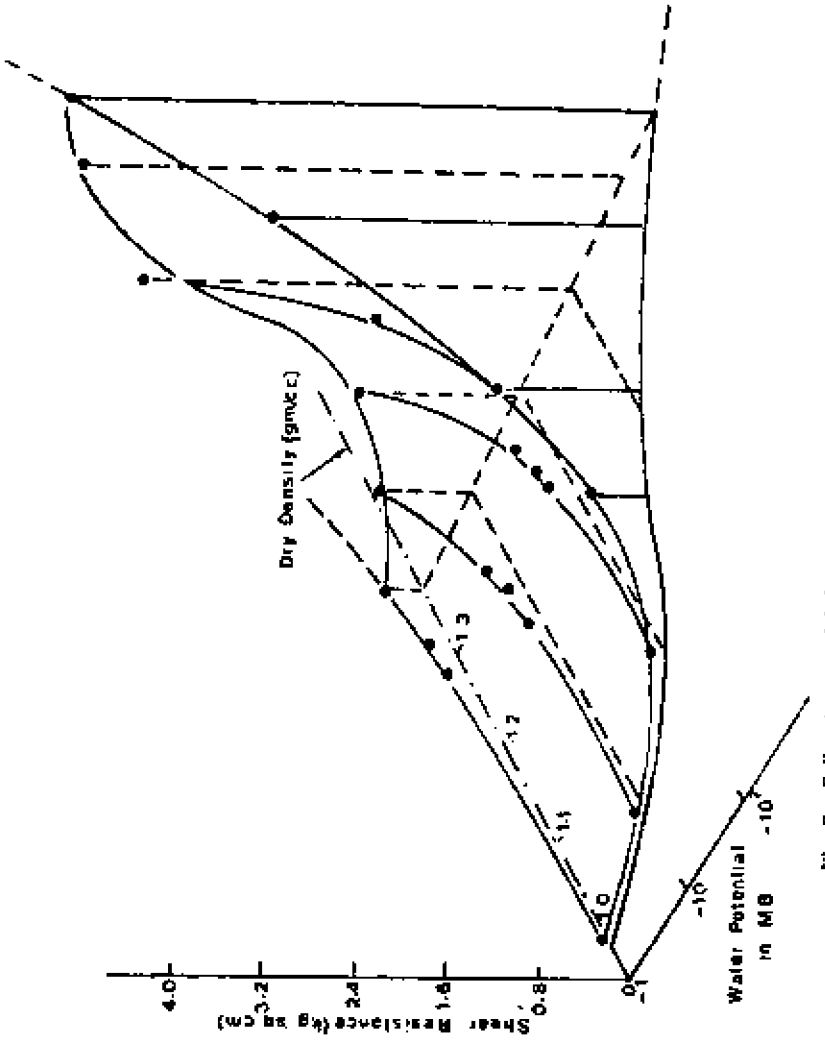

Fig. 9. Soil-water potential-shear strength surface for Sic Rosalie clay.

provide a unique relationship between soil-water potential, shear strength, and dry density. The significance of this form of examination is that the dry density component of soil structure[2] is now incorporated and is seen to be influential in the development of shear strength.

As mentioned previously, the irrecoverable volume change due to fabric distortion, (i.e. dry density changes) can influence the resistance to shear deformation whilst retaining the same energy status. This demonstrates the importance of dry density on the development of water retention and shear strength. The shear strength of the material is seen to depend on the soil-water potential, so long as dry density is taken into account, and thus provides a very useful basis for the examination of the shear strength of partly saturated clay soils

It is evident that, with this method of examination, one is freed from the burden of application of standard models which rely in the fully saturated nature of the soil. In addition, it is not always clear whether the two-parameter failure theory generally used (i.e. Mohr-Coulomb theory) can be usefully applied to describe soil failure during the entire stage of soil unsaturation

WETTING OF SOIL PROFILE AND UNSATURATION / SATURATION

In addressing the problem of prediction of unsaturated soil strength, using any approach which might be feasible, one of the more important requirements is the ability to forecast or to establish beforehand the soil-moisture status (water content and/or degree of saturation). In order to do this, it is necessary to consider the phenomenon of infiltration into the soil arising from input of moisture from the ground surface—through rainfall or any other means. Infiltration, which is the downward entry of water into the soil, is best viewed in terms of the infiltration rate of the soil—i.e. the rate at which a soil in a given condition can absorb water. It is defined as the volume of water passing into a unit area of soil per unit time. One therefore deals with infiltration velocity and capacity of the soil to absorb a certain amount of water. The infiltration rate obviously depends upon both surface and subsurface conditions where particular attention is paid to the initial status of the soil prior to conditions of further wetting.

The general moisture profile and characteristics of infiltration are shown in Figure 10. Note that the general rate of distribution is independent of grain size, even though the time required to wet to a given depth of soil increses with

[2] Soil structure is defined as the resultant action of two components: geometrical arrangements of particles (fabric) and interaction through interparticle forces.

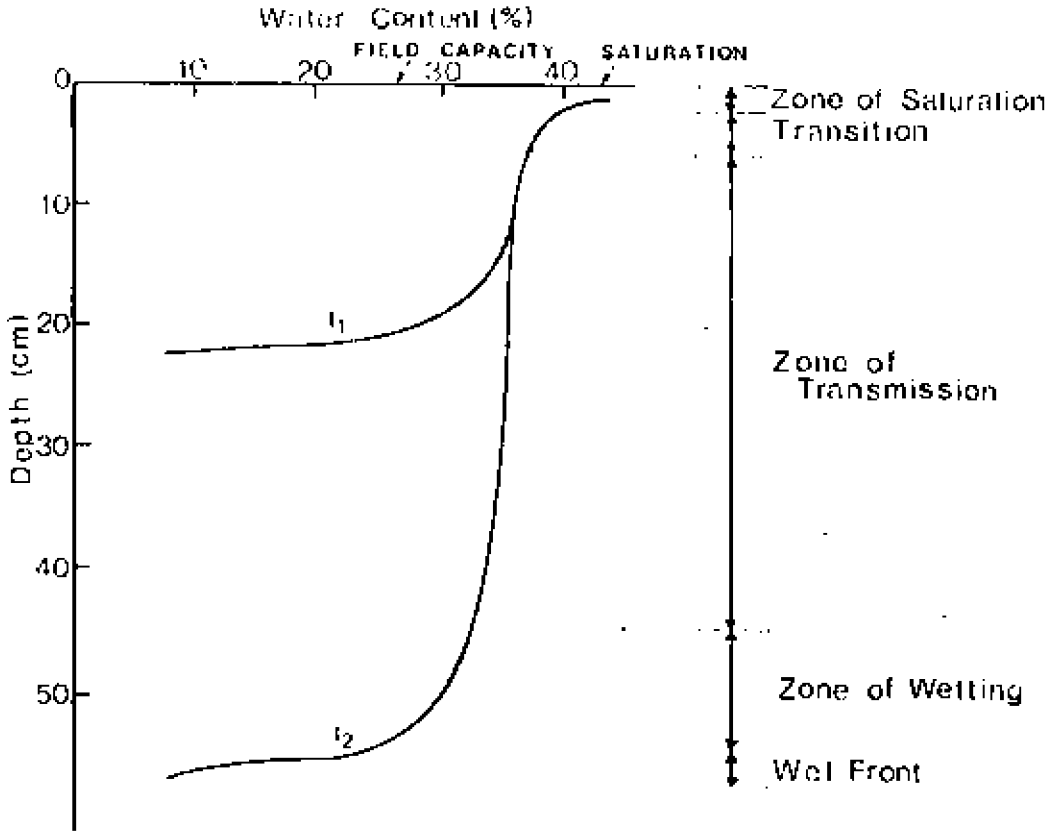

Fig. 10. Water content vs depth profiles for two periods during infiltration.

decreasing grain size. The four parts of the infiltration profile are identified in Figure 10. Note also that the wetting front at any time may be above the standing water table. Recharge of the water table through infiltration will occur very slowly so long as the wet front is above the water table. When the complete wet front and zone of wetting penetrate the water table, a corresponding increase in height of the water table will be observed. Note that the saturation of the soil in the zone of transmission is not necessarily 100%. It is useful to observe that in the downward infiltration zone, the water content in the infiltrated soil will be high. Below the wet front—in the region between the wet front and the standing water table—there exists a layer of soil with lower water contents. This sandwiched layer will decrease in thickness when infiltration progresses further until penetration of the wet front into the water table occurs, or until recharge from the ground surface is diminished.

Changes in soil suction will occur as a result of changes in the water content realised through infiltration. Figure 11 shows a typical set of data which describes the change in soil suction with depth as a function of time from a zero time base, which describes initial infiltration. It is clear that these kinds of information can be obtained for various soil profiles which would allow one to begin to relate soil suction and their changes with resultant shear strength for the soil at various stages of unsaturation — as shown for example in Figure 7.

CONCLUSIONS

It is evident, from the preceding discourse, that the problem of determination of unsaturated soil strength which is pertinent particularly to the difficulties associated with stability analyses, can be successfully evaluated provided one can develop a set of relationships which describe the unsaturated soil strength in relations to the degree of unsaturation and water content. The problems which surround this determination of unsaturated soil strength obviously now can be transferred to those which concern themselves in seeking a set of relationships which permit one to estimate the degree of wetting and the time rate of wetting in the face of rainfall or other surface ponding conditions. With the proper characterization of soil moisture uptake, a knowledge of soil capacity, and the corresponding soil-energy relationships, it now becomes possible to approach the problem of determination for potential instability or present status of stability of a soil mass. The many factors that control soil moisture uptake, water retention, infiltration rate, and moisture cohesion bear overlapping similarity with those which control soil suction. Thus the characterization procedure which requires one to determine the soil suction capability

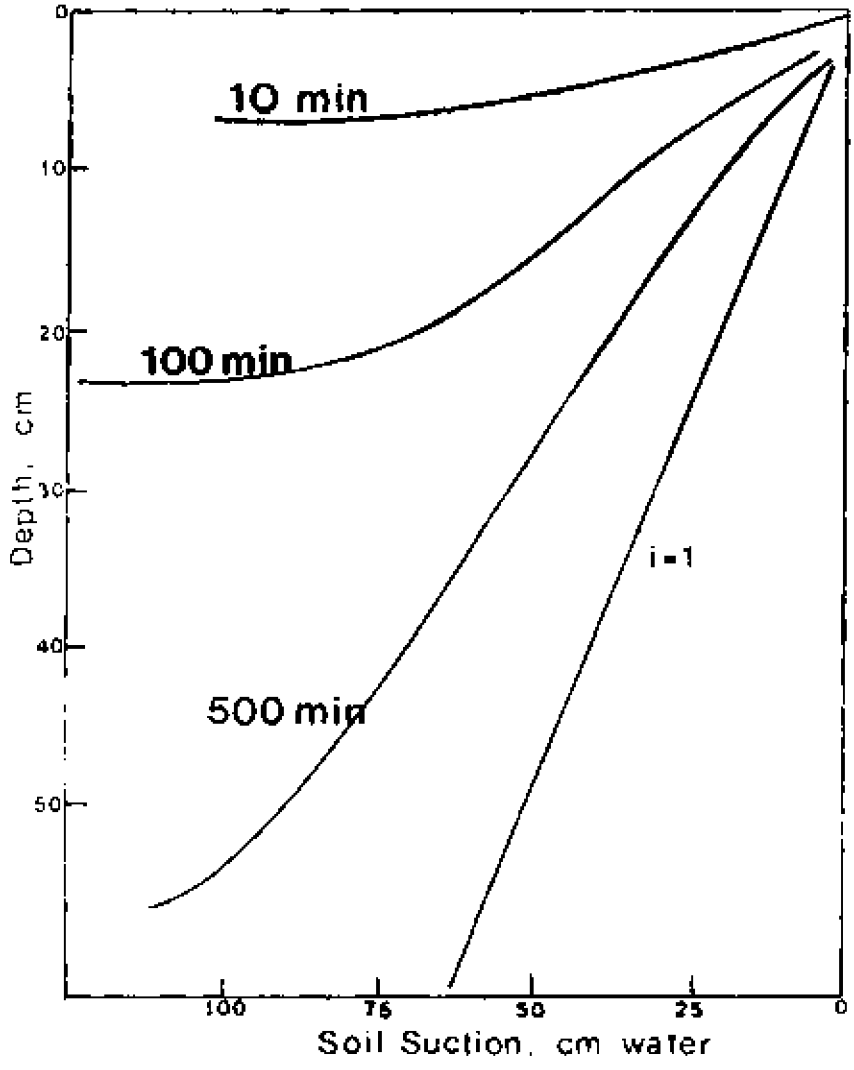

Fig. 11. Soil suction profiles during infiltration at various times.

(soil-water potential) can be used to serve two purposes—i.e. soil characterization for determination of the soil-energy relationships and soil characterization for the purposes of identification of field moisture uptake of soils.

REFERENCES

AITCHISON, G. C. (1965), (Editor), *Moisture Equilibria and Moisture Changes in Soils beneath Covered Areas*, a symposium in print, Butterworths, Australia, pp. 7-21.

CRONEY, D. and COLEMAN, J.D. (1960). Pore Pressure and Suction in Soil, *Proc., Pore Pressure and Suction in Soils Conference*, Butterworths, London, pp. 31-37.

LEWIS, W. A. and ROSS, N. F. (1955), An Investigation of the Relationship between the Shear Strength of Remoulded Cohesive Soil and the Soil Moisture Suction, *Road Research Laboratory, Research Note*, RN 2389/WAL. NFR.

TOWNER, G. C. (1961), Influence of Soil Water Suction on Some Mechanical Properties of Soils. *Journal of Soil Science*, Vol. 12, No.1, pp. 180-187.

YONG, R. N. and WARKENTIN, B. P. (1975), *Soil Properties and Behaviour*, Elsevier, Amsterdam. pp. 109-110.

COMPOSITIONAL EFFECT ON SUCTION OF A RESIDUAL SOIL

by

R.N. Yong, G.T.H. Sweere, M.L. Sadana, Z.-C. Moh and
Y.C. Chiang

Prepared for

ASCE SPECIALTY CONFERENCE
Engineering and Construction in Tropical and Residual Soils
Honolulu, Hawaii
11-14 January 1982

COMPOSITIONAL EFFECT ON SUCTION OF A RESIDUAL SOIL

by

Raymond N. Yong[1] M.ASCE, Govert T.H. Sweere[2a], Madan L. Sadana[2b], Za-Chieh Moh[3] M.ASCE, and Y.C. Chiang[4]

ABSTRACT

The relationship between soil composition and soil structure as revealed from water retention and/or uptake for a soil derived from a moderately to highly weathered granite formation in a tropical region was studied. This relationship is significant in that most of these soils are not fully saturated.

Changes in the immediate local environment will affect the status of the soils - especially in the case of water availability. Since the shear strength and compressibility properties of the soils are to a very large extent dependent on the water content-saturation aspects of the soil, it is necessary to establish basic characterization procedures to allow for prediction of the changes in the moisture regime in the soils. This study provides information on compositional features of a soil obtained from tropically weathered granite. The soil-water relationships are established for the soil and their dependence on aspects of compositional control are shown. Because of the low clay and amorphous material content, very small changes in water content can significantly affect soil performance - especially if the coarser soil particles are coated with the clay and amorphous material.

INTRODUCTION

Of the many problems that underlie the utilization of soil characteristics and properties for prediction of soil performance, the problem of assessment of the role and influence of water content (and degree of saturation) in a partially-saturated residual soil is by far

---

[1] Director, Geotechnical Research Centre, and William Scott Professor of Civil Engineering and Applied Mechanics, McGill University, Montreal, Quebec, Canada.

[2a] Postdoctoral Fellow, Geotechnical Research Centre, McGill University - on leave from Delft University of Technology, The Netherlands.

[2b] Postdoctoral Fellow, Geotechnical Research Centre, McGill University.

[3] Principal and Managing Director, MAA Engineering Consultants (H.K.) Ltd., Hong Kong.

[4] Resident Director, MAA Engineering Consultants (H.K.) Ltd., Hong Kong.

one of the most significant. Whilst one of the most recognizable features of a residual soil is its degree of saturation (partial saturation), and whilst it is indeed known that the water content-percent saturation lumped parameter plays a decided role in the control of the mechanical properties (stress-strain, compressibility, etc.) of such residual soils, the need to continue to seek a more appropriate and accurate soil mechanics models dealing with partly-saturated soils cannot be overstated. By and large tradition has relegated (a) the problem of determination of mechanical properties of partly-saturated soils to one which considers and tests the fully-saturated soil equivalent as a convenient alternative, or (b) the determination of partly-saturated soil properties using procedures which involve empirical correlating factors and other parameters dealing with "measured" pore air pressures, pseudo mechanics theories, dealing with equilibrium established between the various phases, etc. Unfortunately, whilst all these attempts are indeed tacit recognition of the phenomenon of the multiphase interaction, the problem of predicting the performance and behaviour of the partly-saturated residual soil has yet to be successfully solved.

To provide a better means for development of predictive behavioural models dealing with partly-saturated residual soils, it is clear that because of the phenomenon of multiphase interaction, it is necessary to obtain an understanding of the fabric and structure of the soils - especially in regard to the influence exercised by the individual constituents in the soil, i.e. compositional control. In particular, the various kinds of constituents constituting the compositional features which interact and participate in the development of porewater relationships must be well-understood, since water plays a prominent role in the performance of soil material. As the nature of the residual soil is one which is the product of chemical weathering processes, and since the more traditional and classical tools used in soil mechanics classification techniques do not necessarily take into account the requirement for compositional characterization requiring a broader spectrum for detailing of the chemistry of the soil-water system, the present study provides the first-phase reporting of analyses performed on soil samples obtained from three separate coreholes in a soil profile consisting of weathered granite and colluvium overlying the weathered granite.

SOIL SAMPLES AND TEST PROCEDURES

The three coreholes were obtained in the vicinity of Clearwater Bay Road Development III, Kowloon. Soil samples were obtained both in the colluvium and in the weathered granite, with the latter showing the various stages of weathering ranging from completely weathered near the top to a highly weathered zone near the bottom of the corehole profile. The samples taken were 7.6 cm in diameter with lengths varying between 0.3 and 1 m. The depth of sampling varied from 2 to 20 m as shown in Fig. 1, where the initial on-site description of soil samples is provided together with the blow count.

In addition to the standard classification tests, e.g. grain size analyses, consistency limits, the other kinds of tests conducted

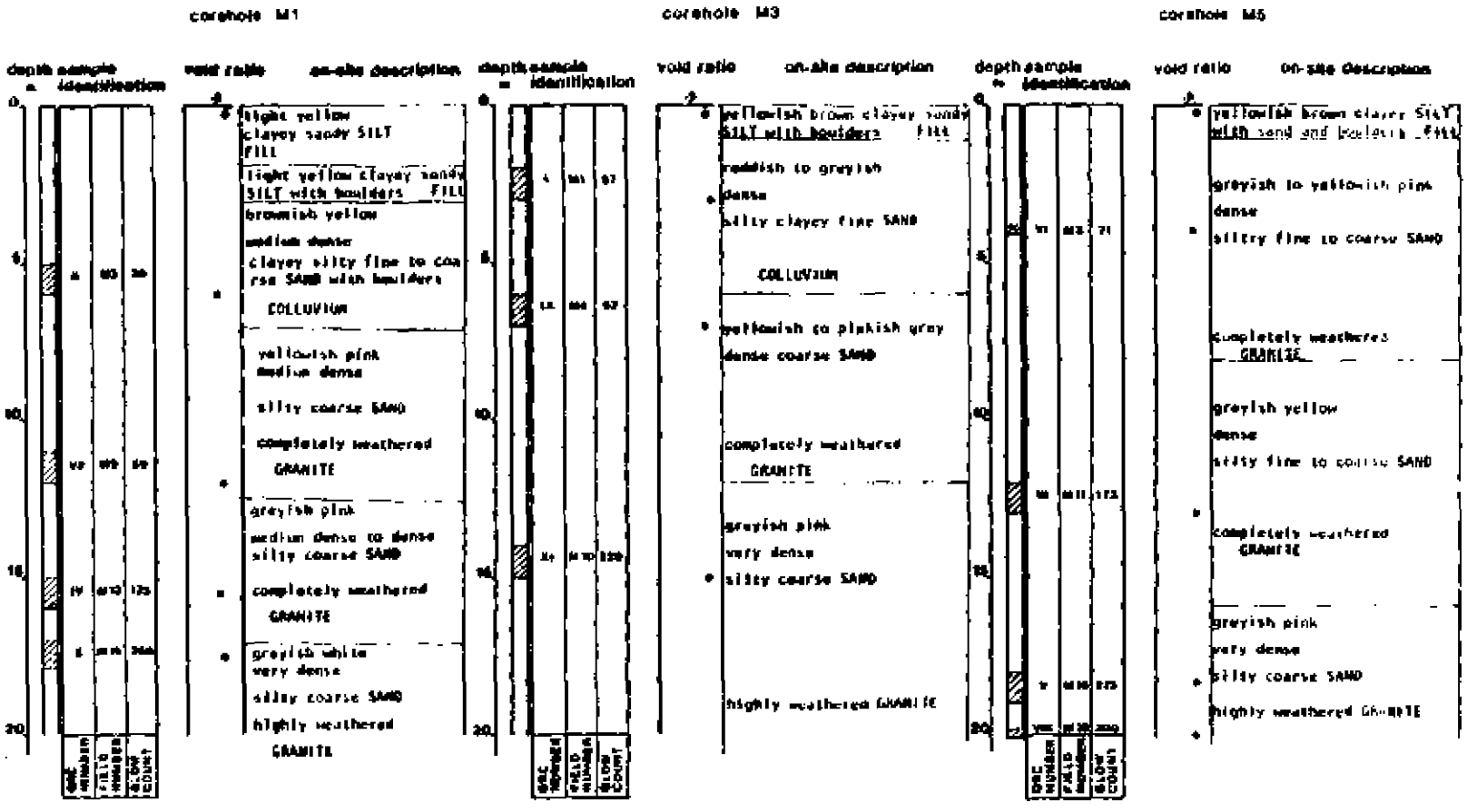

Fig. 1 Depth of Sampling, Sample Identification, Void Ratio and Soil Description for the Three Coreholes

included chemical and mineralogical analyses for determination of the amount of lime removed, organic content, amorphous material content, proportions of clay minerals and chemical analyses of the porewater.

Soil suspensions obtained after amorphous material removal were used for preparation of oriented slides for mineralogical analyses. X-ray diffractograms were obtained and the peak heights for the various minerals compared to those of standard minerals. With such a method, an approximation of the quantities of the specific minerals present in the soils may be obtained. It is necessary to note at this time that because of the high coarse fraction content, mineralogical analyses were only conducted on the fine fractions of the soil samples, and hence the data presented in the results concerned with mineralogy refer only the the fine fraction minerals.

In the procedure used for removal of lime ($CaCO_3$) the soil samples were ground and mixed with sodium acetate, and subsequently heated to 100°C. This resulted in a mixture with a pH = 5. The mixture was then centrifuged and decanted, and analyses made for the calcium and magnesium contents.

The soil samples were treated with hydrogen peroxide for removal of organic material. The dry weight before and after treatment with hydrogen peroxide was indicative of the amount of organic material removed.

The procedure followed for determination of amorphous content in the soil samples was similar to the one reported previously by Yong et al (1979). This pH-dependent dissolution technique has been previously developed by Segalen (1968) for application to tropical soils. In this technique, pH of the soil is decreased with the addition of 8N HCl solution, at which time iron and alumina are dissolved. Subsequently, the pH is increased with the addition of 0.5N NaOH solution which in turn will dissolve silica and alumina. To apply this alternate pH cycling for dissolution of the specific amorphous components, the soil samples are ovendried and treated at room temperature in the cold state with the HCl solution for 20 minutes to allow for dissolution of alumina and iron. Following this, the excess hydrochloric solution is removed by washing and centrifugation of the sample with water. This is followed by the addition of the NaOH and subsequent placement of the samples in a hot water bath for five minutes to permit dissolution of silica and alumina. This alternate washing with HCl and NaOH constitutes one cycle. This cycle is repeated eight times for the same soil sample, and has been found to be effective in the extraction of amorphous materials - e.g. Yong et al (1979).

In the procedures used for porewater analyses, the porewater was extracted from the soil samples using the saturation extract method. Subsequently, the porewater was then analyzed for cations (Na, K, Ca, Mg) and anions (CO_3, HCO_3, Cl, SO_4).

In addition to these characterization tests, soil suction measurements were made using the pressure membrane technique. The

samples were allowed to take in water at pF* = 0 initially, prior to desorption to a pF value of 7. Following this, the samples were then allowed to adsorb in the rewetting part of the soil suction tests. Whilst attempts were made to measure volume change at various stages of desorption-adsorption, it should be recorded that no measurable volume changes were observed.

To better understand and to develop a wider base of appreciation of the various components interacting to provide the entire make-up of the soil, scanning electron microscopy was used for visual examination of the soils. By and large, this was confined to those soil samples which contained the fine material and which allowed for separation of the material into finer quantities.

RESULTS AND DISCUSSION

The particle size grading tests obtained from the results of the particle size distribution tests for all the samples, using the same sample identification numbering scheme as in Fig. 1, are shown in Table I. In the Table, the D_{75}, D_{50}, and D_{25}, i.e. diameters for the 75%, 50% and 25% soil fraction, are shown with the median, deviation, and skewness of the distributed curves. For proper individual particle separation - because of the suspicion that the amorphous material present in the soil might contribute to aggregate particle groupings which would not be easy to disintegrate - samples were mixed with sodium bicarbonate and shaken for 15 minutes before final agitation in an ultrasonic cleaner for another 15 minutes. Following this agitation, the mixture was washed through a 53 micron sieve in order to separate the fine fraction from the coarser fraction.

If one uses the more standard procedure for grain size analysis, it will be seen that the resulting particle size distribution when compared to a Gaussian distribution will appear to be smaller than that which should be obtained from these kinds of samples. Apparently part of the clay fraction appears as silt-sized particles because of the aggregative bonding established between the particles. To confirm this suspicion, the cementing agents were removed, using the chemical treatment method (DCB method) described by Mehra and Jackson (1960). The resultant particle size distributions obtained were subsequently analysed and the values shown in Table I. The skewness, deviation and median were calculated according to - median $Md = \log D_{50}$, deviation $Dv = \frac{1}{2} \log (D_{75}/D_{25})$, skewnness $Sk = \frac{1}{2} \log ((D_{75}/D_{50})/(D_{50}/D_{25}))$

Results from Table I can be plotted in the Md-Dv field as shown in Fig. 2, which according to Lumb (1965) shows that Samples 11 to

---

* Soil suction values are generally expressed on a pF scale. The log of soil suction expressed in centimeters of water is defined as pF, in analogy to pH. A pF of zero for example indicates that the height of a column of water which the soil suction would support is one centimeter.

TABLE I Particle Size Distribution

Sample	D_{75} (mm)	D_{50} (mm)	D_{25} (mm)	Md	Dv	Sk
I	.11	0.004	0.0006	-2.398	1.132	0.308
II	2.00	0.660	0.070	-0.180	0.728	-0.246
III	1.75	0.650	0.098	-0.187	0.625	-0.196
IV	1.85	0.800	0.115	-0.097	0.603	-0.239
V	1.70	0.980	0.200	-0.009	0.465	-0.225
VI	1.50	0.360	0.031	-0.444	0.842	-0.223
VII	2.50	1.150	0.270	0.061	0.483	-0.146
VIII	2.05	1.000	0.200	0.000	0.505	-0.194
IX	2.35	1.150	0.390	0.061	0.390	-0.080
X	2.55	0.950	0.165	-0.022	0.594	-0.166
XI	2.00	0.580	0.038	-0.237	0.861	-0.323

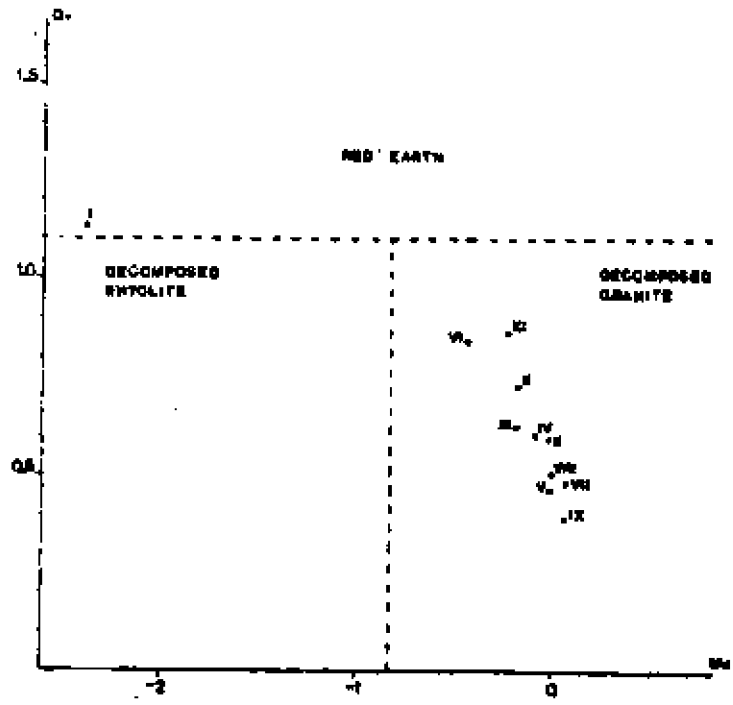

Fig. 2 Soil Classification on Grain Size (according to Lumb, 1965)

XI can be classified from this plot as decomposed granite, whilst Sample I can be classified as red earth. This confirms the initial visual classification shown in Fig. 1.

Figure 3a shows the water content distribution for the soil samples as indicated in the corehole profiles. Superposed on the diagrams are the degree of saturation in the natural state and the water content at saturation point. Note that the saturation point water contents for remoulded soil samples were experimentally measured, and may not accord with theoretical saturation values calculated on the basis of measurements for initial partial saturation void ratios, densities and specific gravities. One of the reasons for any perceived differences may lie in the presence of entrapped air in discontinuous void spaces and aggregate groups, since no attempt is made at this point to disaggregate all the peds or fabric units. The entrapment of air in aggregate units is sometimes encountered in experimental soil saturation techniques using simple water uptake procedures for preparation of saturation extract samples.

The data in Fig. 3a shows that the saturation water content for the remoulded samples appears to become relatively constant in the lower part of the corehole profiles - indicative of the results shown in the distribution of the clay content for each corehole - i.e. D_{25}* for each corehole. Thus, for example, for Samples V and VIII, the D_{25} values are identical, and the D_{25} values for Samples VII, IV and X for corehole MI are of the same order of magnitude.

The calcium and magnesium content together with the organics content superposed are shown in Fig. 3b, and the porewater analyses are shown in Fig. 3c, where the distributions for calcium, sodium, potassium and magnesium in the porewater are shown in the depth profile. The mineralogy and amorphous content distributions are shown in Table 2. It is noted that the amorphous content, even in the small proportions shown, can exercise a significant role in the control of water retention and uptake - as will be shown later.

The soil suction curves shown for the samples from the three coreholes are given in Figs. 4 to 6. Of particular interest are those samples which show measurable differences in adsorption-desorption performances. To provide a better view of these differences Figs. 7 and 8 gather together the soil suction curves for Samples X, V, and VIII (Fig. 7), and Samples I and VI (Fig. 8).

In gathering the two representative groupings of soil suction curves, the intent is to show not necessarily the amorphous content influence, but also to highlight the importance of both the

---

*Note that the D_{25} criterion, i.e. effective maximum diameter of soil particles for the 25% fraction of soil in the sample tested, is a very useful method for quick assessment of the grain size proportion of the soil. If D_{25} is very small, i.e. in the clay size range, the clay content is obviously significant.

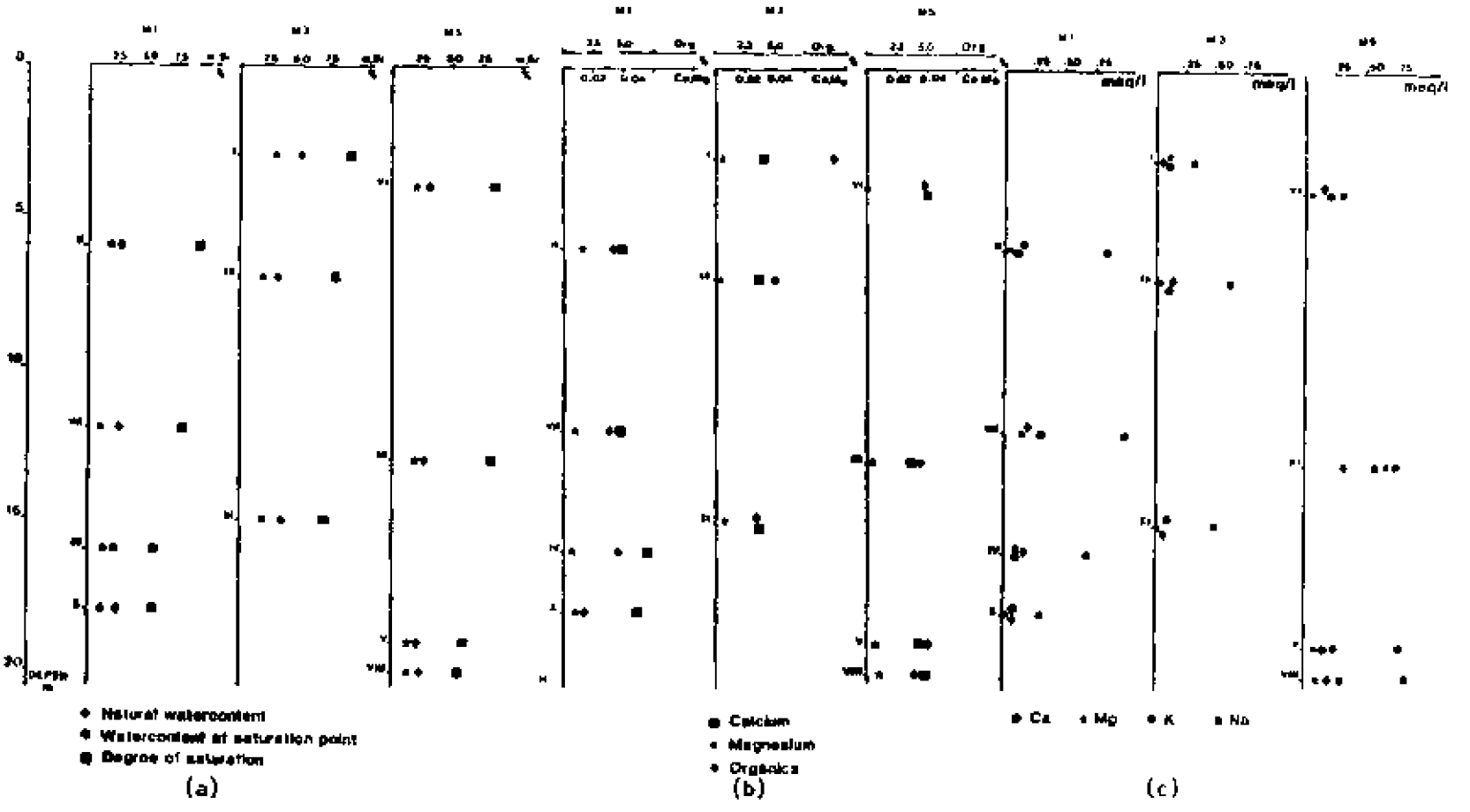

Fig. 3 Water Content, Degree of Saturation, Calcium and Magnesium Contents (derived from lime removal), Organic Content in % of Ovendry Weight and Cation Concentration of Porewater in meq/l Versus Depth for the Three Coreholes

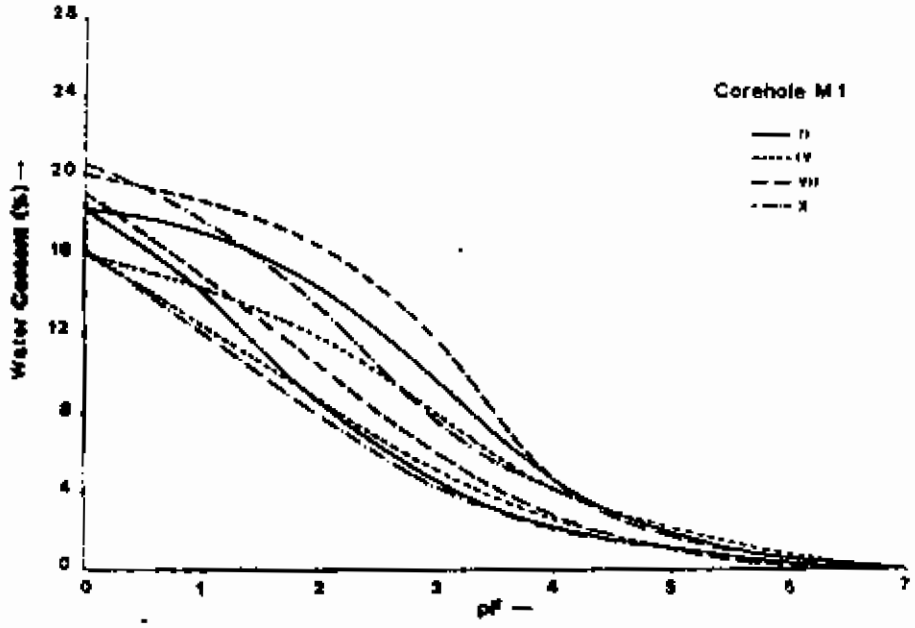

Fig. 4 Soilwater Potential Curves for Samples from Corehole M1

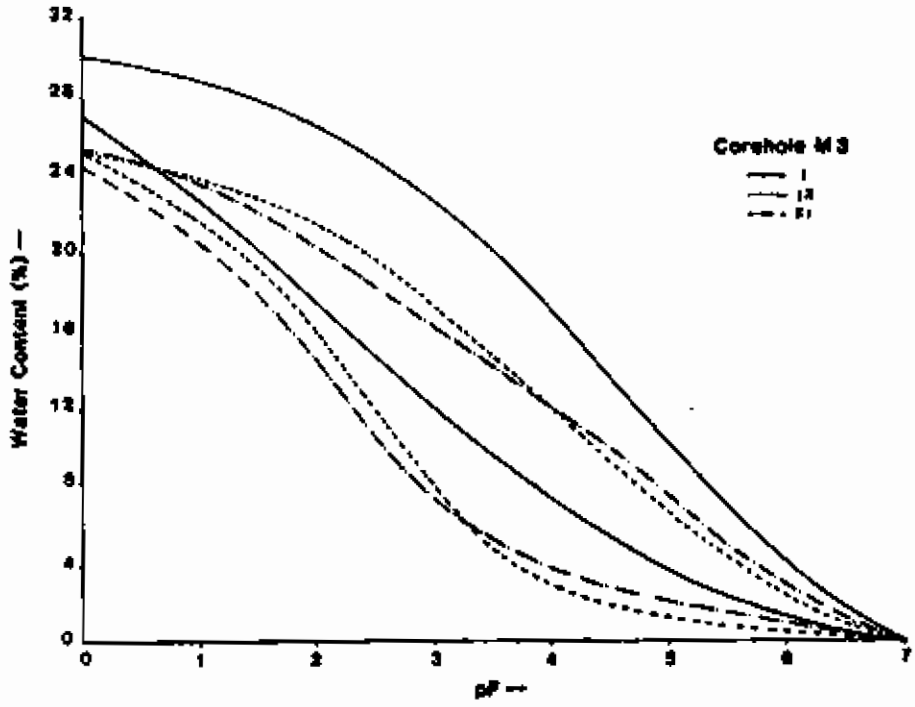

Fig. 5 Soilwater Potential Curves for Samples from Corehole M3

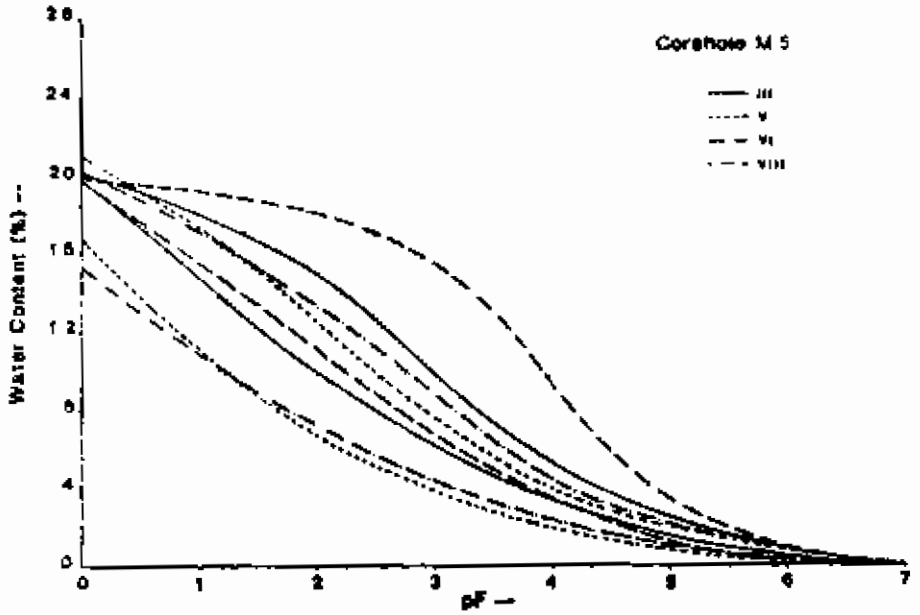

Fig. 6 Soilwater Potential Curves for Samples from Corehole M5

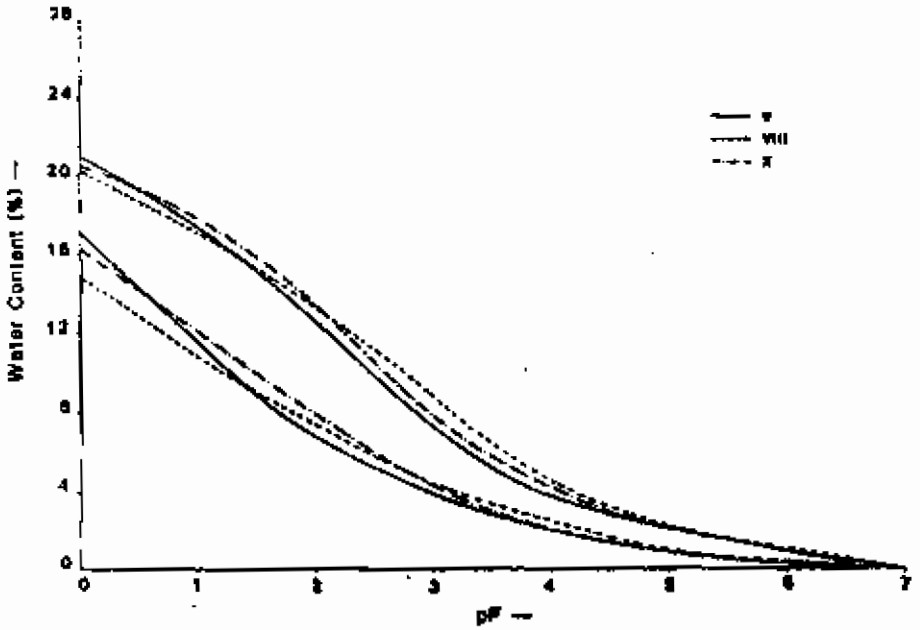

Fig. 7 Soilwater Potential Curves for Samples V, VIII and X

TABLE 2 MINERALOGY AND AMORPHOUS CONTENT DISTRIBUTIONS

		MINERALOGY AND AMORPHOUS MATERIAL CONTENT										
	Corehole	M1				M3			M5			
	Depth (m)	6	12	16	18	3	7	15	4	13	19	20
	Sample No.	II	VII	IV	X	I	IX	XI	VI	III	V	VIII
MINERALOGY*												
Kaolinite		95	84	86	41	64	49	25	97	90	75	97
Mica		1	1	1	25	2	31	39	0	1	1	1
Quartz		4	7	12	22	32	13	31	2	8	23	-
Microcline		-	1	1	3	1	6	5	1	2	1	-
Albite		-	7	1	7	1	-	-	-	-	1	2
AMORPHOUS MATERIAL CONTENT**												
Fe_2O_3		0.23	-	0.65	0.89	1.38	0.74	0.44	1.34	0.64	1.01	0.27
Al_2O_3		-	-	-	-	-	-	-	-	-	-	-
SiO_2		-	0.14	0.12	-	-	-	-	-	-	0.2	0.34

* The presence of each mineral is expressed as a percentage of the total amount of minerals present in the fine fractions of the soil samples.

** The amorphous material content is expressed as a percentage of ovendry weight.

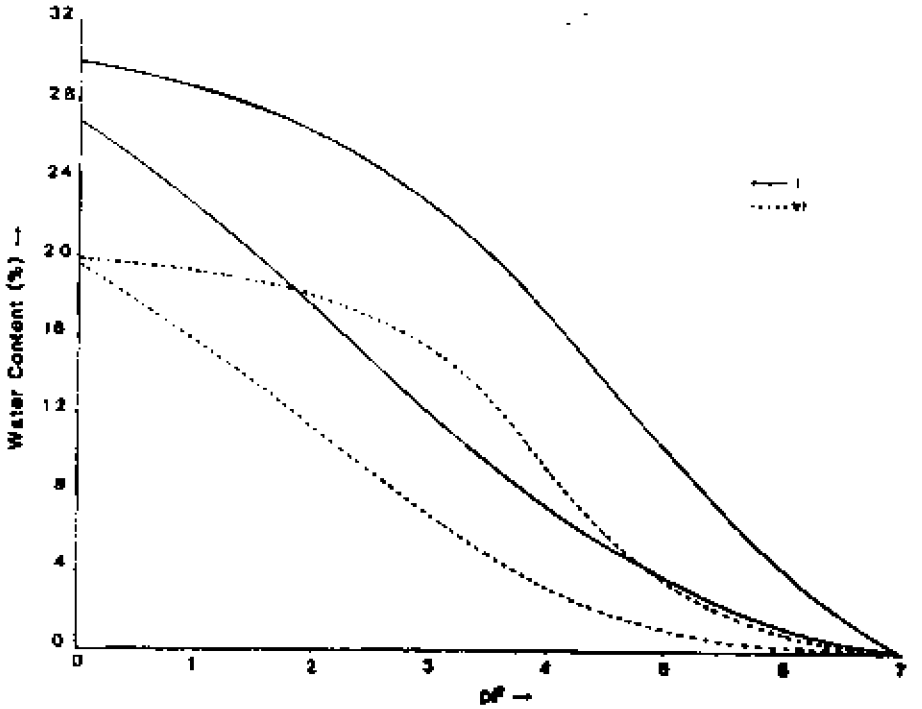

Fig. 8 Soilwater Potential Curves for Samples I and VI

fineness of the fines content (D_{25}) and the percentage of fines. Thus, for example, whilst the amorphous material content for both Samples I and VI are almost identical, the diameter values shown for D_{25} show that this D_{25} diameter is indeed very small. The D_{25} fineness plus the higher percentage of fines for Sample I in contrast to Sample VI is reflected in the contrasting deviation and skewness of Samples I and VI. The soil suction curve for Sample I reflects the material characteristic not only in terms of initial water content, but also in the desorption/absorption characteristics of the material. It should be noted that this is material from the colluvium and not from the weathered granite, as shown also by the data indicated in Fig. 2, and drawn according to Lumb's classification technique. The electron micrographs for the typical samples show that where the amorphous presence is high, the crystallinity of the mineral particles cannot be easily discerned. The amorphous material appears to coat the larger size particles.

The significance of the presence of clay, silt and amorphous materials in the soil suction performance of the soils tested can be discussed in view of the model initially proposed by Yong and Sethi (1977) for clays with a high amorphous content. The results of this study indicate that the basic model can be adapted for the soils studied herein to account for the much lower amorphous content but higher coarse fraction availability. The presence of the high coarse fraction plus proportionately much lower clay and amorphous material contents suggest that the coarse fractions such as gravel and sand are coated with some clay and some amorphous material. Additionally, it would

not be unlikely for clay particles to form aggregate groups (peds) with the amorphous material as bonding agents. To illustrate the model suggested by the results obtained it is necessary to develop a 3-part, or 3-zone adsorption/desorption mechanism model - Fig. 9a.

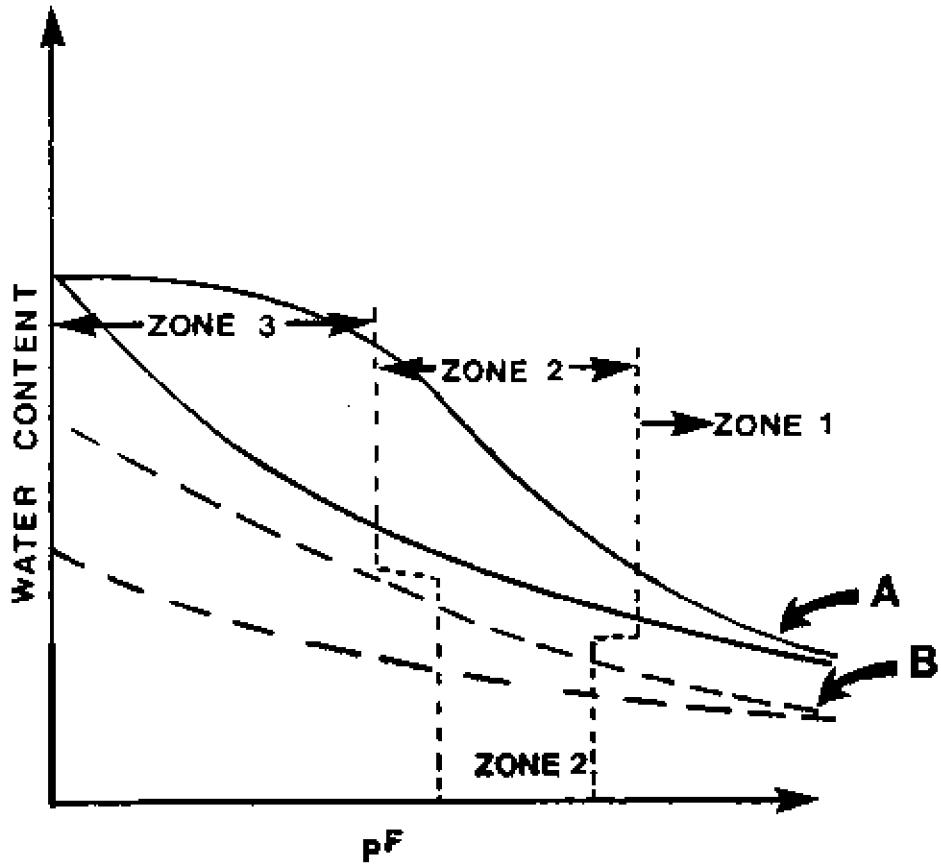

Fig. 9a Typical 3-Zone Desorption/Adsorption Curves - with "Ink Bottle" Effect (Curve A) and Without "Ink Bottle" Effect (Curve B).

In the typical desorption/adsorption curve shown in Fig. 9a as Curve A, the classic ink-bottle effect* is shown as typified in Zone 2. The suction performance is indicative of a uniformly dispersed "uniform" size particle system somewhat similar to silt, where the

* In a series of interconnected pores, the diameter of the pores at mid-points are larger than the necks of the pores. Thus in dry or emptying the points, the water contents reached will not be the same as in the wetting process - bearing in mind the different pore diameters. This is the classic ink bottle effect, i.e. where the neck diameter is smaller than the main pore space. Thus in emptying the smallest diameter will control whilst in wetting the larger diameter will control. This will result in hysteresis. See Fig. 9b and Yong, R.N. and Warkentin, B.P. (1975), Chap. 4,

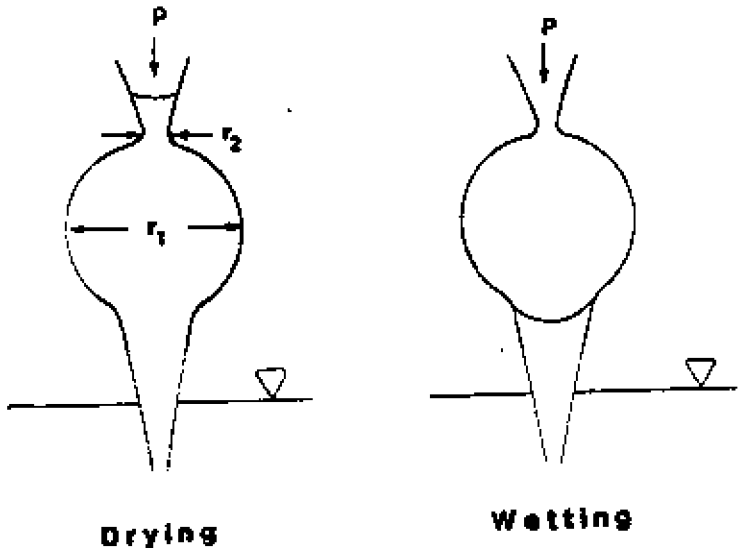

Fig. 9b Hysteresis in Soils Due to Drying and Wetting

adsorption-desorption curves deviate significantly in Zones 2 and 3 as testimony to the "ink-bottle" effect. Note that this applies to Samples I and VI. In the model suggested where the amorphous material would tend to form bonding between clay particles, creating aggregate groups (peds) - it is not uncharacteristic for these peds to be more or less similar in size to the silt particles, thus producing in essence a seemingly uniform-sized soil particle system. Note that the presence of peds was indicated in the tests for grain size distribution as observed earlier.

Water uptake in Zone 1 can be identified with vapour phase phenomena whilst water uptake in Zones 2 and 3 are associated with capillary action in view of the micro-pores and macro-pores respectively. The greater or lesser presence of micro-pores will highlight the greater or lesser "ink-bottle" effect. With the likelihood of ped formation as in Samples I and VI, the deviations between adsorption-desorption performances in Zones 2 and 3 can be quite pronounced.

In the case of Curve B, Zone 2 adsorption-desorption deviation is indeed weak. This is typical of a soil system where particle size distribution does not develop much "ink-bottle" effect in rewetting - i.e. pore size distribution is "well-graded". Samples V, VIII and X shown in Fig. 7 are somewhat similar to Curve B in Fig. 9a. To a greater or lesser extent, all the other samples show suction characteristics not unlike that of Curve A. The Curve B mechanism identified indicates water uptake initially by the clay particles as coating material (plus some minor individual clay particles), followed by micro-pore water uptake. At this time, a little "ink-bottle" effect is apparent for most of the samples in this grouping, but to a considerably lesser extent in comparison to Samples I and VI. The final phase of water uptake is through capillary action identified in Zone 3 - through the macro-pores.

To apply the model further, the soil suction curves for the various samples are analyzed to show the differences in water content for adsorption-desorption as a function of pF. The results are shown in Fig. 10. The curves representing Samples I, II, III, IV, VI, VII, IX and XI are typical of the type of suction performance shown by Curve A in Fig. 9a. The curves representing Samples V, VIII and X in Fig. 10 correspond to the type of suction performance shown by Curve B in Fig. 9a. Note that the "ink-bottle" effect in the curves corresponding to type A in Fig. 10 occurs at about pF3. The clay contents for type A vary from 1.8% to 39.5%, and for type B from 1.7% to 2.1%.

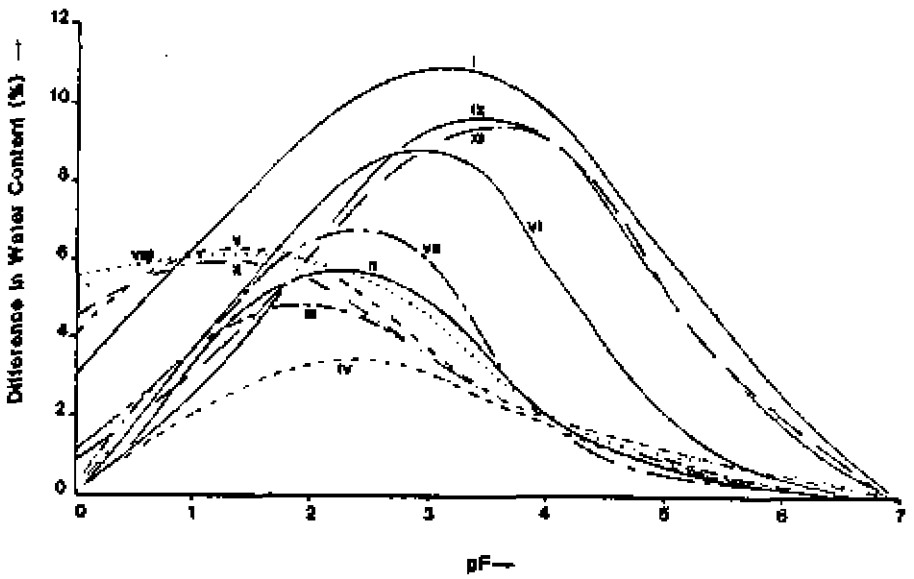

Fig. 10 Difference in Water Content for Adsorption-Desorption as a Function of pF for Samples From the Three Coreholes

The various proportions of clay present can indeed form coatings around the gravel and sand - as shown in Tables 3a and 3b, where surface area measurements for soils have been shown. In the procedure used for the four soil samples studied, (i.e. I, II, VI and VII) the surface area was determined for each sample in its natural state, and also for the various fractions obtained separately from particle size distribution determination. In addition, measurements were also made for soil samples obtained after lime and organics removal. Surface area measurements were made using the EGME (ethylene glycol monoethyl ether) method described by Carter et al (1965). Because of the fact that the measured surface area for the coarse fractions far exceeded the theoretically calculated values for "equivalent" sized spheres, the coarse fractions of some of the samples were "cleaned" using DCB-method and sodium hydroxide treatment. In doing so, coatings of clay and amorphous material would be removed, leading perhaps to a closer accord between measured and calculated surface area of the coarse particles. After this "cleaning" procedure, a substantial reduction in

surface area was observed, but this still far exceeded ideal spherical particle computed surface areas. This is to be expected since the coarse fractions were indeed highly angular totally "non-spherical!".

From the results shown, it is evident that the coarse particles were indeed coated by the clay particles, and also by some amorphous materials. The differences in measured surface areas, both before and after cleaning are testimony to the coating model. Thus the principal of this method is that EGME forms a monomolecular layer on soil particles. Since the amount of EGME needed to cover 1 m^2 of soil particle surface is known (i.e. 2.86 x 10^{-4}g EGME per m^2 of surface), the surface area of the soils can be calculated from the difference in weight of the sample with and without the EGME coating. With the seemingly small amount of clay present, a judicious placement of the clay can indeed affect soil performance considerably. Note that, except for Sample VII, the surface area of the clay particles far exceeds the combined surface area of the gravel and sand. (See Table 3b). Thus, there are sufficient clay particles to coat the larger particles, plus leftover clay particles to form peds with amorphous bonding.

CONCLUSIONS

In this first stage of soil compositional control study for a particular residual soil, attention has focussed on two particular aspects of the problem, i.e. the presence and amount of amorphous material and clay in the soil, and the manner in which these are distributed in the soil. By and large, because of the granular nature of the soil and the low amounts of clay fines and amorphous materials in contrast to the amount of total soil material, it is clear that the degree of saturation is important in the response behaviour of the soil material. It is indeed significant to observe that because of the low amounts of clay fines and amorphous material, any small change in the water content of the material would play a large part in changing the overall mechanical behaviour of the soil - especially if the material forms clay coating and aggregate groups. If the residual soil had a much higher clay fines and amorphous material content, small changes in the water content would not be as significant in the control of corresponding changes in the chemical properties.

The first phase of this study has indeed demonstrated through the characteristic soil suction curves that because of the small changes in water content, no real changes in volume can be measured. However, this does not necessarily indicate that the mechanical properties of the material would not be considerably influenced because of these small changes. In actual fact, the results demonstrate through the shapes of the soil suction curves that a one or two percent overall content difference in the clay fines or amorphous material would serve to dramatically increase or decrease the rate of water uptake - as shown by the adsorption-desorption part of the soil suction curve.

In the continuing study, the shear strengths of the soils are examined in relation to the various stages of water uptake and

TABLE 3a Specific Surface Area in m^2/g for Various Fractions of Samples I, II, VI and VII.

	Sample Number			
	I	II	VI	VII
Total sample, natural state	51.98	12.81	13.84	8.33
Gravel	14.93	1.12	0.70	0.88
Gravel, 'cleaned'	2.15	0.57		
Coarse sand	13.14	2.84	1.33	2.19
Coarse sand 'cleaned'	4.50	2.49		
Medium fine sand	6.57	5.52	2.37	14.23
Fine Sand	9.80	12.31	5.35	14.90
Silt	14.80	32.41	26.38	27.54
Clay	120.42	67.40	55.45	138.21
Total sample, after lime and organics removal	47.07	9.67	10.85	7.06

NOTE: In order to compare the surface area of the total sample to the sum of the surface areas of the constituting fractions, the latter should be added up proportionately to their presence in the total sample (as indicated by the particle size distribution).

TABLE 3b Comparison of Surface Area in m^2 for the Combined Gravel and Sand Fraction Versus Clay Fraction, as Present in 100 g of Total Soil Material*

	Sample Number			
	I	II	VI	VII
Gravel + Sand Fraction	317.04	21.78	120.86	210.98
Clay Fraction	4756.59	308.64	560.04	343.43

* Computed from particle size distribution and specific surface area, as indicated in Table 3a.

relationships describing the rate of water uptake and corresponding changes in the material properties will be shown.

ACKNOWLEDGEMENTS

The input and assistance provided by Dr. A.J. Sethi is acknowledged by the authors. This study is part of the overall study on compositional control of soils undertaken at McGill University, under grant financing from the Natural Sciences and Engineering Research Council of Canada, Grant No. A-882.

REFERENCES

1. Carter, D.L., Heilman, M.D., and Gonzalex, C.L. (1965) Ethylene Glycol Monoethyl Ether for Determining Surface Area of Silicate Minerals. Soil Science, Vol. 100, No. 5, pp.356-360.

2. Lumb, P. (1965) The Residual Soils of Hong Kong. Geotechnique, No. 15, pp. 181-194.

3. Mehra, O.P. and Jackson, M.L. (1960) Iron Oxide Removal from Soils and Clays and Clay Minerals, No. 7, pp. 317-327.

4 Segalen, P. (1968) Note sur une méthode de détermination des produits minéraux amorphes dans certain soils à hydroxides tropicaux. Cahier ORSTOM, Série Pedologie, No. 6, pp. 105-126.

5. Yong, R.N., Sethi, A.J. and LaRochelle, P. (1979) Significance of Amorphous Material Relative to Sensitivity in Some Champlain Clays. Canadian Geotechnical Journal, No. 16, pp. 511-520.

6. Yong, R.N. and Sethi, A.J. (1977) Influence of Amorphous Material on Soil Performance and Its Relation to Environmental Weathering. Proceedings, Specialty Session on Geotechnical Engineering and Environmental Control, Tokyo.

7. Yong, R.N. and Warkentin, B.P. (1975) Soil Properties and Behaviour, Chapter 4. Elsevier Scientific Publishing Company, Amsterdam.

ANALYSES OF HONG KONG RESIDUAL SOIL SLOPES

by

Prapote Boonsinsuk, and Raymond N. Yong

prepared for

ASCE SPECIALTY CONFERENCE

Engineering and Construction in Tropical and Residual Soils

Honolulu, Hawaii

11-14 January 1982

ANALYSES OF HONG KONG RESIDUAL SOIL SLOPES

by

Prapote Boonsinsuk[1], M.ASCE and Raymond N. Yong[2], M.ASCE

ABSTRACT

The current procedures for designing cut slopes in Hong Kong residual soils are reviewed. It is evident that the stability of slope in such soils is predominantly governed by the strength of partially-saturated soils and the effect of rainwater infiltration. The shortcomings of the design approaches adopted at present appear to be the lack of an appropriate constitutive relationship for the unsaturated soils and an analytical model for evaluating slope stability which properly accounts for rainfall intensity.

A suitable method for analysing and/or designing cut slopes in residual soils which undergo high annual rates of rainfall is outlined. This can be achieved by assessing the intensity of rainfall which will affect slope stability. Such a consideration should lead to a better design procedure for slopes formed in residual soils.

INTRODUCTION

Slope failures in Hong Kong residual soils occur frequently during the wet season (from May to September) in which the average annual rainfall is about 80 in (2000 mm) with the highest recorded daily rate of about 21 in (530 mm). One of the most common types is in the form of mudslides carrying loose fill or in-situ soil, often with rock boulders, downslope at high speeds during periods of heavy rain. The other type of equal significance is failure of cut slopes and natural slopes characterized by shallow slip surfaces extending to depths of approximately 10 to 20 ft (3 to 6 m). The consequences of such failures can be disastrous to human lives and properties especially when these events occur within highly populated areas. One of the most

---

[1] Research Associate, Geotechnical Research Centre, McGill University, Montreal, Canada; formerly Geotechnical Engineer, Scott Wilson Kirkpatrick & Partners, Hong Kong.

[2] Director, Geotechnical Research Centre, and William Scott Professor of Civil Engineering and Applied Mechanics, McGill University, Montreal, Canada.

severe landslides experienced in Hong Kong was in June 1972 in which more than a hundred people were killed and several roads and buildings were badly damaged (Hong Kong Government, 1972).

To prevent disastrous slope failures, the Hong Kong Government commissioned a detailed study on the landslide potential of the existing slopes (Beattie and Attewill, 1977) and introduced new regulations which required comprehensive ground investigation and proper design under the supervision of specialized geotechnical engineers for all major site developments. Reports on site investigation and proposals for site formation have to be checked by the Government. In order to outline the basic approach in slope design, the Hong Kong Government published the 'Geotechnical Manual for Slopes' in November 1979 which provides general design procedures for local soil conditions. However, the problem of identification of the actual mechanism of slope failure has yet to be solved. This problem is indeed important and needs to be solved since many steep slopes standing at considerable heights have survived years of heavy rainfall whilst others have failed. Without such an understanding of slope failure mechanics, it is apparent that only conservative design approaches will be adopted by prudent designers, resulting thereby in extensive precautionary design measures, e.g. cutting at flat angles, installing anchors, building retaining walls, etc.

Needless to say, there are several schools of thought regarding the mode of failure and strength parameters currently used for slope design in Hong Kong. The various differences often lead to lengthy discussions between the checking authority and the designer, on the choice or use of the proper design criteria, sometimes to such an extent that a complete re-design is necessary.

The concepts underlying design of cut slopes in in-situ residual soils generally adopted in Hong Kong will be presented herein to identify the problems encountered. Possible amendments to improve the current design consideration will be discussed.

GENERAL SOIL PROPERTIES

The abundant residual soils forming the natural slopes of Hong Kong are the products of in-situ decomposition of the parent rocks by the processes of weathering which have been relatively active due to the sub-tropical climate, high temperatures and heavy seasonal rains. The thickness of the residual soil mantle varies extensively and can be as deep as 200 ft (60 m). Along the lower parts of steep natural slopes, the in-situ residual soils are frequently overlain by colluvial (slopewash) material of various thicknesses which were transported downslope by torrential rainstorms. There are two major rock types: granite and volcanics (Fig. 1), both being of igneous origin. The granitic rocks are, in general, widely jointed with joint spacings between 1 ft (300 mm) and 10 ft (3 m) while the volcanic rocks are closely jointed at spacings ranging from 2 in (50 mm) to 1 ft (300 mm). Both rocks vary considerably in composition and colour. The geology of

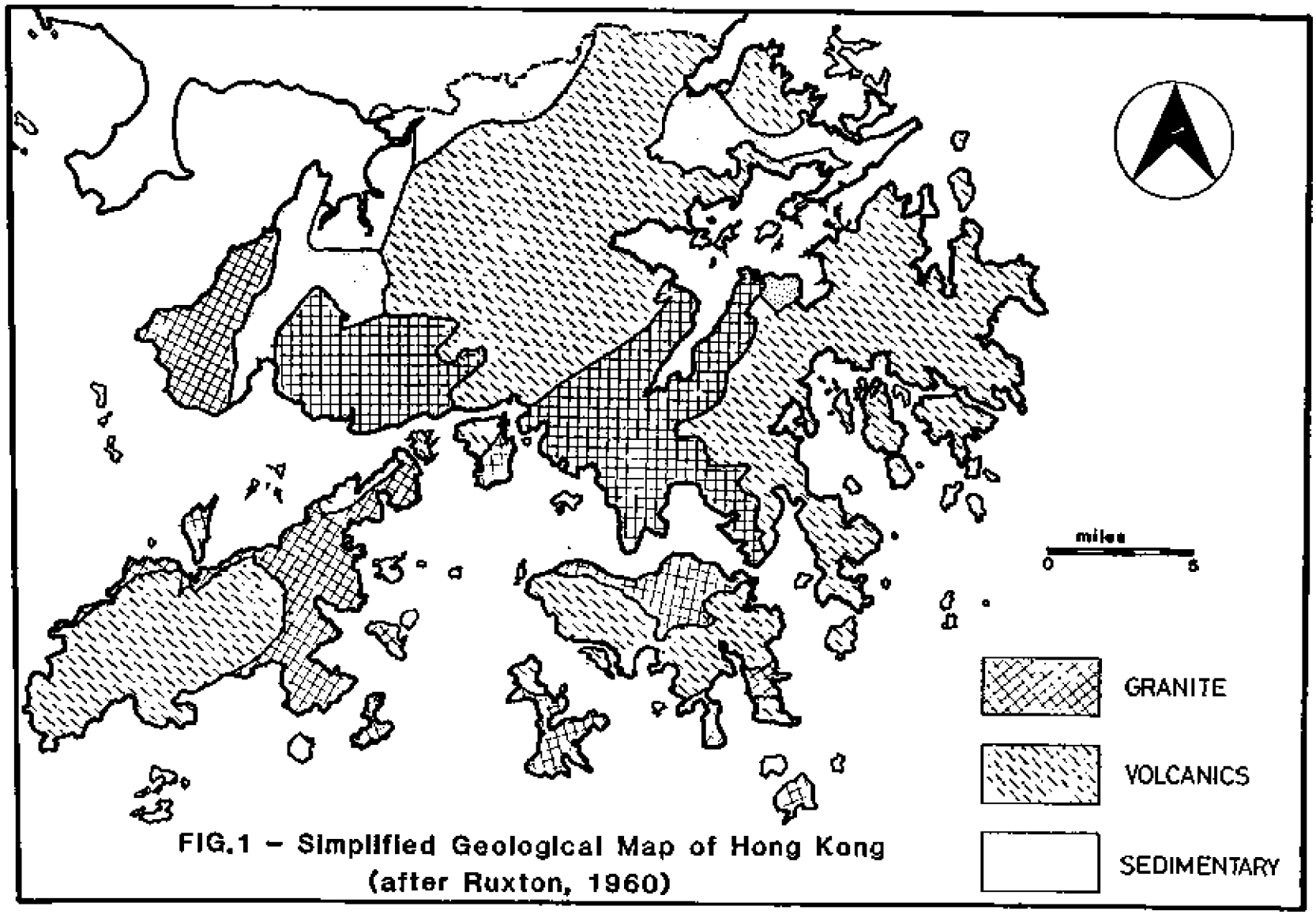

FIG.1 – Simplified Geological Map of Hong Kong
(after Ruxton, 1960)

Hong Kong has been studied in detail by Ruxton (1960) and Allen and Stephens (1971).

The residual soils derived from granitic rocks (decomposed granite) are usually coarse grained (sandy) whilst those from volcanic rocks (decomposed volcanics) are fine grained (silty). When undisturbed, relict joint planes and some fabric of the parent rocks can be identified except in the surface structureless soil. To be specific, the residual soils referred herein include the topsoil, containing no recognizable rock texture, and soil derived from completely decomposed rock, weathered in place, with distinguishable rock texture and relict joints. The major clay mineral resulting from the weathering of both granitic and volcanic rocks is halloysite (Lumb and Lee, 1975). In the natural state, the residual soils are generally unsaturated and the degree of saturation, depending on the seasonal rainfall, varies between 0.7 and 1, occasionally reducing to 0.5 at shallow depths and on exposed surfaces during the dry season.

When unsaturated, most residual soils appear to have a high cohesive strength. This cohesive strength drops to low values or even zero upon full saturation (Lumb, 1965 & 1975). Such a behaviour is considered to be the result of the release of soil suction when the soil begins to take in more water in the wetting process. The measured values of soil suction for undisturbed specimens at about 0.75 degree of saturation, for example, range from pF 3 to pF 4.5 (2 to 60 klp/ft^2 or 100 to 3000 kPa). Lumb notes that the reduction in strength, which seems to be more pronounced in the decomposed volcanics, does not appear to be caused by the collapse of soil structure due to saturation.

The permeability of the decomposed granite obtained from laboratory and field tests has been found to be of the same order, between 3×10^{-5} ft/s (10^{-5} m/s) and 3×10^{-6} ft/s (10^{-6} m/s) with the mean value of about 2.5×10^{-5} ft/s (8×10^{-6} m/s). However, the permeability of the decomposed volcanics exhibits a much higher variation in laboratory and field tests. The mean field value has been calculated to be about 5×10^{-6} ft/s (1.5×10^{-6} m/s) compared to the mean laboratory value of about 6×10^{-8} ft/s (2×10^{-8} m/s) which demonstrates the important role of joint planes on permeability in this soil. Detailed properties of the in-situ residual soils of Hong Kong have been studied earlier by Lumb (1965 & 1975).

CURRENT DESIGN APPROACHES

The customary approach for analysis and/or design of slopes in Hong Kong residual soils, in general, consists of selection of an appropriate method of stability analysis, evaluation of strength parameters and groundwater interpretation. Different design approaches frequently result in proposals for different stabilization measures, sometimes in total disagreement. The following discussions are aimed at highlighting the design procedures currently adopted and their suitability. At present, for high risk slopes, the minimum factor of safety (F) required is 1.4 in association with a 1 in 10 year return period rainfall and 1.12 with 1 in 1000 year return period.

Method of Slope Stability Analysis - Amongst the numerous methods of slope stability analysis available, the one used most for practical design appears to be the Janbu routine method (Janbu, 1954) using non-circular failure surfaces. Its popularity stems from the fact that it can be easily hand-calculated or programmed in small computers and the non-circular failure surfaces conform to the failure surfaces observed. In order to search and locate the critical slip surface (i.e. the one having the minimum factor of safety), the mathematical equations describing the slip surface configuration, normally circular or log-spiral in shape, can be used to generate a succession of slip surfaces. With the development and ready availability of sophisticated small computers, the entire process of calculation using a substantial number of slip surfaces can be carried out in a relatively short time.

Other methods of slope stability analysis are employed occasionally. For quick preliminary calculations, simplified stability charts often provide useful results, particularly when groundwater can be incorporated in the analysis, e.g. Hoek's charts (Hoek and Bray, 1977). Since these stability charts cannot account for the effects of layered soil profile, nor complicated slope configuration, their use is therefore unsuitable for detailed design of high slopes. The Bishop simplified method (Bishop, 1954) is sometimes used when circular surfaces with large radii are likely to represent the probable failure surfaces. The variations of strength parameters and groundwater levels in Hong Kong soils are so high that an extremely detailed method such as the method proposed by Morgenstern and Price (1965) is seldom used for routine design.

As stated above, the Janbu routine method is normally employed in practice for slope stability analysis in Hong Kong. However, Janbu's method considers only the moment equilibrium of individual slices but not necessarily for the whole sliding mass. Its use should therefore be limited to elongated shallow slip surfaces, otherwise serious error would arise when the method of analysis is applied to deep slip surfaces (Nonveiller, 1965). Furthermore, a survey on the effectiveness of the 'in house' computer programmes used in slope stability analysis, which has recently been conducted by the Hong Kong Government, reveals that a large discrepancy can occur in the computed factors of safety from different programmes - for the same slope! The main reasons are different methods of programming, data processing and application of the method of slices.

Strength Parameters - The effective stress concept is adopted in all stability analyses so that the physical state of stress in both saturated and unsaturated conditions can be expressed. When fully saturated the effective stress is defined as:

$$\sigma' = \sigma - u \qquad (1)$$

where σ' = effective stress, σ = total normal stress and u = pore water pressure. For partially-saturated soils, Bishop (1959) has proposed the following equation:

$$\sigma' = \sigma - [u_a - \chi(u_a - u_w)] \qquad (2)$$

where u_a = pore air pressure, u_w = pore water pressure and χ = an empirical parameter depending on the degree of saturation. At present, there are no recommended values of χ or any proper expression available for determining the effective stress in the unsaturated soils of Hong Kong. However, when back-analysing some existing steep slopes known to have been stable for a number of years, the factor of safety is often found to be much less than 1.0 which is theoretically incompatible. Whilst one explanation may be because the strength parameters (i.e. the cohesion intercept c' and the angle of internal friction ϕ' in the Mohr-Coulomb failure criterion) obtained with test data from triaxial tests on saturated samples are too low, the other plausible reason could obviously be that present methods of evaluation of partly saturated soil strength are totally inadequate. Since the bulk of the soil mantle is in fact partially saturated, the existence and influence of soil suction in the soil pores cannot be discounted. For simplicity equation 2 is sometimes used as:

$$\sigma' = \sigma - u^* \qquad (3)$$

where u^* is the soil suction (negative value) obtainable by back analysis. The use of the soil suction (u^*) is normally associated with very low values of c'. Whilst this seems logical, a reliable value of soil suction for use in design is not easily sought. The use of back analysis to determine the soil suction implies that the values of soil suction will also depend on the slope and slip surface geometry. This however, is contrary to soil particle interaction knowledge where ample experience and investigation have shown that compositional characteristics, together with soil structure participate in establishing the soil-water potential - i.e. soil suction (Yong and Warkentin, 1975). A case in point is the soil suction study recently conducted on Hong Kong soil showing the effects of composition on soil suction and soil fabric (Yong et al, 1982). At present, the behaviour of the unsaturated residual soils is being investigated both in laboratory and in-situ conditions by the Hong Kong Government and other interested parties.

In present day technique, the strength parameters (c', ϕ') to be used in design are customarily derived from triaxial compression tests on saturated samples using both drained and undrained conditions. Although the undrained situation seems unsuitable for Hong Kong residual soils due to their relatively high permeability, it is sometimes used for comparison with the drained tests. The cohesion intercept (c') evaluated from the drained triaxial tests should be the lower limit and hence conservative for designing the slope angle at one particular height. Soil specimens are obtained mostly by the Mazier sampler (Beattie and Chau, 1976). The results of the triaxial tests are normally grouped according to the dry density, standard penetration resistance and/or the degree of weathering observed in the specimens so that representative strength parameters for each soil stratum can be determined. In this manner, the shear strength tends to increase with depth which represents the actual behaviour since the degree of

weathering decreases with depth. All triaxial test results in terms of effective stress are accumulated in the p'-q diagram from which the strength parameters for design are evaluated, usually by least-squares fitting.

The most pronounced difference in conducting triaxial tests for Hong Kong residual soils is likely to be the single-stage and multi-stage testing procedures. In the single-stage tests, each soil specimen is subject to one assigned loading condition until failure. Several individual soil samples are sheared at different confining pressures to produce test information for interpretation in terms of a Mohr-Coulomb envelope. In the multi-stage tests, each sample is tested to failure at a constant confining pressure similar to the single-stage test, after which, it is reconsolidated under a higher confining pressure and shearing is repeated. A series of 3 different confining pressures acting on each individual sample is normally used. The failure criterion for each stage is controlled by the maximum principal stress ratio (σ_1'/σ_3') which can normally be reached at low strain. Typical stress-strain relationships for multi-stage tests are presented in Fig. 2. In general, there is no sharp peak at low strains and strength at high strain is not determined particularly in the first two stages so as to limit the degree of distortion in the test specimen. The absence of any well-pronounced peak in the stress-strain relationship could imply that bonding between soil particles is relatively low.

The main advantage of the multi-stage test is that an 'identical' sample is tested throughout the three stages whereas three different specimens are used in the single-stage test to obtain the Mohr-Coulomb envelope. The multi-stage test is adopted primarily to overcome the high degree of nonuniformity inherent in Hong Kong residual soils. However, it suffers from the fact that a weak failure plane may develop from the previous stage which will eventually lead to specimen failure along that weak plane, reducing thereby the likelihood of obtaining separate failure points in each stage of test. For residual soils of which the true cohesion, if any, is derived predominantly from the weathering process of its parent rocks, each stage of the multi-stage test will reduce, if not destroy, such cohesion which is unlikely to recover through consolidation. A correction procedure for this phenomenon in the multi-stage test has been proposed by Wong (1978).

Several attempts have been made to clarify the major factors which govern the shear strength behaviour of Hong Kong residual soils. Sweeney and Robertson (1979) have shown that single-stage and multi-stage tests yield similar strength envelopes regardless of whether the confining pressures of the first-stage tests are lower than or equal to in-situ stresses. This is thought to reflect the granular nature of the completely decomposed granite samples tested. Furthermore, tests conducted at the in-situ moisture condition agree well with the test results of laboratory-saturated samples which seems to indicate that the contribution of soil suction to its shear strength is in fact negligible. There is also no significant effect from the sampling procedure between the Mazier and dry percussion techniques.

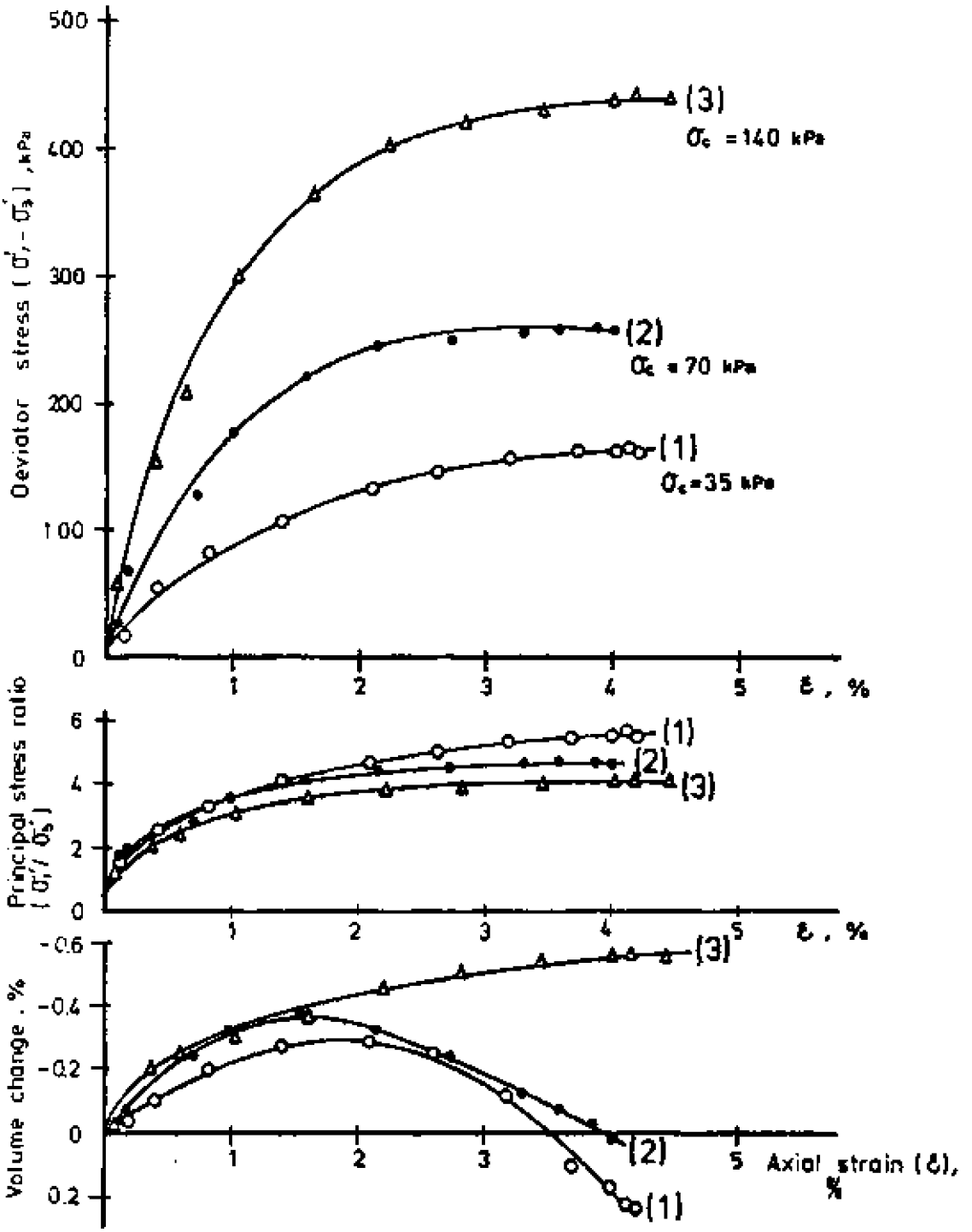

Decomposed Granite , depth 6.0 m . γ_d = 1.454 Mg /m³

Consolidated Drained, with back pressure

C' = 19.5 kPa ϕ' = 34.7°

FIG.2 - Typical Stress-Strain Relationship of Multi-stage Triaxial Test

A typical p'-q diagram presented in Fig. 3 illustrates the results of triaxial tests under various dual conditions, i.e. single and multi-stage, drained and undrained, saturated and unsaturated. The dry densities of the specimens tested were between 94 and 100 lb/ft^3 (1.5 and 1.6 Mg/m^3) with very low plasticity indices. In general, single-stage tests using a small range of confining pressures often yield negative values of cohesion intercept (if derived by the method of least squares) while such a problem seldom arises in multi-stage tests. For shallow slope failure, the stresses within the soil mass are comparatively low and below those used normally in the triaxial tests commercially available. The strength envelope will, therefore, have to be extrapolated in accord with the designer's judgement. Although it is customary to rely on linear extrapolation, some will adjust the value of c' to zero and use soil suction (u^a) instead. Several investigations are being conducted to clarify the shear strength behaviour of Hong Kong residual soils in the low stress range in addition to other factors such as the influence of relic joints, stress relief, etc. It appears from the p'-q diagram in Fig. 3 that different testing procedures seem to have only a slight effect on Hong Kong residual soils.

From the preceding discussion, it is obvious that selection of strength parameters for Hong Kong residual soils depends mainly on "engineering judgement". In order to achieve the required factor of safety of 1.4, a small change in the cohesion intercept or the soil suction can significantly affect the final design. In consequence, sensitivity analyses are often conducted by varying the strength parameters. Such an approach acknowledges the fact that the theoretical factor of safety against slope instability is not an exact value - as specified by current requirements.

Groundwater - Perhaps the design ingredient which is the most difficult to attain is the representative groundwater level to be used in the analysis. Whilst subsoil conditions can be identified by site investigation and strength parameters for design can be found to vary within a narrow range, groundwater can change drastically depending on rainfall intensity/duration and local geological structures. During the dry season, groundwater is often found to be near the interface between the in-situ soil and the bedrock. This level will rise and fluctuate considerably in the wet season. It has been reported that a rise in groundwater level up to 40 ft (12 m) occurred as a result of a tropical storm in one location whilst another piezometer located nearby recorded only a 10 ft (3 m) rise (Sweeney and Robertson, 1979).

As the soil profile is multi-layered in nature as a result of different weathering activities and geological origin, it is possible that a perched water table may exist, particularly during rainfall (Fig. 4). With this in mind, two piezometers will sometimes be installed in the same drillhole but at two different levels near the interfaces between various subsoil strata. It is still difficult, however, to identify a potential impermeable layer within the residual soil mantle since all tested values of permeability (laboratory or field)

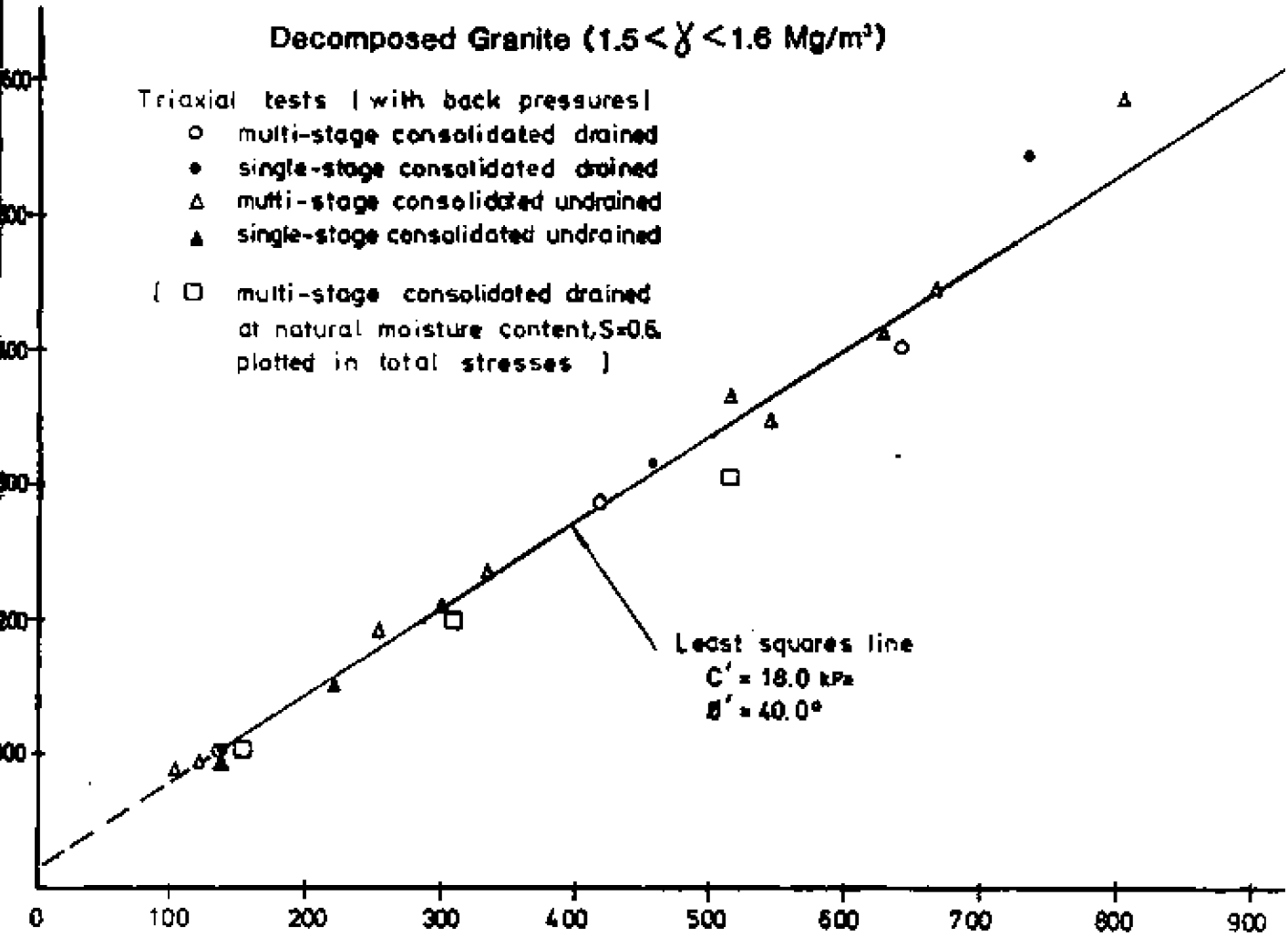

FIG.3 – TYPICAL p'–q diagram $p' = \frac{1}{2}(\sigma_1' + \sigma_3')$, kPa

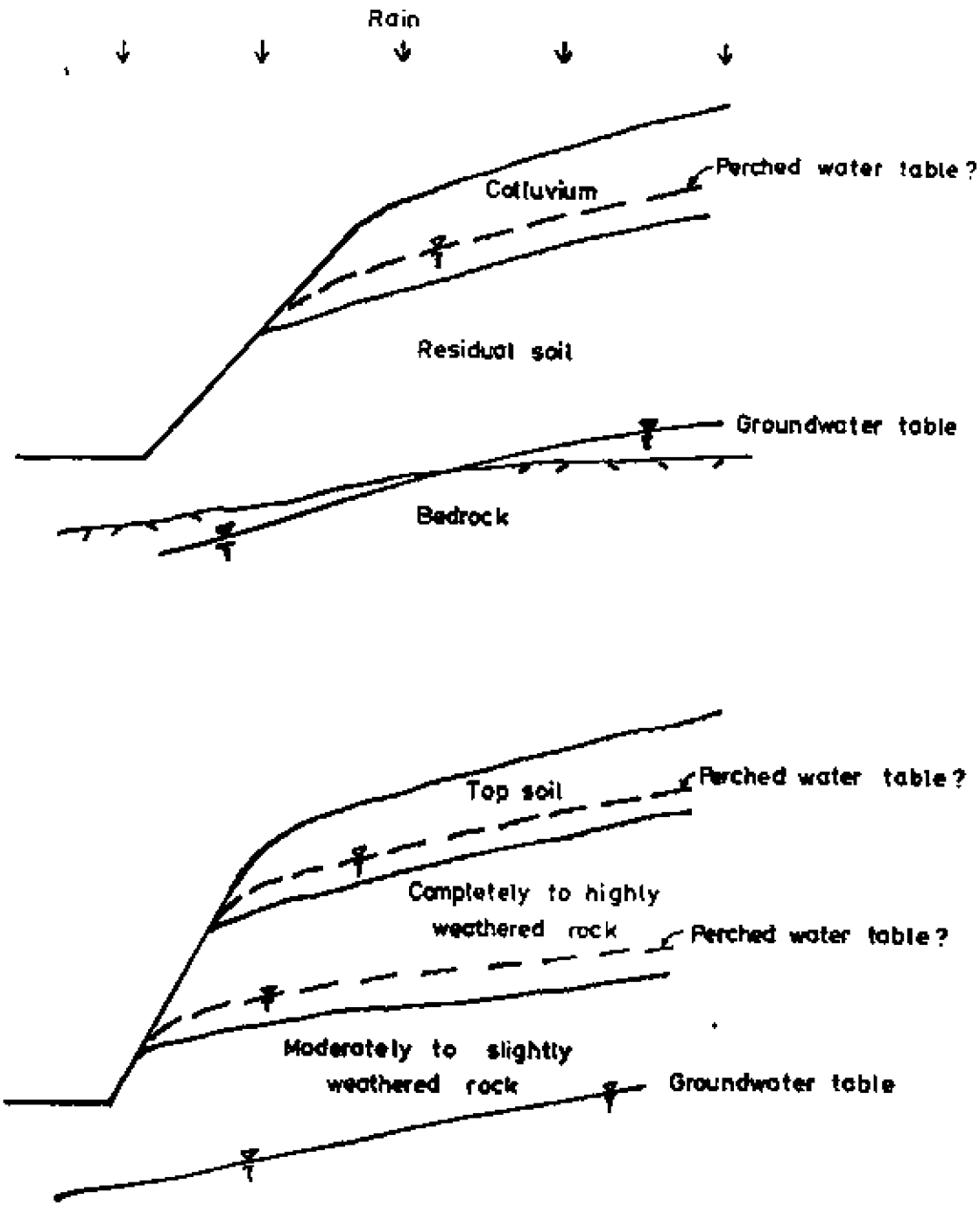

FIG.4 – Probable Occurrence of Perched Water Table

produce results with the same order of magnitude. Consequently the piezometers are monitored closely with special frequent readings during periods of heavy rain. An automatic piezometer-monitoring system is sometimes used to provide continuous readings. In general, any existence of perched groundwater is difficult to prove although slope failure due to the presence of an isolated water table is not uncommon. For safe design, the perched water level is always assumed where appropriate although its hydraulic head is subjective. The groundwater level behind a slope face is sometimes controlled by installing horizontal drains, occasionally with vertical caissons filled with filter material.

Based on general observations that the groundwater table rises during the wet season, it is customary to establish the maximum groundwater level monitored during the wet season as the base level in design. A certain rise is then added in accordance with the statistical rainfall return period required (normally 1 in 10 year and 1 in 1000 year) as recommended by Beattie and Chau (1976).

The amount of such a rise is sometimes assumed to be equal to the depth of the wetting band descending from the existing surface to the base groundwater level. This depth is calculated by the simplified expression proposed by Lumb (1975) as follows:

$$h = \frac{kt}{n(S_f - S_o)} \qquad (4)$$

where h = depth of wetting front, k = coefficient of permeability, n = porosity, S_o = initial degree of saturation, S_f = final degree of saturation, t = duration of rainfall.

The rise in the groundwater level is often assumed to be 1 m for the 1 in 10 year storm (required F = 1.4) and 3 m for the 1 in 1000 year storm (required F = 1.12). Such an approach is generally accepted, where possible, although it is not strictly followed. This is due to the obvious doubt concerning the advance distance of the wet front, i.e. whether or not it is physically equal to the rise in the groundwater table. In a special situation of 'dry' slope, a different approach will have to be considered to account for the various storm return periods.

POSSIBLE MODIFICATION IN CURRENT APPROACH

It would appear from the preceding discussion that a rigorous assessment of slope stability in unsaturated residual soils is extremely complicated. Apart from the problems in establishing strength parameters and groundwater characteristics, an analytical model will have to be developed to take into account the effects of seasonal change in subsoil moisture profile caused by both complex rainfall pattern and groundwater fluctuation. To achieve this aim, one would have to understand the real mechanisms involved in such a situation. A typical subsoil profile of a cut slope in unsaturated residual soils

shown graphically in Figure 5 will generally consist of four different zones. The top zone where infiltration is active during rainfall followed by evaporation undergoes substantial changes in its moisture content throughout the depth of the wetting front. The next layer is the equilibrium zone where slight changes in moisture content would occur unless the wetting front advances much further. Above the groundwater table is the capillary zone where the degree of saturation is likely to be close to saturation due to capillarity and fluctuation of the groundwater. The fourth zone is the saturated soil stratum underneath the groundwater table which develops positive porewater pressure. Under a prolonged rainfall in which the wetting front can advance to a great depth, any rise in groundwater level due directly to infiltration of rainwater from its immediate vicinity will depend primarily on the thickness of the three zones above the groundwater level. It might be possible that once the wetting front reaches the top of the capillary zone which should be near saturation due to high suction, the groundwater table might rise abruptly to that level if the rain is continuous. The amount of rise will depend mainly on the infiltration rate, the flow velocity of the groundwater, the geological structure, the rainfall intensity and duration.

In the simplified model developed by Yong et al (1982), saturation zones leading to changes in soil stress-strain behaviour have been used in the calculation procedures for slope stability. It is understood that the more sophisticated analytical model will need to incorporate complicating issues and situations in the subsoil profile as shown in Figures 4 and 5. Should the worst condition be designed for, i.e. highest groundwater level associated with fully-saturated mantle above, the result would be very conservative and uneconomical. Thus, there is certainly a need to understand the behaviour of unsaturated soil from the slope stability point of view.

In Hong Kong where failures of slopes are closely related to rainfall, several attempts have been made to form an appropriate analytical model for assessing slope stability in such a manner. One of these is the customary approach which assumes a certain rise in the groundwater level according to the specified storm return period. However, its applicability is restricted to slopes with groundwater within their immediate vicinity. For 'dry' slopes in which groundwater does not exist or is located at considerable depths below the slope face, such a method would imply that the slope stability is independent of rainfall, obviously a doubtful concept unless all its exposed surfaces are totally covered by an impervious layer. Furthermore, the rise in groundwater level due directly to infiltration of rainwater requires that the wetting front reaches the original groundwater level at a faster rate than the groundwater flow velocity. Should the shear strength of the residual soil within the wetting band drop to a low value that would cause instability, the slope would fail before any rise in groundwater could take place. In consequence, if such a model is used together with non-zero soil suction, it would imply that there remains some soil suction within the wetting band which would help in stabilizing the slope or otherwise, the rise in groundwater is not caused by direct infiltration.

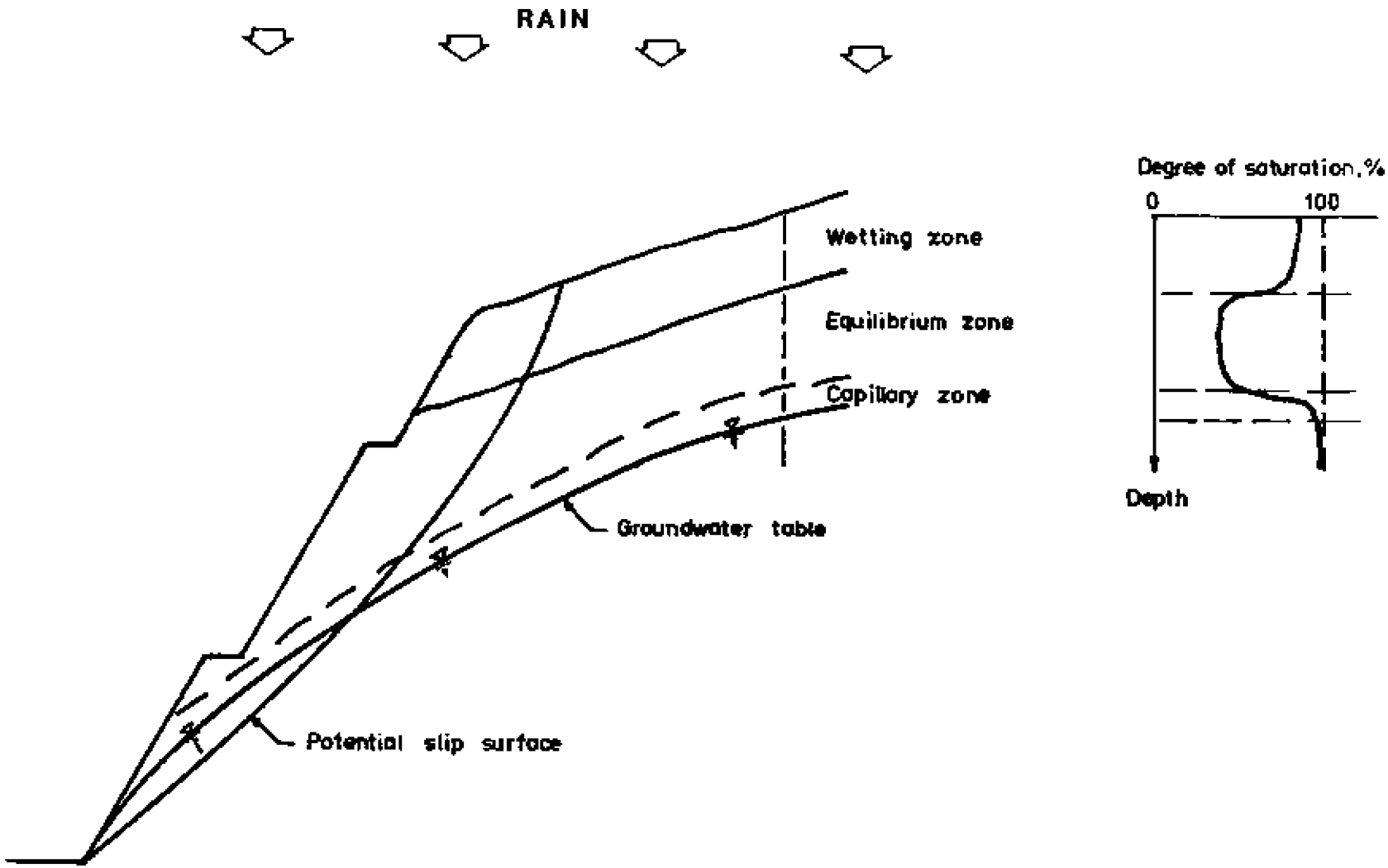

FIG.5 – Typical Profile of Moisture Content Variation in Unsaturated Soil

Based on the common knowledge that the shear strength and the soil suction of an unsaturated soil decreases with increasing moisture content, together with the available means for calculating the advance of wetting front (Lumb, 1962; Wong and Yong, 1973), it is possible to form an analytical model capable of determining the rainfall intensity that would cause slope failure. The shear strength of Hong Kong residual soils has been demonstrated to decrease with increasing degree of saturation and the cohesion could drop to zero when fully saturated (Lumb, 1965). Thus it can be postulated that the shear strength of the unsaturated soil within the wetting band is decreased as a result of higher moisture content which, in turn, increases the degree of saturation since volume change due to wetting for Hong Kong soils should be small. With such a hypothesis, the slope stability during rainfall can be easily assessed. This approach has been proposed by Lumb (1962) but rarely used in routine design, obviously due to the unclear influence of direct rainwater infiltration on slope stability which has yet to be verified through detailed field study. Furthermore, such an approach will have to be modified to cater for the behaviour of groundwater frequently observed during the wet season.

It can be concluded that there are two different opinions regarding the mode of slope failure in Hong Kong residual soils; one assumes that failure is caused by rising groundwater table and the other by saturation of the top soil mantle due to rainwater infiltration without producing positive hydraulic pressure. In practice, both modes of failure are incorporated in the design by using shear strengths of saturated specimens for the unsaturated zone and sealing the exposed surfaces with an impervious layer. In some cases such as natural slopes or grassed slopes, infiltration cannot be completely prevented. Hence the effect of infiltration on slope stability still remains to be solved.

To compare the validity of these two analytical approaches, the factor of safety of a dry slope standing at 55^{o} and 33 ft (10 m) high will be calculated. For simplicity, the bulk density (γ) and the angle of friction (ϕ') are kept constant at 125 lb/ft^3 (2.0 Mg/m^3) and 35^{o} respectively. The slope is cut into a thick mantle of decomposed granite with a permeability of 2.5×10^{-5} ft/s (8×10^{-6} m/s). The cohesion (c') is assumed to be 0.4 kip/ft^2 (19 kPa) which could be considered as an integration of two physical components, the true cohesion (c_t') of 0.2 kip/ft^2 (10 kPa) and the apparent cohesion (c_a') of 0.19 kip/ft^2 (9 kPa) due to soil suction (u^*) of 0.27 kip/ft^2 (12.9 kPa). The values of c_a' and u^* used herein are the upper limits for loose decomposed granite often adopted for slope design in Hong Kong. It should be noted that the factor of safety for the dry condition is 1.4 which meets the current requirement. In other words, combining the upper limits of cohesion and soil suction will result in a slope standing at 10 m high with a maximum angle of 55^{o}. Although slopes of such dimensions are common in Hong Kong, preventive works will normally be required to meet current standards.

Two modes of failure are considered herein. First by assuming that the cohesion (c') drops to zero within the wetting band

in which the soil is fully saturated, the factor of safety can then be calculated as a function of the depth of the wetting front (h). The result shown in Figure 6 was based on the stability chart for dry slopes prepared by Houk and Bray (1977) and the average conesion was approximated as $((H - h)/H)\ c'$. The second mode considers that the soil suction u^s or the apparent cohesion (c'_a) is reduced to zero by the wetting front while the true cohesion (c'_t) is unaffected. The factor of safety was then calculated in the same manner using the average cohesion as $c'_t + ((H - h)/H)\ c'_a$.

The resultant factor of safety shown in Figure 6 exhibits the sensitivity to the advance of rainwater infiltration as would normally be expected. The slope would fail when the wetting front penetrates to a critical depth and, on its path, causes severe reduction in the shear strength. The most critical situation occurs when the conesion (c') is completely destroyed and the failure of the slope is imminent if rainwater infiltrates about 6 m into the soil mantle. Should there be no perched water table within the slope, failure would be triggered by infiltration, not rising groundwater and the soil mass within the wetting band would fail gradually following the advance of the wetting front. On the other hand, if the true cohesion (c'_t) exists infiltration alone could not cause slope instability. In this case, there would be no need to protect the slope with an impervious layer; grassing should be adequate.

To cater for the common observation in Hong Kong that, during any severe rainstorm, many slopes fail while others still stand, the proper analytical method should be able to determine the rainfall that could cause slope failure. This can be achieved once the rate of infiltration and its effect on the shear strength can be correctly described. For the purpose of illustration herein, equation (4) can be written as $v = k/(S_f - S_o)\ n$, where v = rate of infiltration, and used by adopting the following parameters: $k = 2.5 \times 10^{-5}$ f/s (8×10^{-6} m/s), $S_f = 1$, $S_o = 0.75$, and $n = 0.4$. Provided that continuous rainfall prevails such that water percolates into the soil mass uninterrupted, the rainfall duration which is critical to slope stability can be assessed as shown in Figure 7.

It is evident that the duration of rainfall considerably affects the slope stability. If the rainwater infiltration does reduce the cohesion of the soil to a negligible value, the critical rain duration would be about 20 hours or a total rainfall of about 23 in (580 mm) (calculated from the saturated permeability k, being the limit of the infiltration rate v) which is very severe compared with the average annual rainfall of 80 in (2000 mm). Under such a rainstorm, many slopes would fail by direct rainwater infiltration. In the case of the non-zero true cohesion, more severe rainstorms would be necessary to cause slope instability. Obviously, infiltration will cause slope failure before any groundwater rise is possible particularly when there is no impervious layer present.

From the preceding discussion, the following observations can be made:-

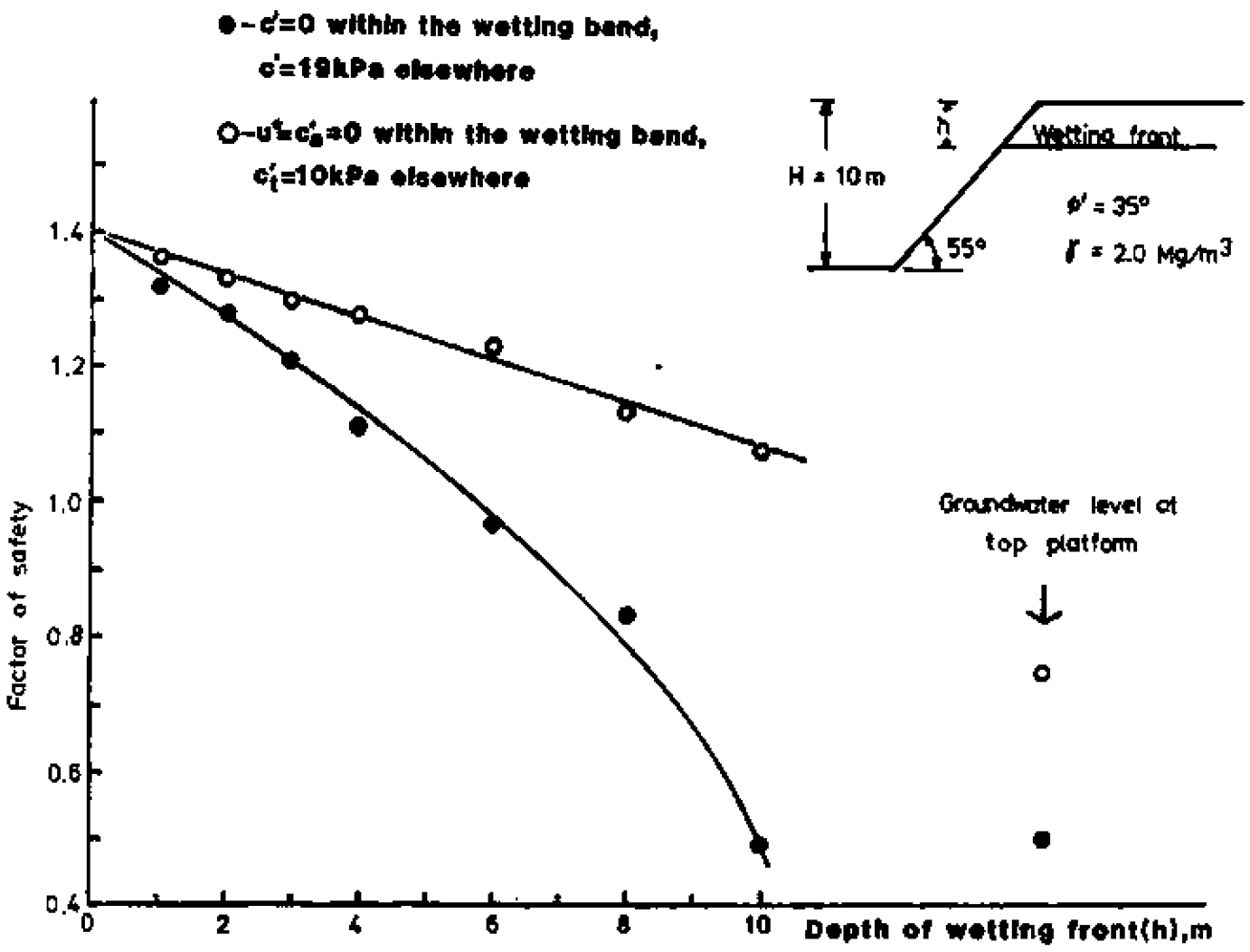

FIG.6 – Effect of Rainwater Infiltration on Factor of Safety

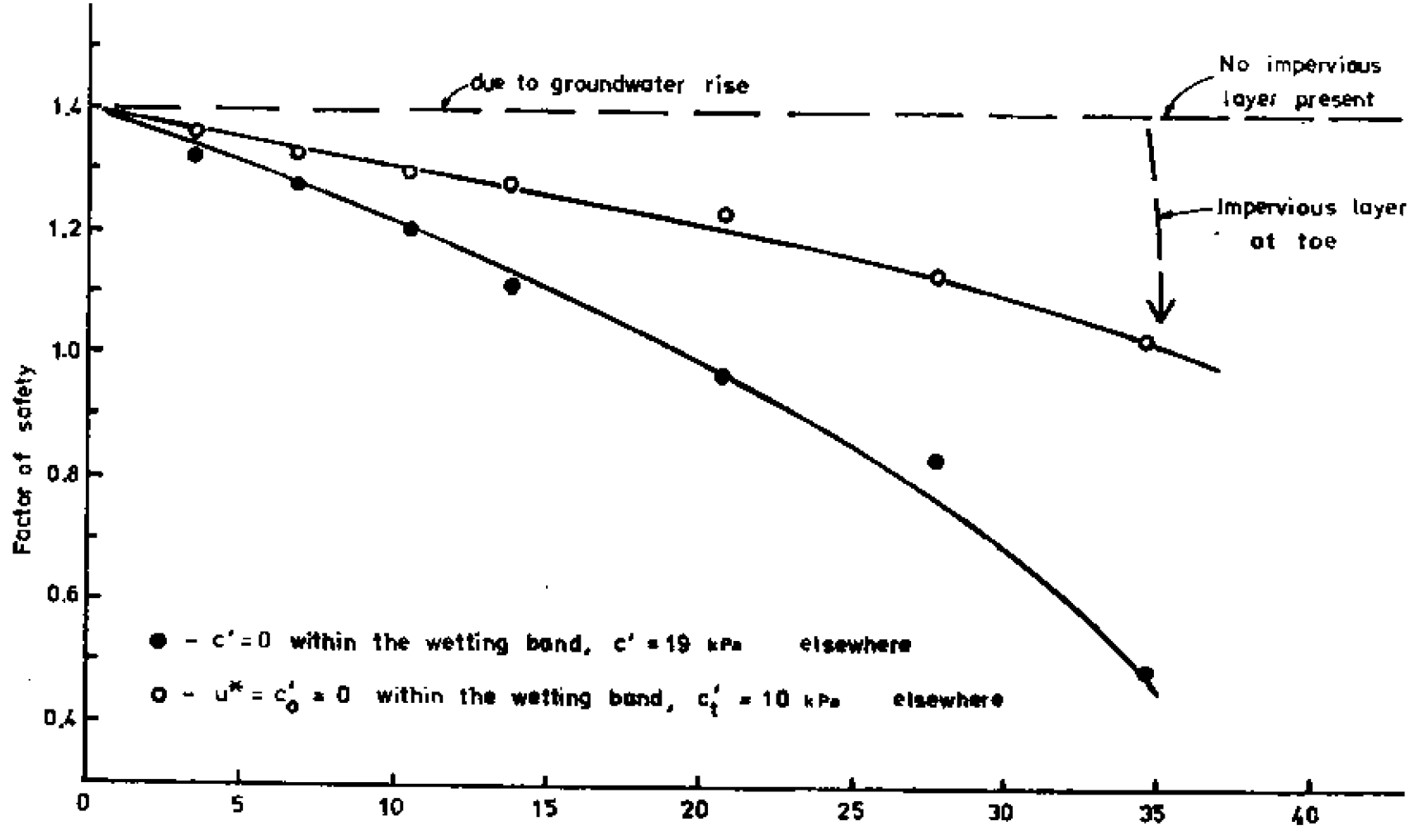

FIG.7 - Effect of Rainfall Duration on Factor of Safety

1) The analytical approach for design should be selected by considering the actual subsoil conditions encountered. Routine approaches should not be used without reservations.

2) For dry uniform slopes, failure would be induced by direct rainwater infiltration, not be rising groundwater.

3) If there is no true cohesion, or if the apparent cohesion in the near-saturation state within the wetting zone is extremely low, then infiltration will cause slope failure prior to any rise in groundwater.

4) If there is a substantial amount of true cohesion, both infiltration and rise in groundwater, if possible will have to be considered.

CONCLUSIONS

The problems of slope stability in Hong Kong residual soils arise from the fact that many slopes have failed whilst others survive through similar periods of rainfall or storm. Although it is obvious that slope failures are closely associated with rainfall, the actual mode of failure is still unclear. Slope instability could be caused by direct rainwater infiltration, thereby increasing the pore pressure and/or raising the underlying groundwater level. Without understanding such a mechanism, only conservative design approaches can be adopted. To be realistic, each slope has to be analysed individually according to the probable mode of failure which in turn depends on the subsoil conditions. The routine design approach should be used only when appropriate. Undoubtedly the behaviour of unsaturated residual soils upon partial or full saturation need to be studied further.

ACKNOWLEDGEMENT

The authors wish to thank the Partners of Scott Wilson Kirkpatrick & Partners for permission to quote triaxial test data presented in this paper.

REFERENCES

1. Allen, P.M. and Stephens, E.A. (1971), Report on the Geological Survey of Hong Kong, Hong Kong Government Press, 107 p.

2. Beattie, A.A. and Attewill, L.J.S. (1977), A Landslide Study in the Hong Kong Residual Soils, Proc. 5th Southeast Asian Conference on Soil Engineering, Bangkok, pp. 177-188.

3. Beattie, A.A. and Chau, E.P.Y. (1976), The Assessment of Landslide Potential with Recommendations for Future Research, Hong Kong Engineer, Vol. 4, No. 1, pp. 31-44.

4. Bishop, A.W. (1954), The Use of the Slip Circle in the Stability Analysis of Slopes, Proc. European Conference on Stability of Earth Slopes, Stockholm, Vol. 1, pp.1-13.

5. Bishop, A.W. (1959), The Principle of Effective Stress, Teknish Ukeblad, 106: No. 39, pp.859-863.

6. Hoek, E. and Bray, W.J. (1977), Rock Slope Engineering, Institute of Mining and Metallurgy, London, 402 p.

7. Hong Kong Government (1972), Final Report of the Commission of Inquiry into the Rainstorm Disasters, November, 91 p.

8. Hong Kong Government (1979), Geotechnical Manual for Slopes, November, 227 p.

9. Janbu, N. (1954), Application of Composite Slip Surfaces for Stability Analysis, Proc. European Conference on Stability of Earth Slopes, Stockholm, Vol. 3, pp.43-49.

10. Lumb, P. (1962), Effect of Rain Storms on Slope Stability, Symposium on Hong Kong Soils, Hong Kong Institution of Engineers, pp.73-87.

11. Lumb, P. (1965), The Residual Soils of Hong Kong, Geotechnique, Vol. 15, No. 2, pp.180-194.

12. Lumb, P. (1975), Slope Failures in Hong Kong, Quart. J. Engineering Geology, Vol. 8, pp.31-65.

13. Lumb, P. and Lee, C.F. (1975), Clay Mineralogy of the Hong Kong Soils, Proc. 4th Southeast Asian Conference on Soil Engineering, Kuala Lumpur, pp.1-41 to 1-50.

14. Morgenstern, N. and Price, V.E. (1965), The Analysis of the Stability of General Slip Surfaces, Geotechnique, Vol. 15, pp.79-93.

15. Nonveiller, E. (1965), The Stability Analysis of Slopes with a Slip Surface of General Shape, Proc. 6th International Conference on Soil Mechanics and Foundation Engineering, Montreal, Vol. 2, pp.522-525.

16. Ruxton, B.P. (1960), The Geology of Hong Kong, Quart. Geology Soc., London, Vol. 115, pp.233-260.

17. Sweeney, D.J. and Robertson, P.K. (1979), A Fundamental Approach to Slope Stability Problems in Hong Kong, Hong Kong Engineer, October, pp.35-44.

18. Wong, H.Y. (1978), Soil Strength Parameter Determination, Hong Kong Engineer, March, pp.33-39.

19. Wong, H.Y. and Yong, R.N. (1973), Engineering Problems in Unsaturated Soils, Civil Engineering and Public Works Review, pp.759-765.

20. Yong, R.N. and Warkentin, B.P. (1975), Soil Properties and Behaviour, Elsevier Scientific Publishing Co., Amsterdam.

21. Yong, R.N., Siu, S., and Sciadas, N. (1982), Stability Analysis of Unsaturated Soil Slopes, Proceedings, ASCE Speciality Conference on Engineering and Construction in Tropical and Residual Soils, Hawaii.

22. Yong, R.N., Sweere, G.T.H., Sadana, M.L., Moh Z.-C. and Chiang, Y.C. (1982), Compositional Effects on Suction of a Residual Soil, Proceedings, ASCE Specialty Conference on Engineering and Construction in Tropical and Residual Soils, Hawaii

STABILITY ANALYSIS OF UNSATURATED SOIL SLOPES

by

R.N. Yong, S.K.H. Siu and N. Sciadas

Geotechnical Research Centre
McGill University
Montreal, Canada

prepared for

ASCE Specialty Conference

Engineering and Construction in Tropical and Residual Soils

Honolulu, Hawaii

11-14 January 1982

STABILITY ANALYSIS OF UNSATURATED SOIL SLOPES

by

Raymond N. Yong[1], M.ASCE, Steven K.H. Siu[2] and Nicolas Sclades[2]

ABSTRACT

This study utilizes the finite element method for analysis of the stability of an unsaturated soil slope where consideration is given to the effect of changes in the soil moisture regime in view of rainfall. To allow for rainfall effects on the slopes, the analysis takes into consideration the percolation of rainwater from the imposed rainfall - with assumed assignment of saturation (wet) penetration into the soil. Since the infiltrating rainwater will create a transient moisture regime, the solution to the problem of stability must consider changes in the degree of soil saturation and the associated changes in the stress-strain relationships of the affected soil regions.

The technique utilizes a relationship between soil strength and degree of saturation and the implementation of a time incremental solution procedure, given in terms of changing saturation zones with time. This allows one to march downwards and also inwards from the slope to accommodate changes in the moisture regime and the associated changes in soil stress-strain.

The solutions should show patterns of soil element strain distress with the penetrating saturation front which allows for an understanding of the development of slope stability.

INTRODUCTION

A very prominent characteristic of residual soils found in tropical climates is the lack of complete saturation of such soils. Because of the initial unsaturated state, it is not uncommon for the soils to lose strength rapidly upon further wetting to saturation. The common belief is that the high negative pore pressures which exist in these soils in the unsaturated state produce resultant strengths which become progressively reduced as water content is increased. When this occurs,

---

[1]Director, Geotechnical Research Centre and William Scott Professor of Civil Engineering and Applied Mechanics, McGill University, Montreal, Canada.

[2]Professional Research Assistants, Geotechnical Research Centre, McGill University, Montreal, Canada.

during rainstorm seasons, the water content continues to increase - due to infiltration, percolation, etc.; shear strength decreases and natural landslides, mud flows, and general slope failures can occur in initially metastable slopes.

In this study, the problem of percolation of rainwater, or infiltration, is considered by assigning saturation levels to the subsoil in the slope under examination. The interest is this particular study is not so much the accuracy in modelling rainfall and infiltration but the use of a simple model of soil saturation level and associated development of soil instability because of the deterioration in soil strength - leading to slope failure.

STRESS-STRAIN REPRESENTATION AND APPLICATION

To provide input for analyses, the stress-strain results obtained from conventional triaxial testing of an initially unsaturated residual soil from South Africa (obtained from decomposed granite) were used. The soil was a yellowish-brown silty clay with distinct lumps of ¼ to 1½ in. (1.0-3.0 cm). The properties of the soil were as follows:

Specific Gravity = 2.71
Natural Water Content = 19.5%
Liquid Limit = 39%
Plastic Limit = 15.5%
Density = 112.5 pcf (18 KN/m^3) at 100% saturation

The grain size distribution is shown in Fig. 1 and the typical stress-strain curves obtained for the soils, backpressured to full saturation for the three confining cell pressures, are shown in Fig. 2. In the absence of "accepted" concensus for partly saturated soil shear strength testing, it was felt that at least this technique of reference full saturation strength would be useful since this presumably represents the "weakest" strength. Note that there is a large difference between the peak and residual strengths for all the samples tested.

It is useful to observe that the application of the finite element analysis does not require involvement of the C and ϕ parameters associated with the Mohr-Coulomb failure criterion. This point becomes particularly important when the unsaturated soil strength of the material is considered. For application of the stress-strain curves (data) to analyses, the two common methods used for simulation of the data are (a) digital, and (b) functional. In the former, the stress-strain curves are represented by coordinate pairs of points which are then used as input into the computer. The points on the curve are chosen at appropriate positions to permit calculation of the tangent moduli required in the finite-element method.

In functional form, the stress-strain curve is represented by a mathematical function. This technique requires one to specify a functional form which can closely represent the actual stress-strain

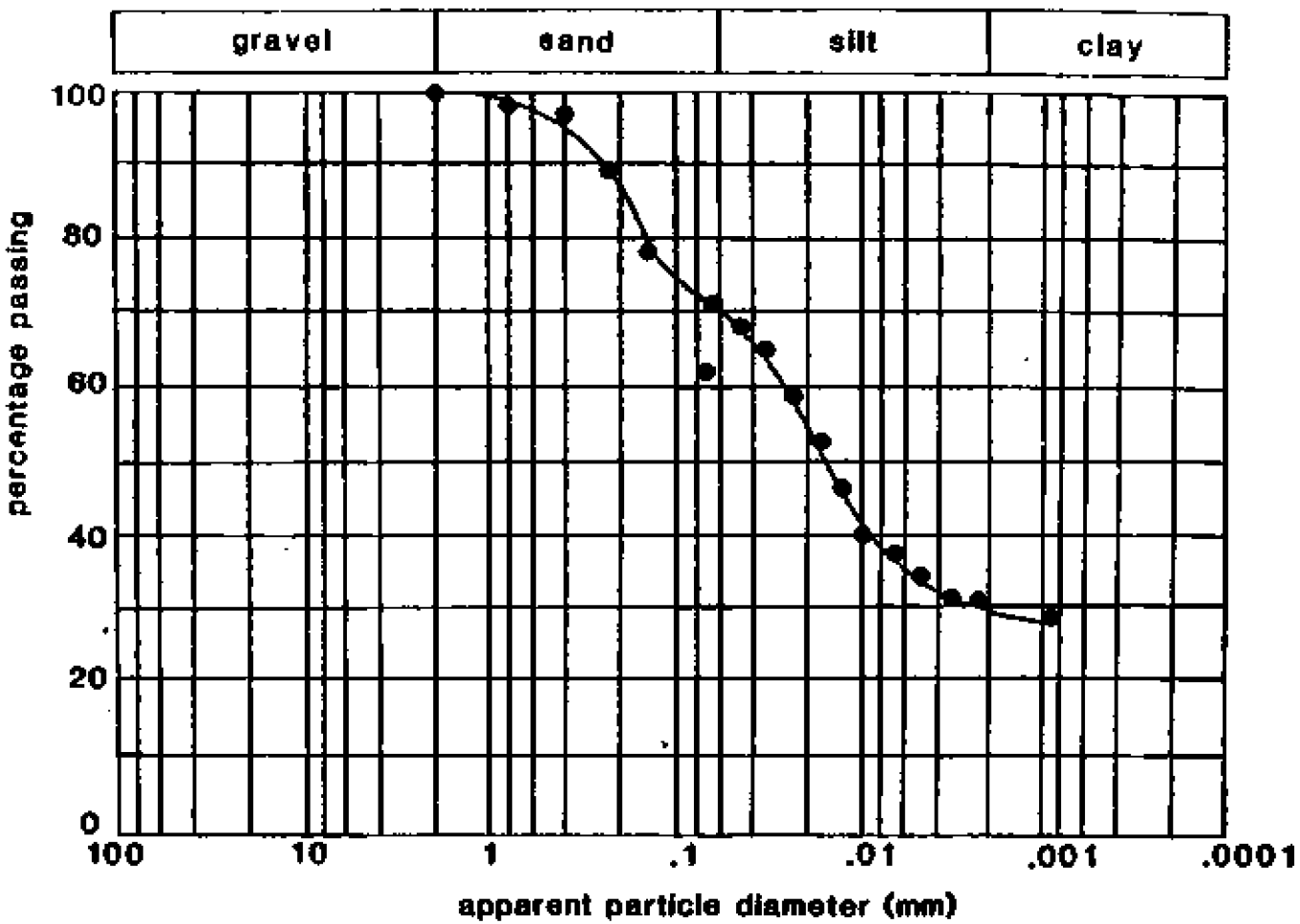

Fig. 1 Grain Size Distribution for Residual Soil

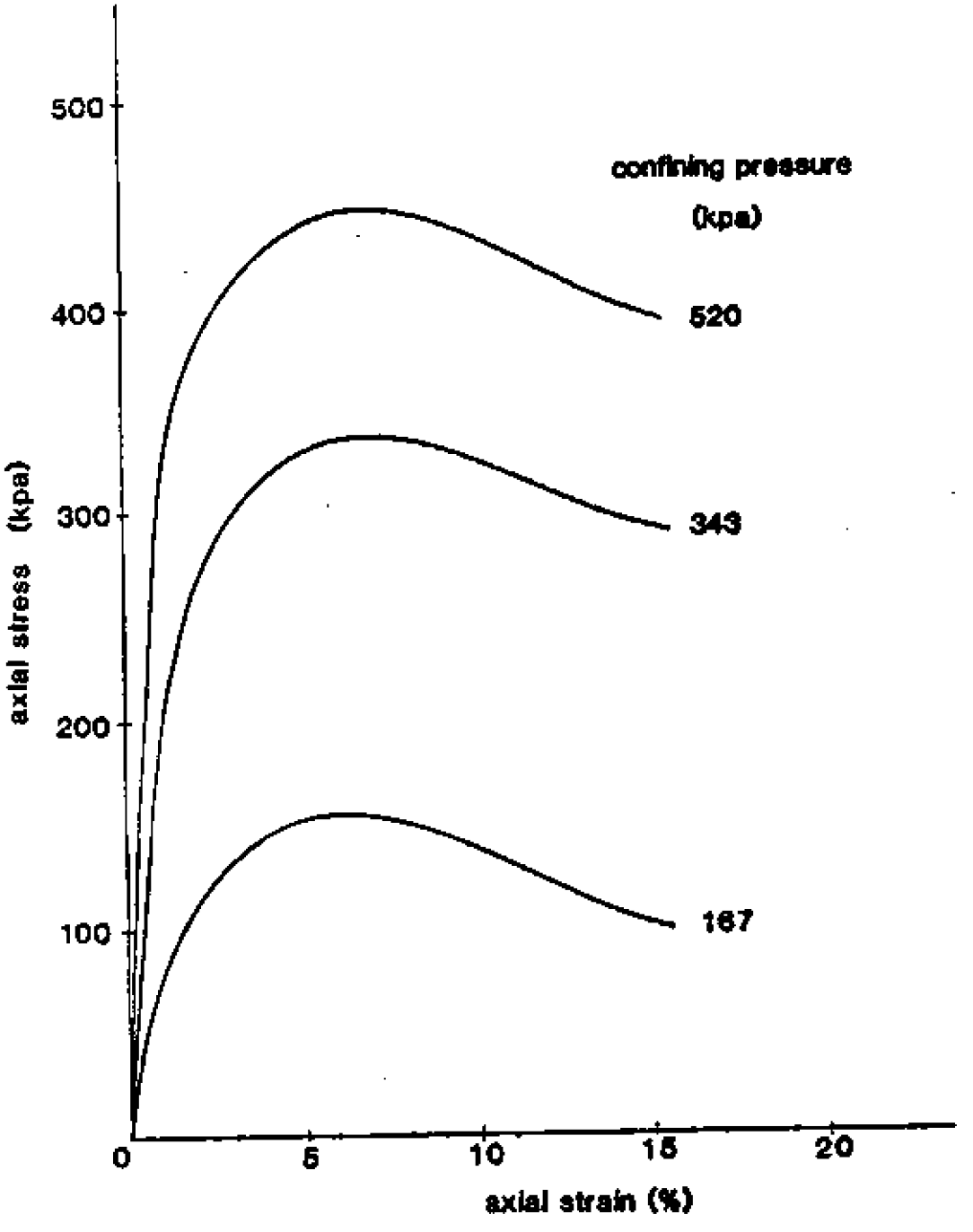

Fig. 2 Stress-Strain Curves for Soil Tested with Back-Pressure Saturation τ_c = Confining Pressure

curve. Since the stress-strain curves of the soil shown in Fig. 2 exhibit a significant strain softening effect which is not conveniently mathematized, a digitized form for representation of the stress-strain curves would be more appropriate. Consequently this study uses a digital form of representation with small intervals to reduce the error in calculation of the values of tangent moduli and the values of stress or strain which lie between points at which the values are digitized.

For computational purposes and application, the direct iteration method was used. To illustrate the procedure, the following steps were taken: for the first iteration, the trial value of initial tangent modulus chosen calculates a pair of stress-strain values at the first iteration. A check is made to compare the results with the stress-strain relation. If a large discrepancy is observed, a second iteration is started with the stiffness value equal to the slope of the chord joining the origin and the endpoint of first iteration as shown in Fig. 3. The procedure is repeated until the difference obtained is within the allowable value. This procedure is necessary because of the distinct strain softening nature of the soil.

In this direct iteration method, while convergence occurs relatively fast, the rate of convergence still depends on the initial trial value of the tangent modulus in the first iteration. The better the first approximation is, the faster the solution converges. Convergence is controlled by the assigned allowable margin of error - i.e. 15% margin is assumed in this solution - and the calculated value of the tangent modulus is compared to the actual value to satisfy the requirements. In actual application, the convergence of the iteration is seen to be very quick.

APPLICATION OF FINITE ELEMENT ANALYSIS

To develop the analysis which accounts for the infiltration of water into an initially unsaturated soil slope, an assumed 45^{0} slope with a height of 172.25 ft (52.5 m) was chosen for the study. In performing the analysis for slope stability, the initial conditions assumed for the status of the slope are: slope is unprotected from surface infiltration during rainfall, i.e. rain water can infiltrate into the soil through the slope surface and from the top of the slope, (b) the initial degree of saturation of the soil is constant throughout the whole soil mass prior to infiltration, (c) as rain water infiltrates into the slope, changes in water content and saturation are divided into saturation zones and are described by saturation contours which change with time as infiltration progresses.

Saturation contours at three different stages of infiltration are shown in Figs. 4a through 4c. Note that these are assumed distributions and also that the levels of saturation have been chosen arbitrarily to represent three stages of wetting exposure of the soil slope. The intent of this representation is to permit implementation and development of the method of analysis for the problem under study. It is recognized that a more sophisticated infiltration model will need

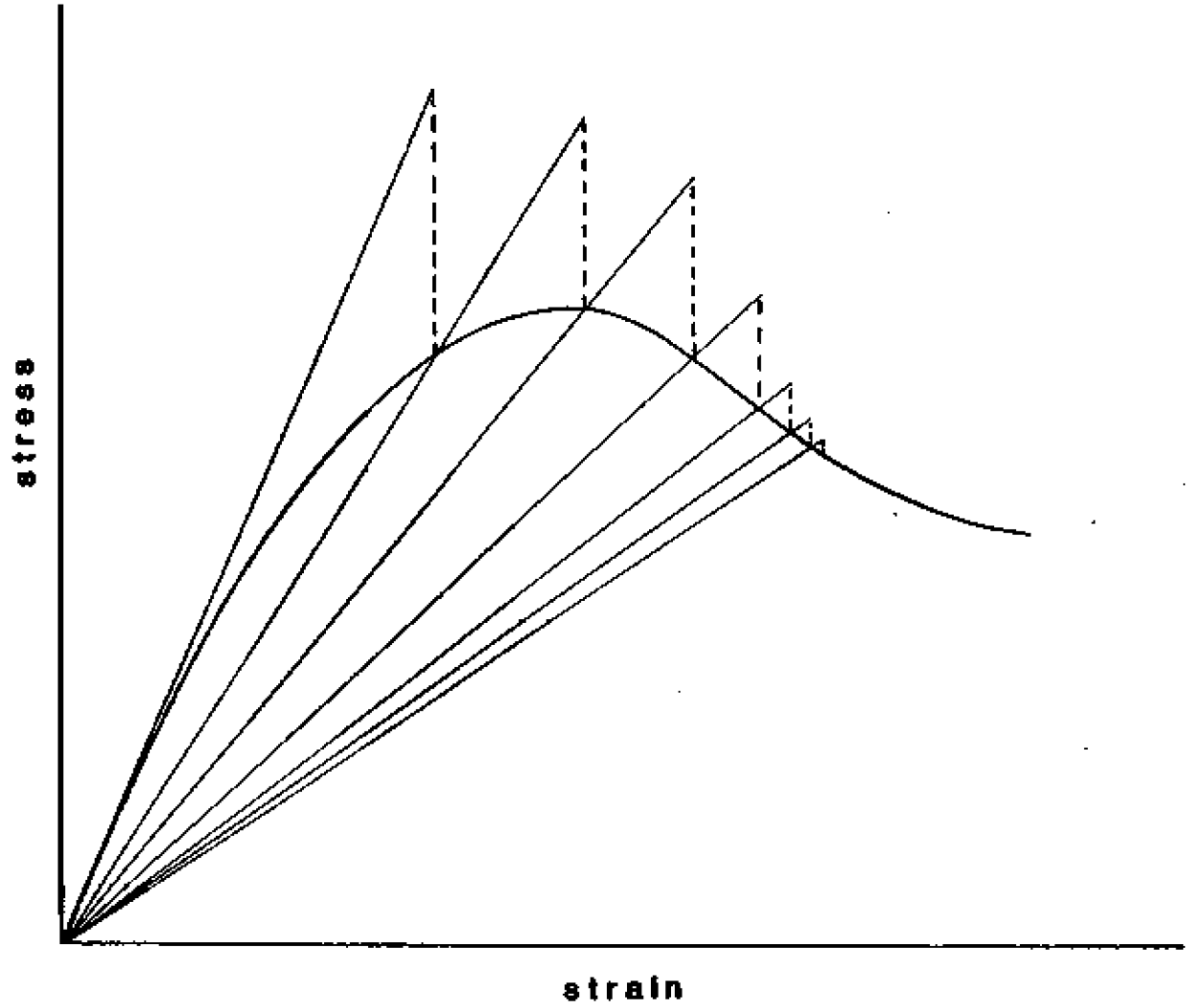

Fig. 3 Direct Iteration Method Used for Application of Finite Element Analysis

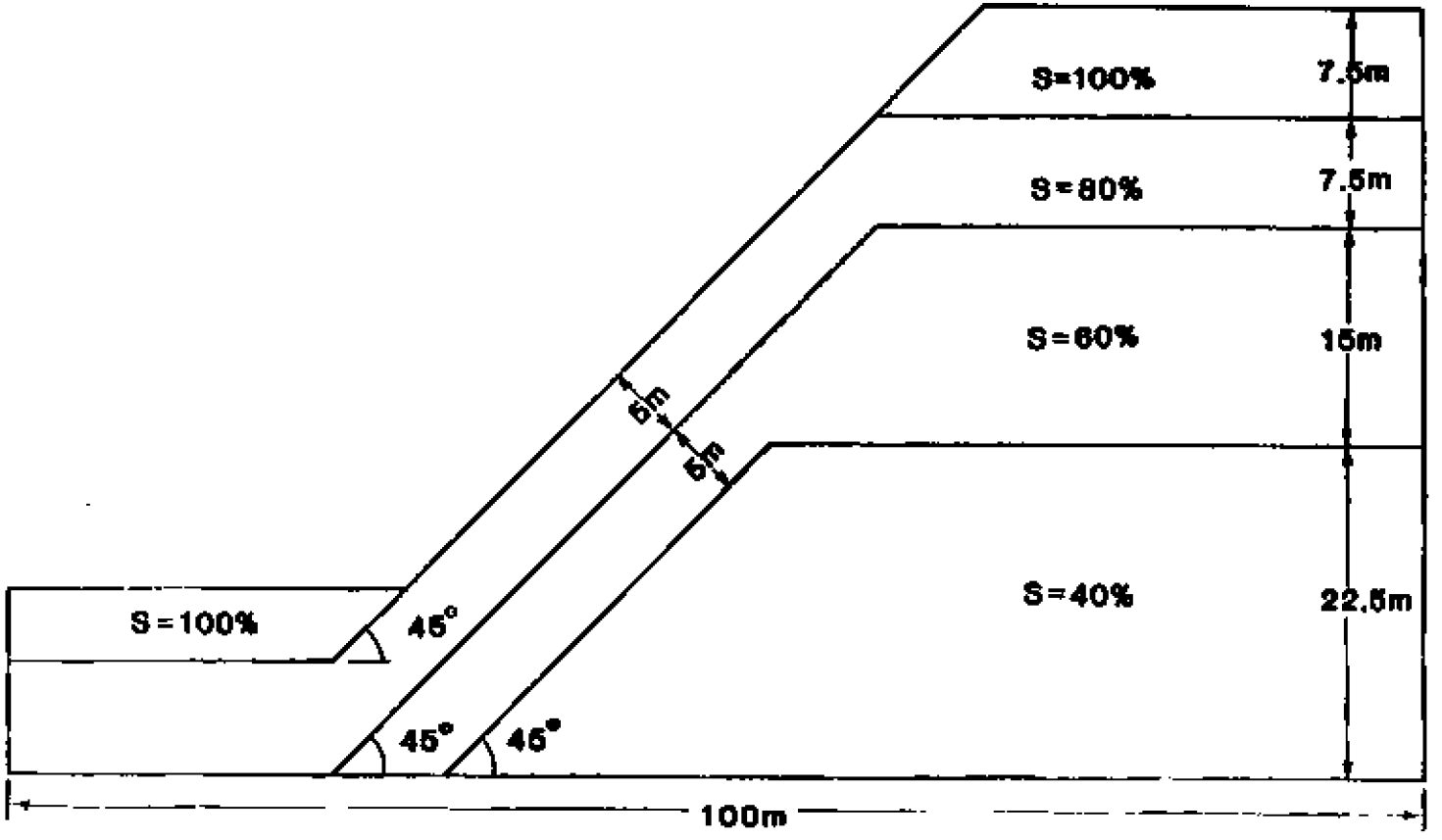

Fig. 4a Assumed Infiltration Pattern, Stage I, Showing Initial Penetration of Saturation (Wet) Front After Time t_1

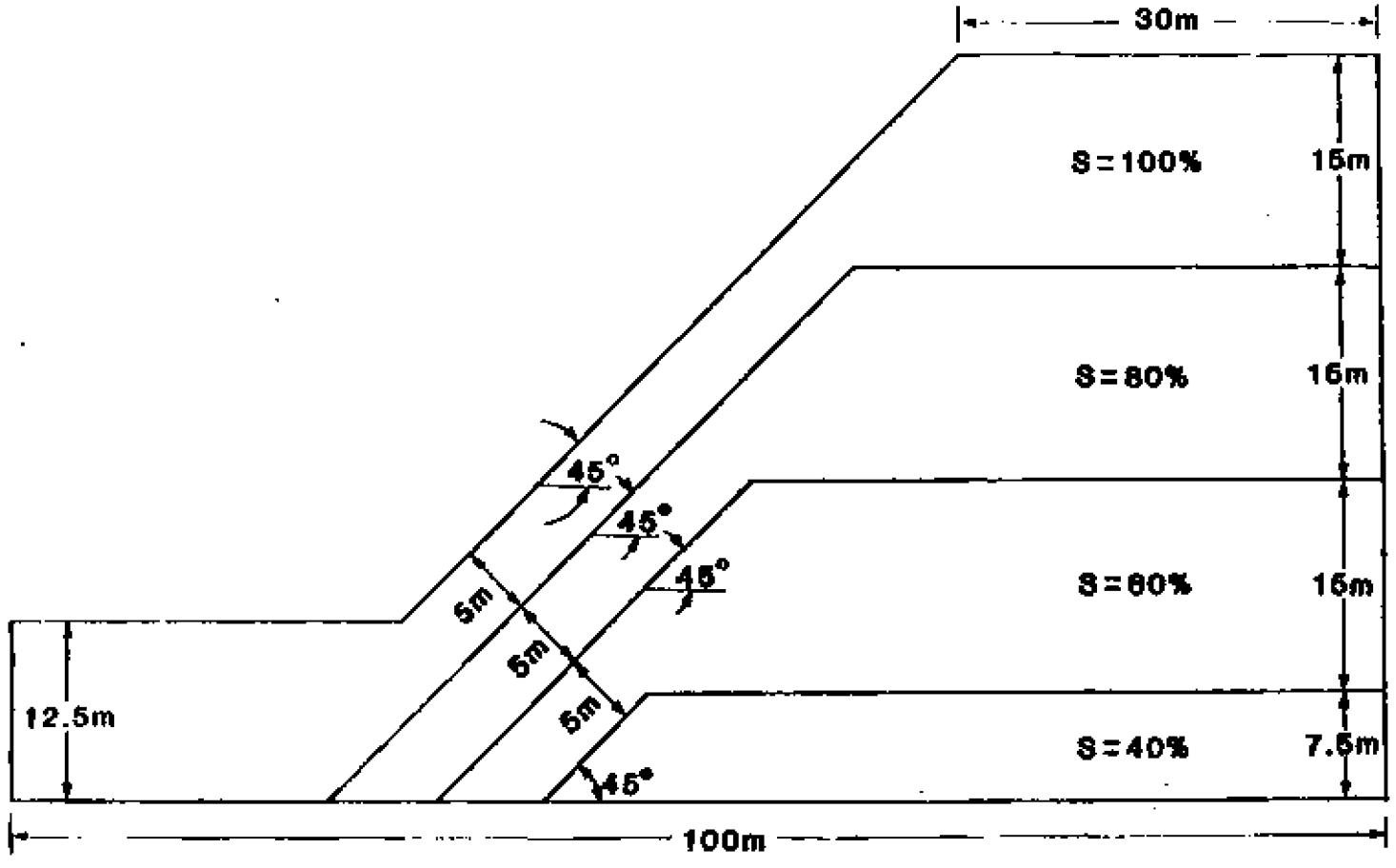

Fig. 4b Assumed Infiltration Pattern, Stage 2, Showing Penetration of Saturation (Wet) Front After Time t_2. Note: $t_2 > t_1$

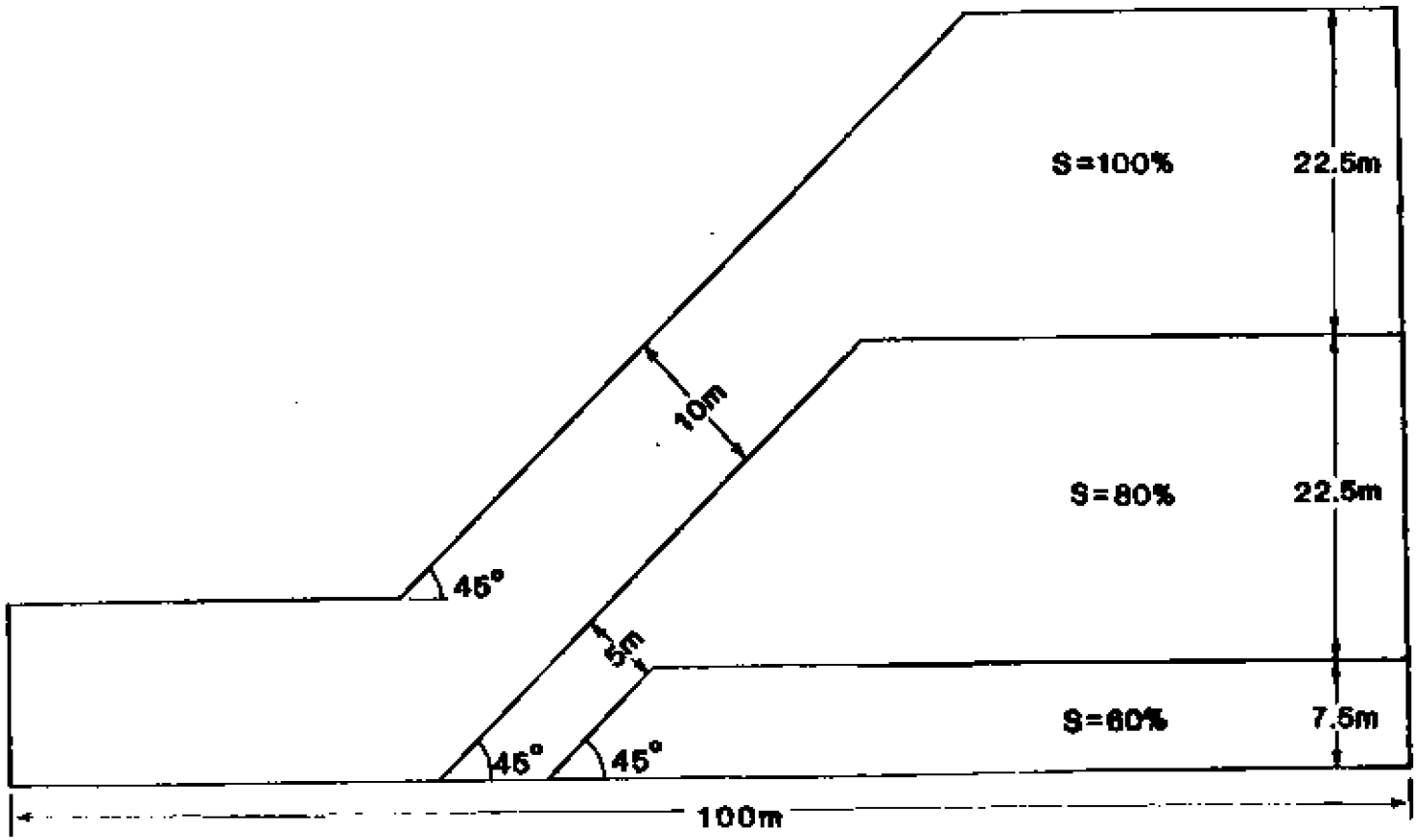

Fig. 4c Assumed Infiltration Pattern, Stage 3, Showing Penetration of Saturation (Wet) Front After Time t_3, where $t_3 > t_2 > t_1$.

to be developed. Until such is available, the use of saturation zones is indeed useful as input values for the finite element method of analysis.

The finite element mesh used is shown in Fig. 5. This slope is assumed to be of infinite width - allowing for plane strain analysis - and the soil is considered as isotropic. The isoparametric element concept has been used as a basis for element formulations.

In the procedure used to account for the confinement of a soil mesh element, it was recognized that the axisymmetric triaxial (test) stress condition which equated the intermediate and minor principal stresses was not directly representative of the in situ lateral stresses developed in the actual field problem. Since the magnitudes of the intermediate and minor principal stresses of a soil mass element would be different, and since the field lateral confining stress may not necessarily be equal to the minor principal stress, it was decided that for the computational purposes the confinement in an element could be represented as an average of the magnitudes of the intermediate and minor principal stresses induced at the centroid of the element. To implement the finite element analysis, the following steps are used:

Step 1	Calculate the state of stress of an element based on an initial assumed tangent modulus,
Step 2	Calculate the new tangent modulus from the stress-strain nonlinear curves based on the stress-state calculated in Step 1,
Step 3	Calculate the stress-state based on the new modulus,
Step 4	Repeat Step 2.

The schematic flow diagram identifying the above is follows:

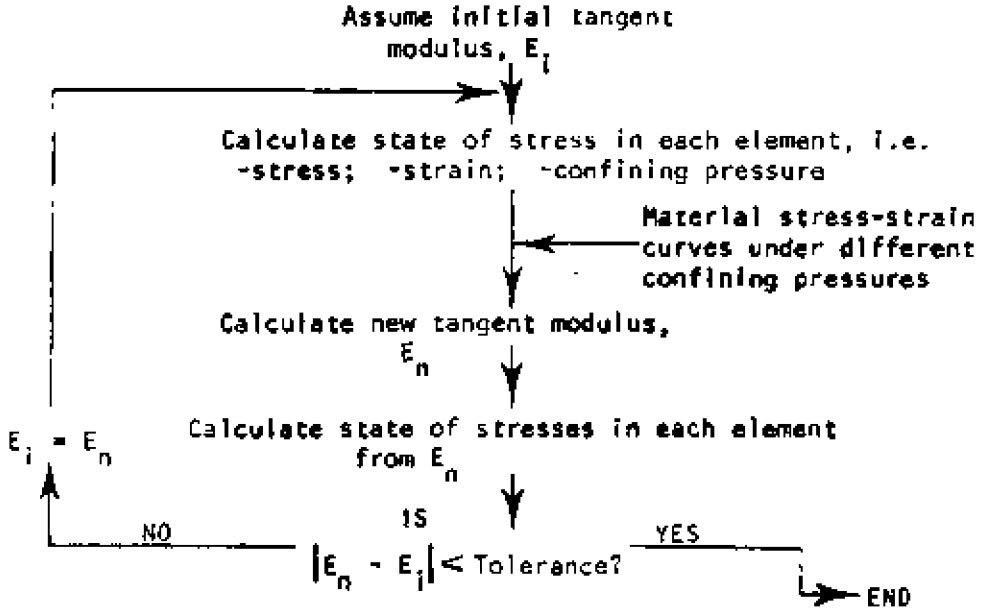

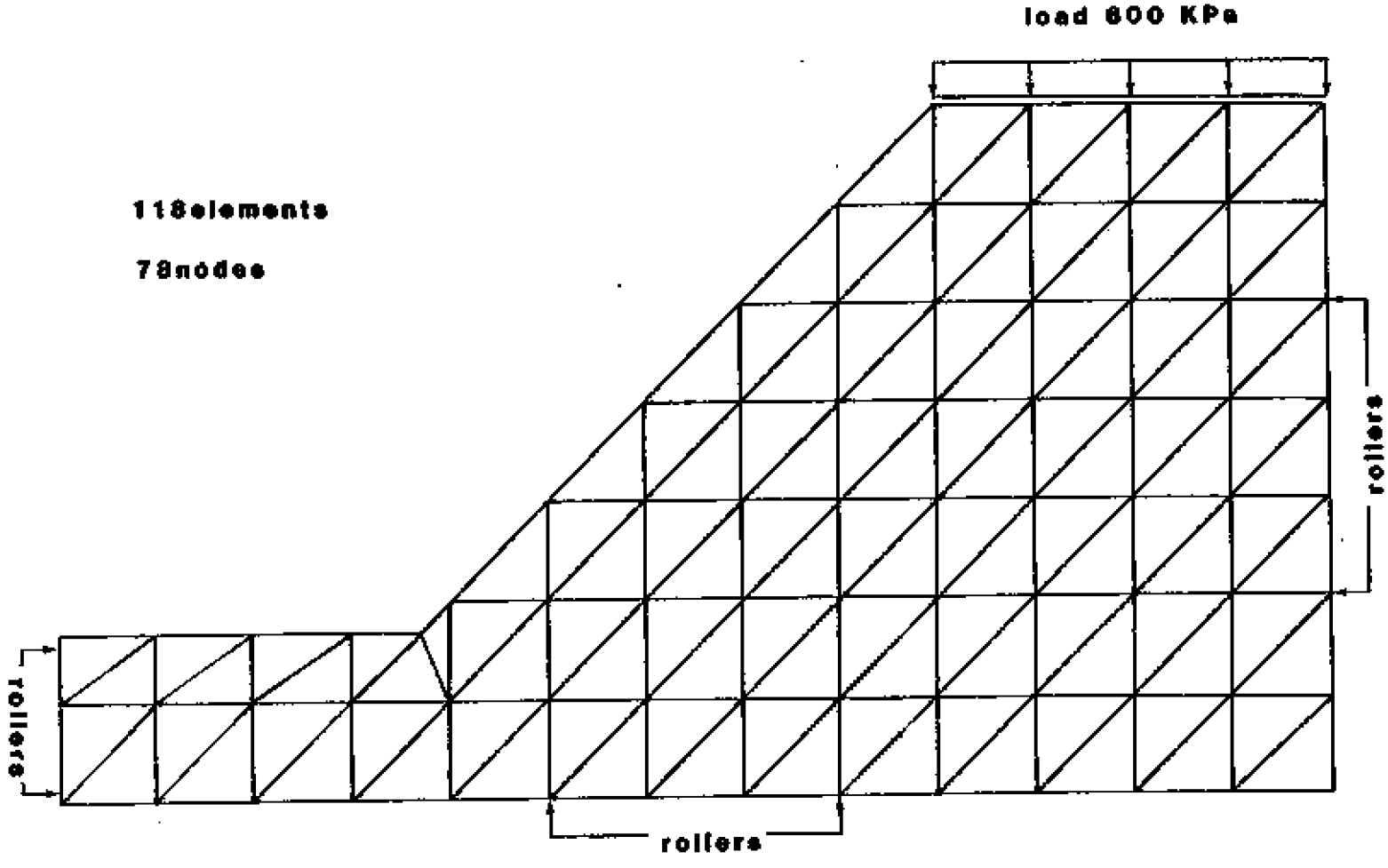

Fig. 5 Finite Element Discretization and Boundary Conditions

Linear interpolations were performed to compute intermediate values in a curve and also between curves at different confining pressures.

Since tensile stresses will exist in some of the elements at each iteration, the no-tension analysis requires that elements with tensile stresses induced in the first iteration are marked. Following the first iteration, equilibrating nodal forces are applied for the elements with tensile stresses. As the finite element analysis continues, the iterations are also continued until the zones are relieved of tensile stresses through redistribution in the adjacent regions.

The effects of the weight of the soil at the various saturation levels were taken into account in the analysis of the problem. The weight of the soil at the particular saturation level was calculated according to the total constituents in the volume contained by each element (area in 2-D analysis), and distributed equally onto each node. The process was cumulative, such that at a specific node the total load due to self weight was composed of the contributions of all elements containing that node.

Several finite element analyses were performed using three different saturation contours representing three time stages of iteration. A surcharge load of 87.1 psi (600 KPa) was applied to the top of the slope and the analysis carried on until clearly defined failed elements were observed within the slope. Elements were considered as failed when the element strain exceeded 15%. The stress-strain curves used to represent the strength of the soils in the various contoured regions of saturation, i.e., 40, 60 80 and 100% saturation were adjusted in accordance with a simplified assumption (model) which tied the peak and residual strength to the saturation level of the soil. This model is described further in the following discussion dealing with the application of the simplified Bishop's method of analysis. Figures 6a through 6c show the strain contours developed in the slope for the saturation stages 1, 2 and 3 shown respectively in Figs. 4a, 4b and 4c. Note that stage 3 shown in Fig. 6c is "academic" since the slope will have failed in the earlier stage 2 situation - as will be seen later in Figs. 7b and 7c.

To provide a basis for comparison of finite element analysis results, the simplified Bishop's method was used to perform a stability analysis for the slope with the same saturation zones shown in Figs. 4a through 4c. Since the stress-strain curves of the soils exhibit peak and residual strengths and since their values differ by more than 18%, separate analyses were made using both peak and residual values for determination of the corresponding shear strength parameters. To account for the effect of saturation on the stress-strain values, a simple model which accounted for strength changes with saturation was used. In this model, the peak and residual strengths of 90% saturated soils were assumed to increase by 10% above the strengths of the 100% saturated soils, and the strengths of the 80% saturated soils were 1.1 times larger than the strengths of the 90% saturated soils. Similarly, the strengths of the 60% saturated soils were $(1.1)^4$ times greater than the strengths of the 100% saturated soils. Using the appropriate increased strength

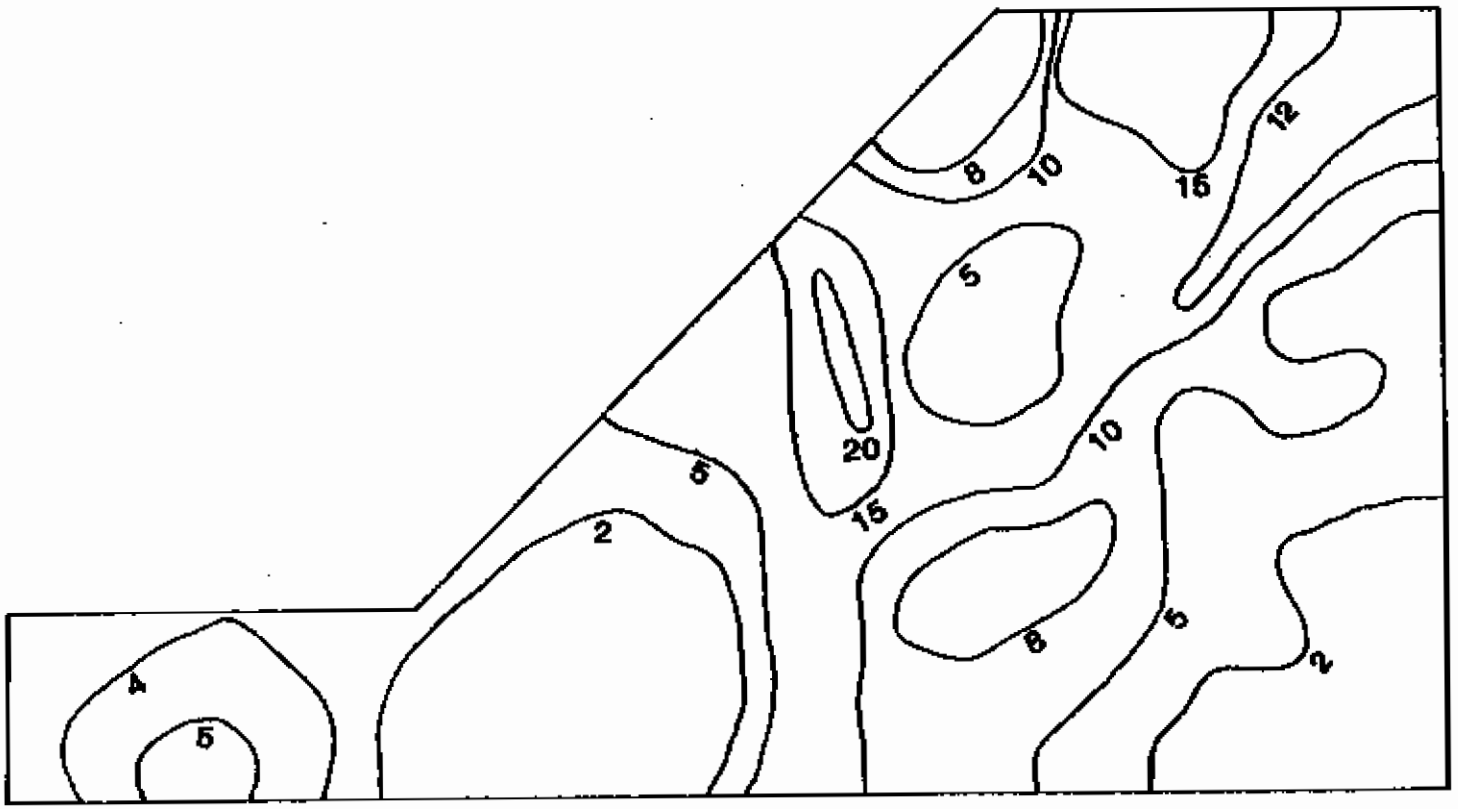

Fig. 6a Strain Contours Corresponding to Saturation Penetrations Shown In Fig. 4a

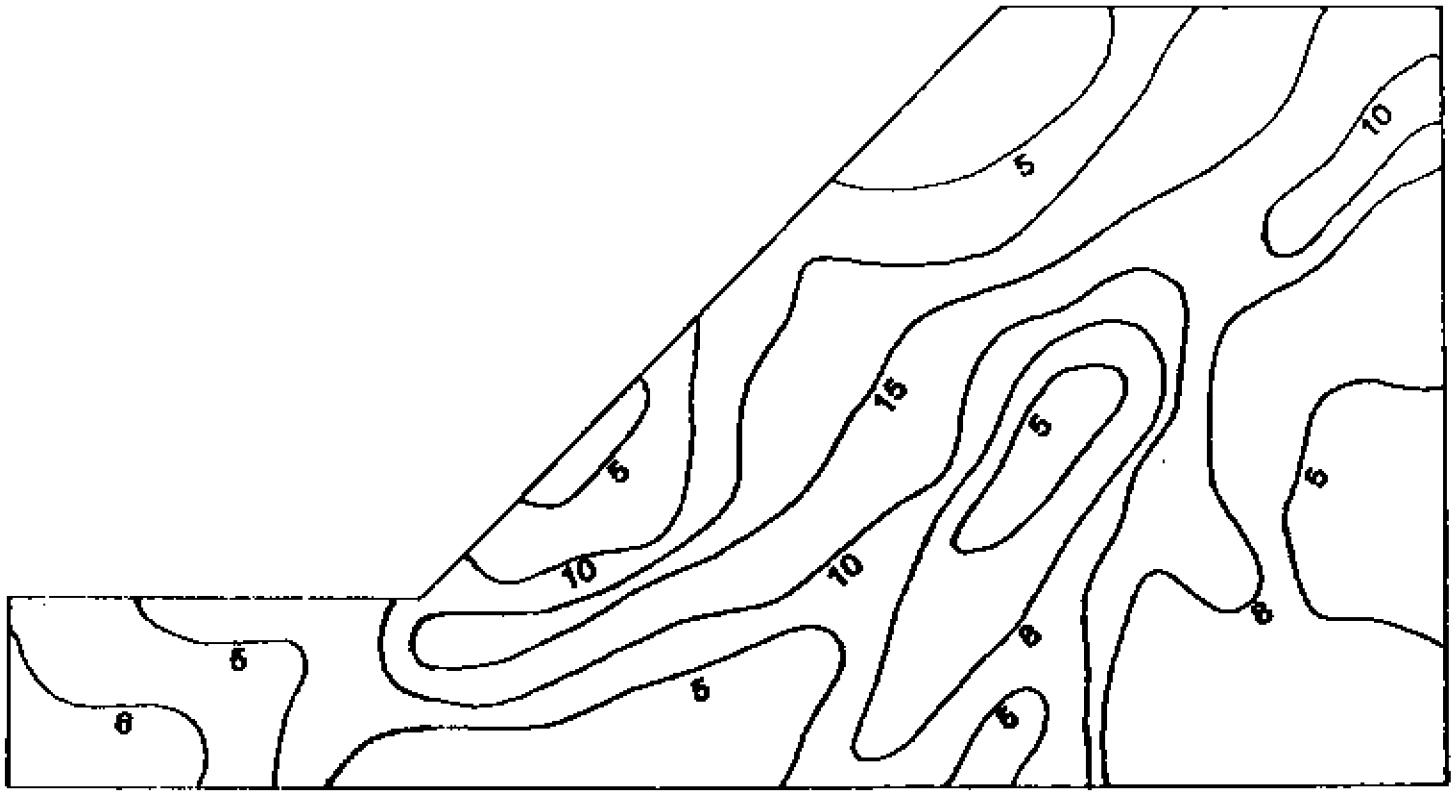

Fig. 6b Strain Contours Corresponding to Saturation Penetrations Shown in Fig. 4b

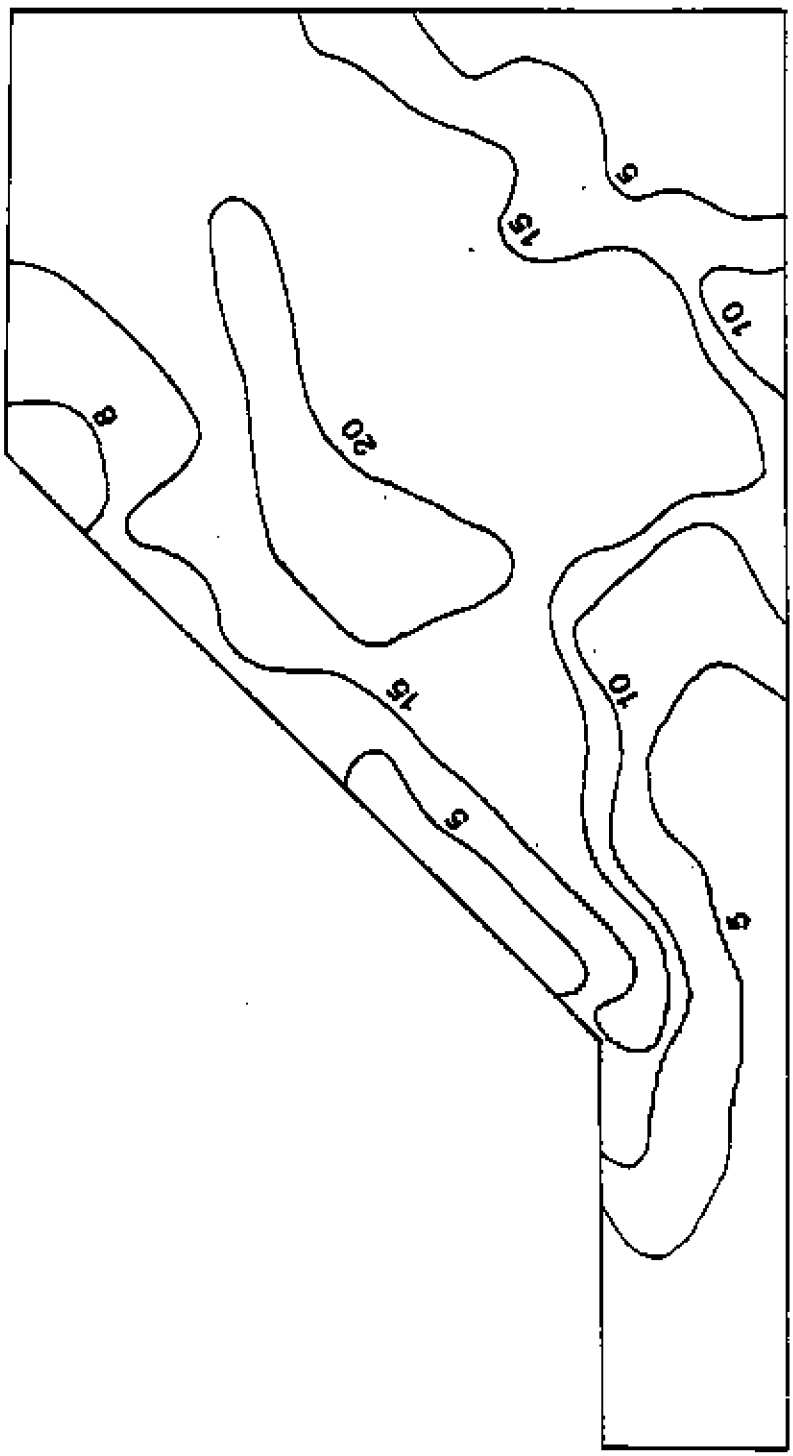

Fig. 6c Strain Contours Corresponding to Saturation Penetrations Shown in Fig. 4c

values, the corresponding Mohr-Coulomb shear strength parameters can be obtained for the particular soil saturation level, and appropriate computations for slope stability can accordingly be made. Table 1 shows the various values used in the simplified Bishop analysis. Note that the applicability of a Mohr-Coulomb failure criterion to the unsaturated soils tested is not being debated at this time. The question is begged since the intent of this study is to test or examine the development of a stress-strain method used in the analysis of unsaturated soil slopes. It is readily acknowledged that the simplifying assumptions concerning strength changes with saturation level in the simple model cannot be easily defended. However, the rationale for the model lies in the observation that strength does indeed decrease as saturation increases, and vice versa. With proper data, it would not be difficult to construct a similar type of model. Note that it is not the model that is really important but the methodology used in conjunction with a finite element analysis - i.e. the use of saturation zones and associated stress-strain phenomena for analysis of unsaturated soil slopes undergoing infiltration leading to slope failure. The slip circles computed with the simplified Bishop method of analysis are shown in Figs. 7a through 7c together with the results from the finite element analysis. In the diagrams, the elements showing strains exceeding strain-at-peak stress (approximately 7 to 8%), but less than 15% (i.e. "failed" strain) are indicated as shaded elements. The figures show that in stage 1 (Fig. 7a), "failure" of the slope does not really occur although identifiable elements within the slope show degrees of strain distress. This is compatible with the values of the factors of safety derived from the limit equilibrium analysis using the simplified Bishop method.

In Fig. 7b where Stage 2 saturation occurs after time t_2, it is noted that progression of the saturation wet front has caused a greater strain distress. The F.E. analysis shows a continuous failed zone which corresponds to the limit analysis solution - as identified by the low factors of safety computed by the simplified Bishop method.

Stage 3 saturation penetration is "academic" since slope failure will have already occurred. However, for completeness, and for the purpose of illustration of the analysis which considers the transient saturation of the soil, the results shown in Fig. 7c dramatically illustrate the full effect of deep saturation penetration. Extreme strain distress is shown over a large region in the soil slope. The limit analysis shows the bounding failure surfaces as indicated by the failure circles in Fig. 7c.

CONCLUSIONS

As stated earlier, the intent of this study is not to show that the finite element analysis can again be applied to yet another slope stability problem, but to try to indicate the feasibility of incorporating a simple set of assumptions that recognize the distribution of water content of the soil constituting the slope and the associated differences in soil strengths. The simple stress-strain-saturation

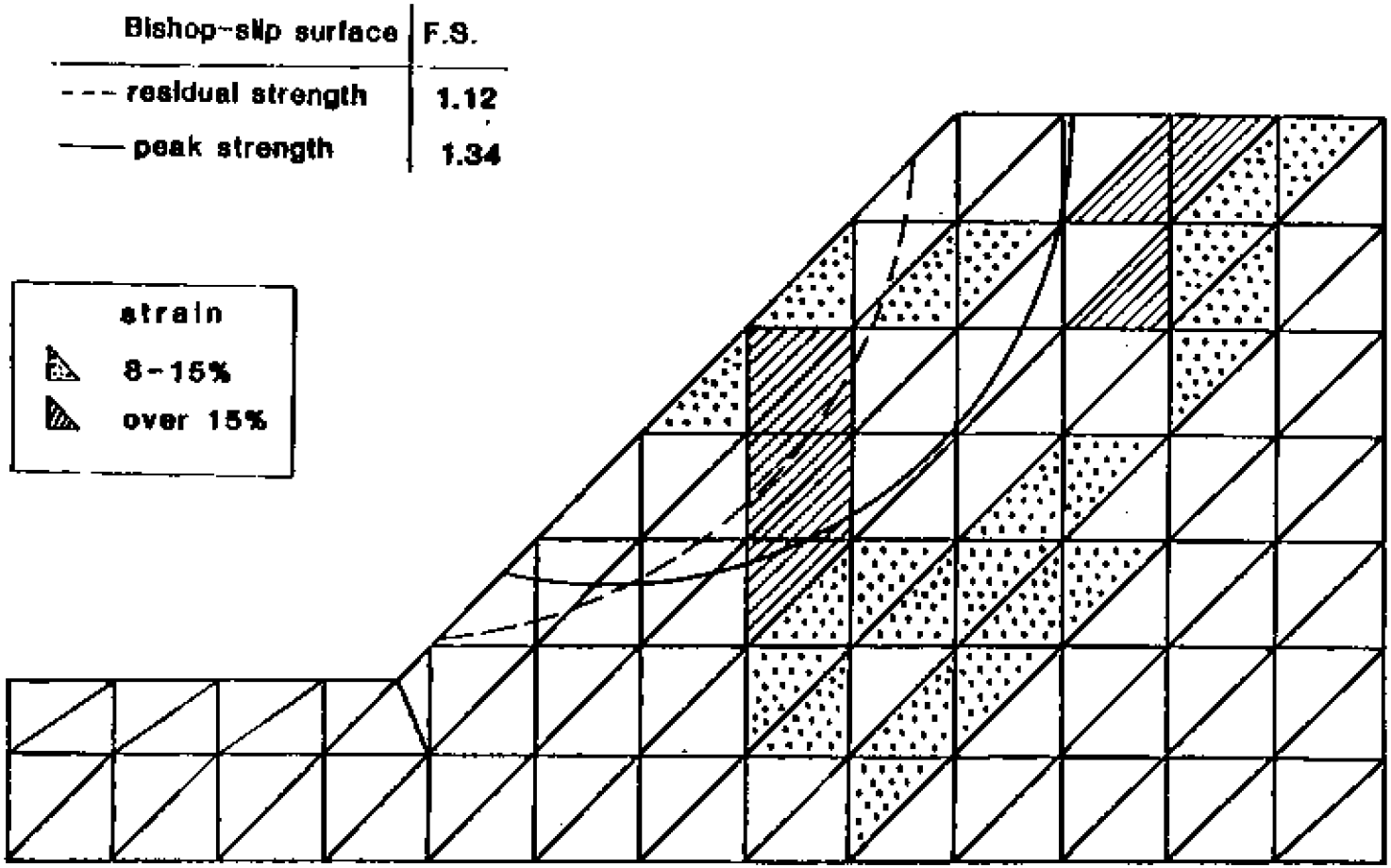

Fig. 7a Stage I - Soil Element Strain and Limit Analysis

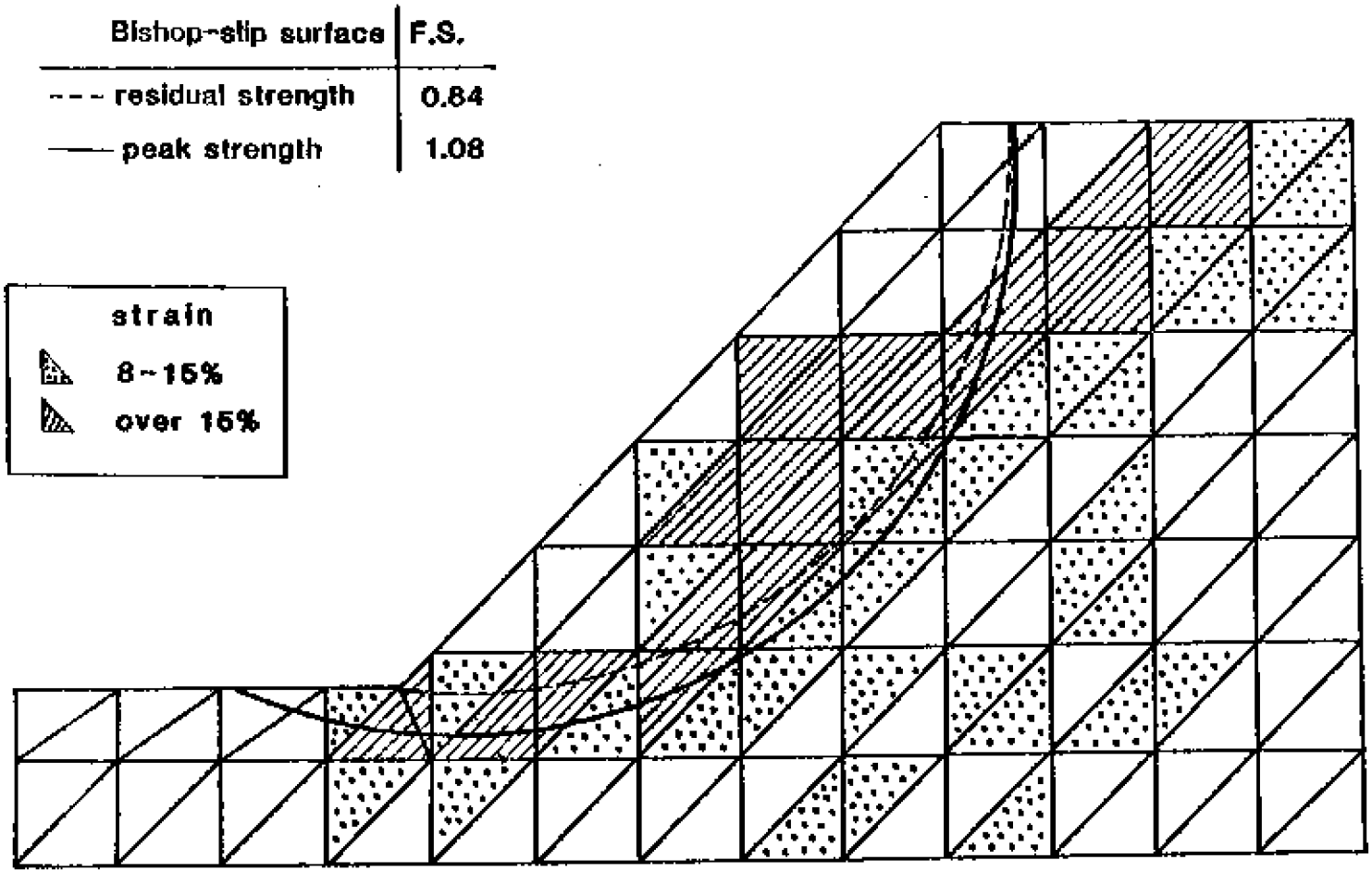

Fig. 7b Stage 2 - Soil Element Strain and Failure Surfaces from Limit Analysis. Note the Strain Distress in the Various Elements

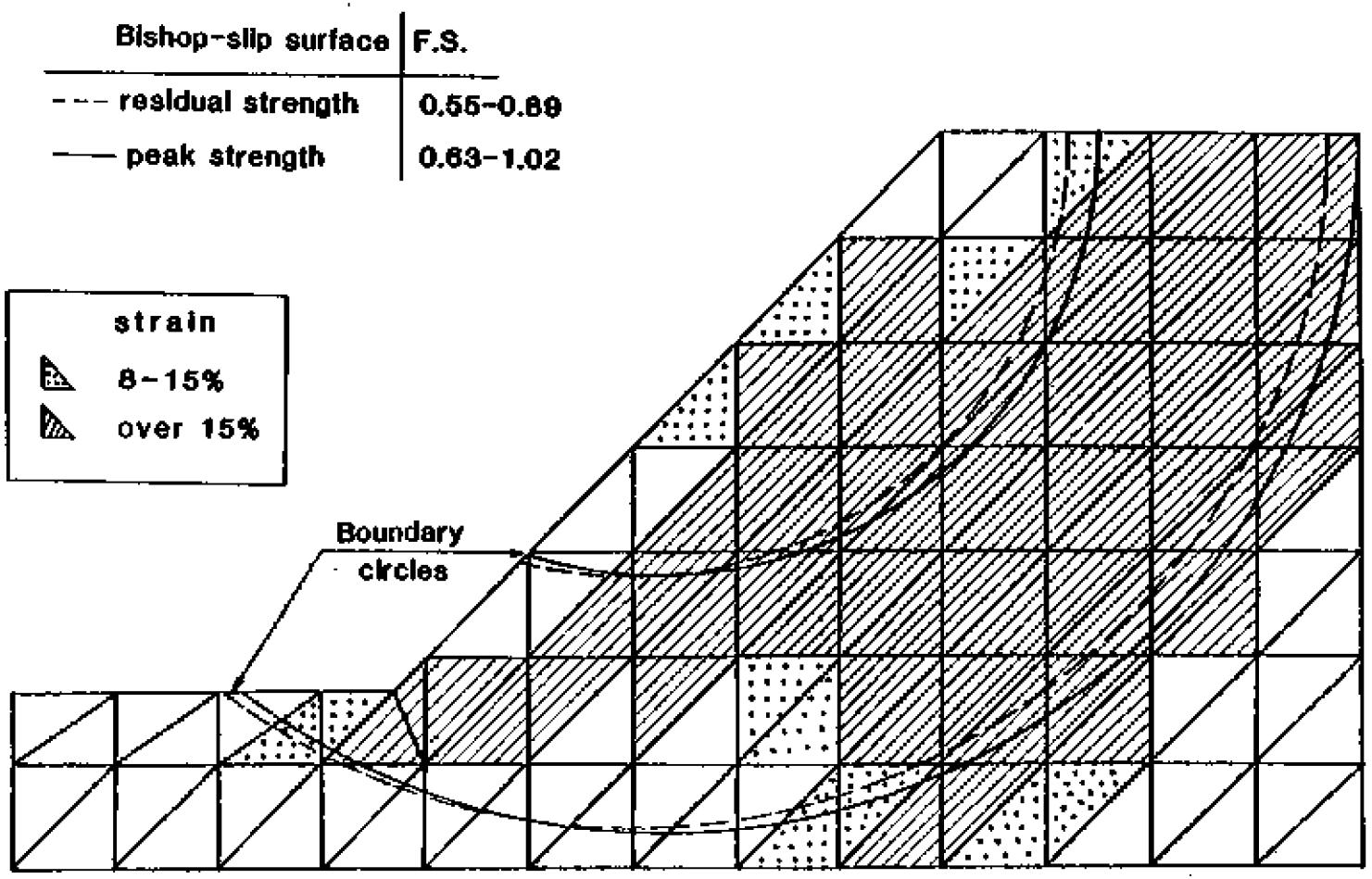

Fig. 7c Stage 3 - Slope Failure and Soil Element Strain Distress. Note the Vast Distress Region and the Upper and Lower Boundary Failure Surfaces Determined from Limit Analysis

model can be criticized and the need for a data-based stress-strain-saturation model is indeed obvious. However, for the purpose of this study, the assignment of zones of saturation, and the continued penetration of a saturated wet front with elapsed time, identified by moving saturation contours is fundamental to the methodology for analysis. With this technique, the study shows that the finite element analysis can generate analyses which show progressive element strain distress as soil saturation increases.

The finite element analyses of the slope and the considerations identified in Figs. 7a through 7c produce non-circular slip arcs which are seen to be close to the circular slip surfaces predicted by the simplified Bishop method. It is noteworthy that with the finite element analysis which considers the complete stress-strain curve, the prediction of slope failure due to saturation increase of the soil accords closely with the limit slip surface predicted by the simplified Bishop method. The failed elements shown in Figs. 7b and 7c provide a useful feature in the analysis of slope instability in view of the saturation effects in the soils. If other changes in the saturation levels of the soil are made, the method of analysis can produce results similar to those shown in Figs. 7a through 7c. When the infiltration model is developed in terms of a saturation-penetration-time relationship, the analysis can be easily adapted to consider "time" as a direct feature of the overall analysis.

ACKNOWLEDGEMENT

The authors wish to acknowledge the assistance and input provided by Dr. E.A. Fattah. This study was conducted under the Canadian Natural Sciences and Engineering Research Countil (NSERC) Grant No. A-882.

REFERENCES

1. Bishop, A.W. and Henkel, D.J. (1972) *MEASUREMENT OF SOIL PROPERTIES IN THE TRIAXIAL TEST*, 2nd Ed. English Language Book Society, London, 228 p.

2. Christian, J.T. (1968) *Undrained Stress Distribution by Numerical Methods*, ASCE Journal, Soil Mechanics and Foundations Division, Vol. 94, No. SM6, pp. 1333-1345.

3. Clough, R.W. (1960) *Finite Element Analysis in Plane Stress Analysis*, ASCE Proceedings, 2nd Conf. Elec. Computation, Pittsburgh, pp. 345-378.

4. Duncan, J.M. and Chang, C.Y. (1970) *Nonlinear Analysis of Stress and Strain in Soils*, ASCE Journal, Soil Mechanics and Foundations Division, Vol. 96, No. SM5, pp. 1629-1653.

5. Taylor, D.W. (1948) *FUNDAMENTALS OF SOIL MECHANICS*, John Wiley and Sons, New York, 700 p.

6. Yong, R.N. and Hanna, A.W. (1977) *Finite Element Analysis of Plane Soil Cutting*, Journal of Terramechanics, Vol. 14, No. 3, pp. 103-125.

7. Zienkiewicz, O.C. (1971) *THE FINITE ELEMENT METHOD IN ENGINEERING SCIENCE*, McGraw-Hill, London, 787 p.

TABLE 1 Soil Strength Properties and Bulk Densities Used in Simplified Bishop Analysis

Saturation %	Peak Cohesion KPa	Peak Frictional Angle	Residual Cohesion KPa	Residual Frictional Angle	Bulk Wt. KN/M^3
100	6.10	27	4.95	23	18.00
80	17.53	29	14.85	25	17.07
60	34.65	33	29.7	28	16.14
40	61.40	38	49.5	32	15.22

1 KN/M^3 = 6.243 pcf

1 pcf = 0.160 KN/M^3

1 KPa = 0.145 psi

1 psi = 7.0307 KPa